

https://dspace.org/

Equilibrium study of selected ion exchange reactions

Khanyile, Sabelo Mlungisi

2016
http://hdl.handle.net/10539/21275

Downloaded from a DSpace repository. https://dspace.org/

EQUILIBRIUM STUDY OF SELECTED ION EXCHANGE REACTIONS



Sabelo Mlungisi Khanyile (Pr.Sci.Nat.)

A Dissertation submitted to the Faculty of Science, University of the Witwatersrand, Johannesburg in fulfilment of the requirements for the degree of Master of Science.

May 2016

DECLARATION

I, the undersigned, declare that the work presented in this dissertation was carried out by me under the supervision of Professor Luke Chimuka. All sources used in this work have been dully acknowledged. It is being submitted for the degree of Master of Science in the University of the Witwatersrand, Johannesburg, and has not been submitted before for any degree or examination at this or any other university.

_____

Sabelo Mlungisi Khanyile

On this _____ day of _____ 2016

AKNOWLEDGEMENTS

I would like to express my deepest gratitude to my academic supervisor, **Prof. Luke Chimuka** for allowing me to be part of his research team, and for his excellent guidance.

Special thanks go to **Mr Ken Galt** for reviewing my proposal as well as for his excellent ideas. We discussed a number of interesting ideas which, some of them fell outside the scope of this dissertation but are worth to be investigated in the near future.

This work was carried out at Eskom Matimba power station laboratory. Therefore enamours thanks goes to **Mr Tebogo Kubyane**, the Chemistry manager at Matimba power station for granting me permission to carry out this work in his laboratory, and most importantly for making sure that laboratory resources were available for use in this work. I would also like to thank **Ms Maphuti Moloto Garine**, the laboratory supervisor at Matimba power station for her support throughout the course of this work.

Thanks also given to **Mr Cecil Mgqibisa** and Mr **Sidwell Muthavhine** for their support in arranging and supplying candidate ion exchange resins used in this study.

Finally, I owe my gratitude to my dear girlfriend Lisa who always gave me motivation when my work seemed difficult. No words can express my thanks for the support and encouragement she has given me.

ABSTRACT

The thermodynamic and equilibrium data for Na^+/RH^+ exchange reactions were generated using the batch method. The experimental data is unique in that the reactions were carried out at elevated temperatures (50^oC–90^oC), using low level counter ion solutions (0.001100–1.258 mg/l, Na^+). The equilibrium data was modeled against the non-linear Langmuir and Freundlich isotherm models. The model parameters were determined by an iterative approach, using the 'SOLVER' function of Microsoft Excel. The coefficient of determination, R^2 was used to evaluate the goodness of fit. The R^2 values for both models were satisfactory ($R^2 > 0.9$) to a certain extent. From the experimental data, the equilibrium parameters; Selectivity coefficient, $K_{H^+}^{Na^+}$, and Corrected selectivity coefficient K^I were computed. Irrespective of the initial solution concentration, the equilibrium parameters were found to decrease with increasing reaction temperature, indicating a poor uptake of Na^+ from solution by candidate ion exchange resins. Thermodynamic parameters; enthalpy of reaction, ΔH (J/mol.K), and entropy, ΔS (J/mol.K) were calculated from the slope and intercept of the Van't Hoff plot respectively. The reaction's Gibbs free energy change, ΔG was calculated from the values of ΔH, and ΔS, and reaction temperature. Generally, ΔG was positive and increased with increasing reaction temperature, which proved that an elevated reaction temperature favours the reverse reaction. The reactions were found to be exothermic process with negative entropy. The effect of pH on the exchange reactions was also studied. There was a decrease in the equilibrium Na^+ concentration in solution after pH conditioning, with a considerable difference when compared with that obtained from reactions without pH conditioning. The equilibrium quotient was used to define the selectivity coefficient for reactions carried out at varying pH. The equilibrium quotient increased across the initial solution concentration and was highest for reactions carried out at 1.258 mg/L. The equilibrium quotient decreased across the pH range, per initial solution concentration, indicating the pH effect.

TABLE OF CONTENTS

DECLARATION I

AKNOWLEDGEMENTS II

ABSTRACT III

LIST OF FIGURES V

LIST OF TABLES VI

LIST OF ABBREVIATIONS VIII

1. CHAPTER ONE 1

1.1. INTRODUCTION 1

1.2. PROBLEM STATEMENT 3

1.3. MOTIVATION 3

1.4. KEY RESEARCH QUESTIONS 4

1.5. SCOPE OF WORK AND WORK OUTLINE 5

2. CHAPTER TWO 6

2.1. LITERATURE REVIEW 6

2.1.1. Theory of the batch method approach 6

2.1.2. Fundamentals of ion exchange media 6

2.1.3. Preparation of organic ion exchange resins 8

2.1.4. Characteristics of ion exchange resins 11

2.1.5. Theory of condensate polishing 14

2.1.6. Condensate polishing plant configurations 15

2.1.7. Ion exchange equilibria 22

2.1.8. Langmuir Isotherm model 30

2.1.9. Freundlich Isotherm model 31

2.1.10. Langmuir and Freundlich model parameters determination 32

2.1.11. Ion exchange equilibrium isotherm plot 34

3. CHAPTER THREE 36

3.1. EXPERIMENTAL METHODS 36

3.1.1. Materials 36

3.1.2. Candidate ion exchange resins 40

3.1.3. Methods 41

4. CHAPTER FOUR 45

4.1. RESULTS AND DISCUSSION 45

4.1.1. Exchange capacity 45

4.1.2. Optimum contact time 46

4.1.3. Ion exchange equilibria 47

4.1.4. The pH effect 77

5. CHAPTER FIVE 84

5.1. CONCLUSION 84

5.2. RECOMMENDATION 85

5.3. REFERENCES 86

5.4. APPENDIX 93

LIST OF FIGURES

Figure 1: Typical water-steam cycle for Eskom direct dry cooled power generating plant. 1

Figure 2: Typical ion exchange resin manufacturing processes 9

Figure 3: Schematic of styrene-DVB ion exchange resin copolymer network [31] 10

Figure 4: Condensate scavenger configuration 16

Figure 5: Cation/Anion mixed bed configuration 17

Figure 6: Lead cation resin-mixed bed configuration 18

Figure 7: Separate bed configuration 19

Figure 8: Tripol configuration 20

Figure 9: Triobed configuration 21

Figure 10: Typical ion exchange equilibrium isotherm plot 35

Figure 11: Filtration apparatus 38

Figure 12: Experimental setup for ion exchange reactions 38

Figure 13: Set up for UPW production 39

Figure 14: Experimental setup for exchange capacity measurements 39

Figure 15: Removal of Na^+ ions from solution by Ambersep 252 H as a function of contact time at 25°C, C_{in} = 2.0 µg/L 47

Figure 16: The variation of Langmuir constant, K_L with reaction temperature 49

Figure 17: Experimental and predicted ion exchange equilibria for Na^+/RH^+ reactions at varying reaction temperatures using resin type; (a) ambersep 252 H , (b) amberjet 1600 H, (c) SGC 650 H, and (d) PPC 150 H 53

Figure 18: Separation factor for the Na^+/RH^+ exchange reaction and varying initial solution concentration and reaction temperature 56

Figure 19: Variation of selectivity and corrected selectivity coefficients with initial counter ion solution and temperature 63

Figure 20: The Van't Hoff plots for Na^+/RH^+ exchange reactions 77

Figure 21: The effect of pH on Na+ exchange by candidate ion exchange resins at varying reaction temperature (C_o = 0.001100 mg/L) 80

Figure 22: The effect of pH on Na+ exchange by candidate ion exchange resins at varying reaction temperature 83

LIST OF TABLES

Table 1: List of chemicals 36

Table 2: Typical ion exchange resin physical and chemical properties 40

Table 3: Ion exchange capacities of candidate resins 45

Table 4: Constants for equilibrium isotherm models for exchange reactions involving; Ambersep 252 H, Amberjet 1600 H, SGC 650 H, and PPC 150 H resins 49

Table 5: Selectivity coefficients for the Na^+/RH^+ reaction at varying initial solution concentration and reaction temperatures 58

Table 6: Equilibrium and Thermodynamic parameters generated using; (a) Ambersep 252 H, Amberjet 1600 H, and; (b) SGC 650 H, PPC 150 H 64

Table 7: The effect of pH on Na^+ exchange at varying reaction temperature 93

Table 8: Equilibrium quotient variation with pH at varying reaction temperature for reactions involving Ambersep 252 H 94

Table 9: Equilibrium quotient variation with pH at varying reaction temperature for reactions involving Amberjet 1600 H 95

Table 10: Equilibrium quotient variation with pH at varying reaction temperature for reactions involving SGC 650 H 96

Table 11: Equilibrium quotient variation with pH at varying reaction temperature for reactions involving PPC 150 H 97

LIST OF ABBREVIATIONS

1hr:30 min:	One hour thirty minute
Å:	Angstrom
BWR:	Boiling water reactors
^{o}C:	Degrees centigrade
DVB:	Divinylbenzene
Eq/L:	Equivalent per liter
EPRI:	Electric power research institute
g:	Grams
ΔG:	Gibbs free energy
ΔH:	Enthalpy change
H^+:	Hydronium ion
H_2SO_4:	Sulphuric acid
ICP-OES:	Inductively coupled plasma optical emission spectroscopy
IUPAC:	International union of pure and applied chemistry
K:	Kelvin
K_D:	Distribution coefficient
K_T:	Thermodynamic equilibrium constant
K_A^B:	Selectivity coefficient
K':	Corrected selectivity coefficient
mL:	Millilitre
mg/L:	Milligrams per litre
N:	Normality
Na^+:	Sodium ion
NaCl:	Sodium chloride
Na_2CO_3:	Sodium carbonate
—$N^+(CH_3)_3^+$:	Quaternary ammonium ion
NaOH:	Sodium hydroxide

NH_3/NH_4^+:	Ammonia/ammonium ion mixture
$NH_4^+(aq)$:	Aqueous ammonium ion
NLLS:	Nonlinear least square
NRTL:	Non-random two-liquid model
OH^-:	Hydroxide ion
pH:	P function of the hydronium ion
PT:	Pitzer model
PWR:	Pressurised water reactors
R^2:	Coefficient of determination
RH^+:	Hydrogen form ion exchange resin
RNa^+:	Sodium form ion exchange resin
RMSE:	Residual root mean square error
ΔS:	Entropy change
—$SO_3^-H^+$:	Sulphonic functional group
SS:	Sum of squares
TDS:	Total dissolved solids
UNIQUAC:	Universal quasichemical
UPW:	Ultrapure water
µg/L:	Micrograms per litre
$\mu gL^{-1}min^{-1}$:	Micrograms per litre per minute
µS/cm:	Micro Siemens per centimetre
χ^2:	Chi-square

1. CHAPTER ONE

1.1. INTRODUCTION

In the fossil-fuel power generating process, steam generated in a steam generator (boiler) is sent through a series of turbines where it expends most of its thermal energy, exits the low pressure turbine(s) and is channelled through the exhaust steam ducts to the steam condenser where it condenses. The condensate and other clean process drains are recovered and recycled for further steam generation. Recovery and recycling of condensate is of economic importance as it provides means to significantly reduce power generating costs and hence increases the cycle efficiency. Condensate recovery also reduces water consumption as less make up water is required for steam generation. Furthermore, recovered condensate contains less dissolved ionic impurities compared to demineralised make up water. This excludes the presence of any boiler feed water chemical conditioning agent, such as ammonia, which is normally present in excess over any impurities.

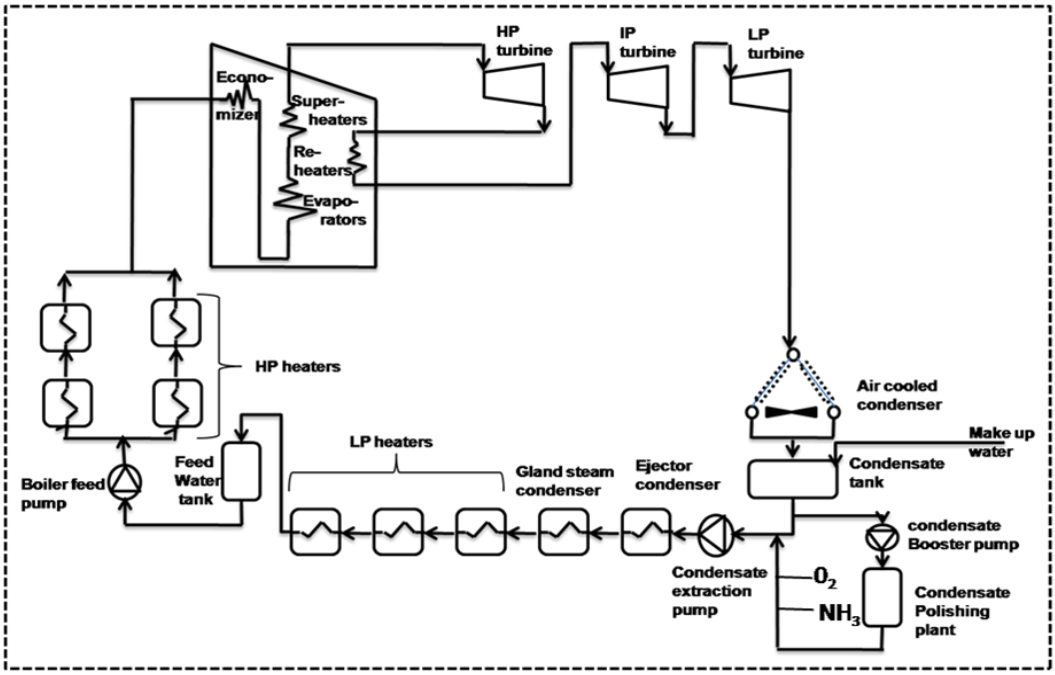

Figure 1: Typical water-steam cycle for Eskom direct dry cooled power generating plant.

Over the years, the move to higher steam temperatures and pressures operating conditions, and in particular to supercritical conditions, has led to the adoption of increasingly exotic alloy materials that, under the temperature and pressure conditions to which they are exposed, have such fine tolerances of impurities that even return condensate is of insufficient purity, necessitating the incorporation of some form of condensate purification. Utilisation of recovered condensate containing high levels of dissolved ionic impurities and suspended particulate matter for steam generation may have a detrimental effect on the useful life of water and/or steam touched power plant components that are susceptible to corrosion. Chemistry induced boiler tube failures for instance, will cause a steam generator to be taken out of service for repairs, the entire power generating unit shut down, resulting in production losses and repair costs. Dissolved ions are the major cause of corrosion in the water–steam cycle, whilst suspended particulate (corrosion product) tend to deposit and build-up on boiler tubes, causing tube overheating, and facilitating under-deposit corrosion leading to boiler tube failures. Chemical impurities may enter the water-steam cycle in a number of ways including; contaminated boiler feed water chemical conditioning agents, contaminated ion exchange resins regeneration chemicals, resin leachate (especially new resin), contaminated make-up water, incorrect (or incorrectly applied) materials during outage maintenance, etc.

Condensate purification by means of filtration, powdered resin, and deep bed using ion exchange resin is not uncommon in power plant [1-4]. Termed “Condensate Polishing” [3,2,5,7], this is a widely established and accepted ion exchange resin technology which plays a critical role in power generating processes, both fossil and nuclear (boiling water reactors, BWR, and pressurized water reactors, PWR) [3,6,7,8]. Figure 1 show a typical water–steam cycle for Eskom direct dry cooled fossil power generating Unit fitted with ion exchange condensate polishing plant. The majority of Eskom condensate polishing plants operates well in the temperature range of 35–50°C, and pH of up to 8.5. These conditions are found in once through units with wet cooled condensers. In direct dry cooled units, condensate temperatures normally range from 50–75°C, going up to +85°C during hot

summer days, with pH conditions ranging from 9.6 – 10, and is achieved by dosing of ammonia solution. The operation of condensate polishers at these elevated temperatures and pH conditions often results to poor quality condensate (although condensate quality sometimes is within acceptable limits, it is often way above set targets, especially with sodium, chloride, and to a less extent sulfate leakage). This behavior of condensate polishers at elevated temperatures and pH poses a significant challenge to water - steam cycle chemical control in existing power plants, and is a potential challenge to the future direct dry cooled power plants, as more stringent water quality requirements are needed for safe running of these plants. A number of researchers have worked on ion exchange reactions equilibrium studies, extending over a wide range of solution composition, resin types, but narrow range of solution temperatures and pH [3,9,10,11]. There is no published data on ion exchange equilibrium studies carried out at low level counter ion concentrations (µg/L) and at elevated reaction temperatures and pH conditions resembling that of actual condensate polishing conditions.

1.2. PROBLEM STATEMENT

The equilibrium and thermodynamic information of ion exchange reactions play a critical role in predicting condensate polisher performance, and subsequent ion exchange process optimization. Over the years, studies on ion exchange equilibria has focused on reactions involving solutions of binary ion exchange systems at moderate reaction temperatures (≤ 35°C) and high level counter ion concentrations than at elevated reaction temperatures (≥ 50 ^{o}C) and low level counter ion concentrations (µg/L level). Such conditions are applicable in industrial processes such as condensate polishing fossil fuel power generating plants utilising direct air cooled condensers.

1.3. MOTIVATION

Understanding equilibrium and thermodynamic conditions of Na^{+}/RH^{+} exchange reaction at elevated reaction temperatures and pH would help power plant chemists make

meaningful predictions of condensate polisher performance, form a base for optimizing condensate polishing processes, and serve as a baseline when assessing ion exchange resin suitability for elevated temperature and pH condensate polishing. Condensate polishers operated optimally would result in better condensate quality, minimal chemistry induced plant component failures, and prolong plant components useful life. There is limited equilibrium and thermodynamic information on ion exchange reactions particularly Na^+/RH^+ carried out at elevated reaction temperatures (≥ 50^oC) and pH (≥ 9.6). Therefore, this work would be of valuable use to plant operators as well as to current and future designs of ion exchange resin condensate polishers operated at elevated temperature and pH.

1.4. KEY RESEARCH QUESTIONS

This research work seeks to establish answers to the following questions:

1.4.1. Determination of ion exchange equilibrium isotherms for the reaction; Na^+/RH^+ at temperature range; 50 – 90 ^oC using the batch experimental method

1.4.2. Characterization of equilibrium isotherm data using the heterogeneous approach:

a) Determination of the Selectivity coefficients, K_A^B, Corrected selectivity coefficient, K', as well as the Equilibrium quotient, $\Lambda_{Na\text{-}H}$ of the reactions under study

b) Establishing the effect of temperature and pH on the Na^+/RH^+ exchange reaction as well as on the performance of candidate ion exchange resins.

c) Modeling of ion exchange equilibria using non-linear Freundlich and Langmuir isotherm models

1.4.3. Determination of the reactions' Gibb's free energy change, ΔG, enthalpy change, ΔH, as well as the entropy change, ΔS.

1.5. SCOPE OF WORK AND WORK OUTLINE

The focus of this work was on Na^+/RH^+ exchange reaction carried out at varying reaction temperature and pH. The work done on this study consisted of the following:

1.5.1. Chapter two: *Literature review* **-** Fundamentals of ion exchange media, preparation of organic ion exchange resins, theory of condensate polishing, condensate polishing plant configurations, characteristics of ion exchange resins, and ion exchange equilibria

1.5.2. Chapter three: *Experimental Methods* **-** A detailed description of ion exchange resin sample preparation, chemical solutions preparation, experimental set-up, candidate resin ion exchange capacity measurements, and the determination of ion exchange equilibrium isotherms by a batch method.

1.5.3. Chapter four: *Results and Discussion* - Exchange capacity of candidate ion exchange resins, optimum solution – resin contact time, ion exchange equilibria as well as thermodynamic parameters

1.5.4. Chapter five: *Conclusion, Recommendations, and References*

2. CHAPTER TWO

2.1. LITERATURE REVIEW

2.1.1. Theory of the batch method approach

The application of the batch method on ion exchange equilibrium isotherm studies has been successfully applied by a number of researchers [10-16]. The batch method is a straight forward technique, where a predetermined quantity of resin is mixed with a known amount of solution containing counter ion(s) of interest, in a sealable container.

The system is kept under constant agitation, at constant temperature for a convenient period of time. The agitation speed is carefully determined and controlled to minimize the external mass transfer resistance and film diffusion [17,18]. Once equilibrium is reached, separation of the resultant solution can be accomplished by filtering off the resin from the solution and the filtrate analysed for counter ions concentration. According to Limousin *et al* [19], isotherm does not have any intrinsic thermodynamic definition, but depends on the conditions from which it is obtained. A number of authors observed a significant and nonlinear dependence of the solid/solution ratio on the degree of exchange, and the exchange rate is often observed to decrease with the solid concentration [19]. Although this method is straight forward, it is tedious as obtaining many data points from one resin sample may introduce errors due to loss of exchange capacity (especially anion resins) over a period of time. Desirably, new resin samples should be used per experiment to minimise errors associated with capacity loss, and precautions should be taken to ensure that separate experiments are conducted for many data points.

2.1.2. Fundamentals of ion exchange media

Ion exchange resins widely used in condensate polishing are of styrene–divinylbenzene (DVB) copolymer type [2,3,6]. These resins are produced as solid spheres with pore structures and ion exchangeable functional groups for ion exchange capability. In the year 1944, D'Alelio successfully developed cation exchange resins from copolymerisation

of styrene cross-linked with DVB [3]. Polystyrene - DVB anion exchange resins were developed in 1948, patented and introduced in 1949 [3]. The original design of condensate polishing system was introduced in 1954, following the invention of single bed of mixed cation and anion exchange resins in the early 1950's [3]. Strong acid cation exchange resin with sulfonic acid functional group ($—SO_3^-H^+$) and strong base anion exchange resins with quaternary amine functional group ($—N^+(CH_3)_3OH^-$) are chosen from others of similar functional group because, unlike others they exchange almost all types of cations and anions respectively [3,6].

There are two forms of strong base anion exchange resins; type I and type II [3,6]. Type I is of interest to condensate polishing as it consists of quaternary ammonium functional group with three methyl groups bonded to nitrogen atom ($—N^+(CH_3)_3OH^-$). This functional group has the highest basicity amongst commonly used anionic resins, and is normally used when very low reactive silica levels are targeted on treated condensate [20,21]. Type II resins also consist of a quaternary ammonium functional group but with two methyl groups and ethanol group bonded to nitrogen atom ($—N^+(CH_3)_2(C_2H_4OH)OH^-$). This functional group is less basic when compared to that of type I. Type II resin has high levels of reactive silica leakage when compared to type I. Type II resin is also limited with respect to temperature range (maximum application temperature is about 40^oC) [20,21].

The types of ion exchange resin mostly used in deep bed condensate polishing are gel or macroporous type resins [22]. Used mostly in the United States fossil and nuclear utilities [22], gel type ion exchange resins consist of homogeneous gel structure with homogeneous water distribution throughout the resin matrix [22,23]. Gel type ion exchange resins exhibit no porosity when dry, but when wet the porosity is of the order of 30Å or less [23-25]. Resin pore structure is a function of the distance between the polymer chains which vary with the crosslink level of the polymer, the polarity of the solvent, and the operating conditions [23]. Macroporous resins consist of pores of the order of 10^1 to 10^4 Å larger than that of gel resin [23]. The large pores act as a passage for ion transport to the inner parts of the resin bead [26]. Access to internal functional groups through larger resin

pores, and a large surface area gives advantage to macro porous resins over gel resins, giving them usage preference [2]. Furthermore, although macroporous resins have lower exchange capacity than gel type, they exhibit higher mechanical stability and more resistance to oxidation than gel type, making them good contenders for high condensate temperature application [27].

2.1.3. Preparation of organic ion exchange resins

Ion exchange resin manufacturing techniques employed by various resin manufacturers generally are closely guarded secrets and normally not revealed to end users as each manufacturer seeks competitive advantage over others. General ion exchange resin manufacturing techniques range from conventional suspension polymerization, and emulsion polymerization that yield small, but non-uniform resin beads to jetting suspension polymerization, polymerization through a vibrating orifice, and other modern manufacturing techniques that yield uniform particle size resin beads [2,28]. Figure 2 shows a schematic for a typical suspension polymerization synthetic procedure for styrene–DVB based ion exchange resins, and a Jetting process for uniform bead production [2,3,24]. Macroporous (also referred to as Macroreticular) resins are produced when styrene–DVB monomer mixture containing a free-radical initiator is mixed with an inert diluent or porogen which serves as a pore forming agent [2-3]. The reaction mixture is then added into the continuous phase under constant agitation to facilitate homogeneous droplets formation and distribution in the continuous phase. Copolymerization and crosslinking reactions take place in the monomer/diluent droplets and results in the formation of resin beads [2,3,24].

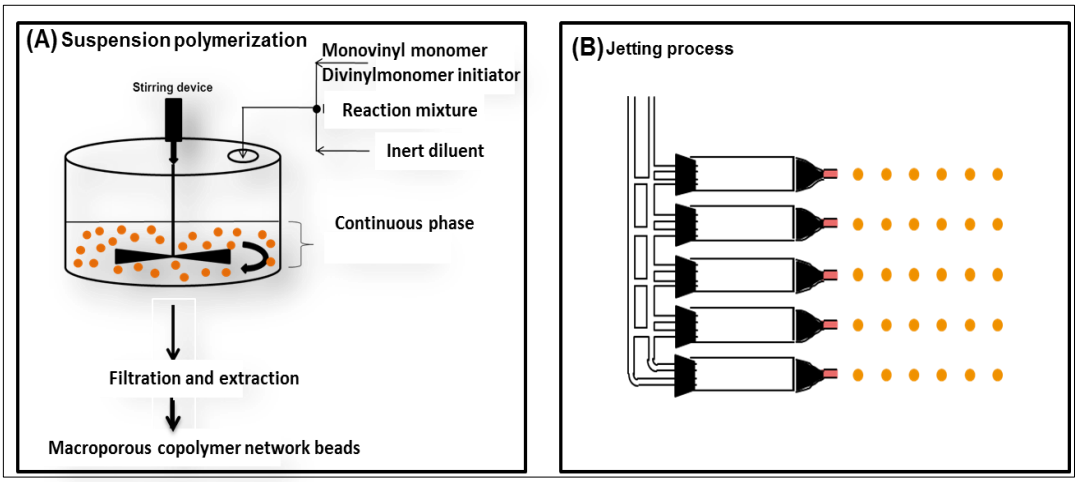

Figure 2: Typical ion exchange resin manufacturing processes

The beads are then extracted with an appropriate solvent to remove the soluble polymers and the diluent from the polymer network. The crosslinker (DVB) and monomer concentration in the reaction mixture, together with the type of the diluent are the main factors determining the porous structure and properties of the copolymer beads [25].

According to IUPAC, macrospores refer to pores of larger than 500 Å, whereas macroporous networks usually have a broad pore size distribution, ranging from 10^1 to 10^4 Å [22,25]. Sherrington [29], stated that the term 'macroporous' is however used to indicate a class of resins which have a permanent, well-developed porous structure even in the dry state. When the reaction mixture consists of styrene-DVB monomer and the polymerisation initiator only, the product generally consists of hard glassy transparent resin beads. When functionalised, the final product is a gel type ion exchange resin. Patented by Rohm and Haas Company [30], the jetting method is a continuous process mostly used to produce uniform size gel type resin beads. Uniform particle size resin offers advantage in that it provides increased exchange capacity, better resin separation for mixed bed operation, better flow and pressure characteristics, better chemical and rinse water utilisation, and simplicity since fewer resins are required [3].

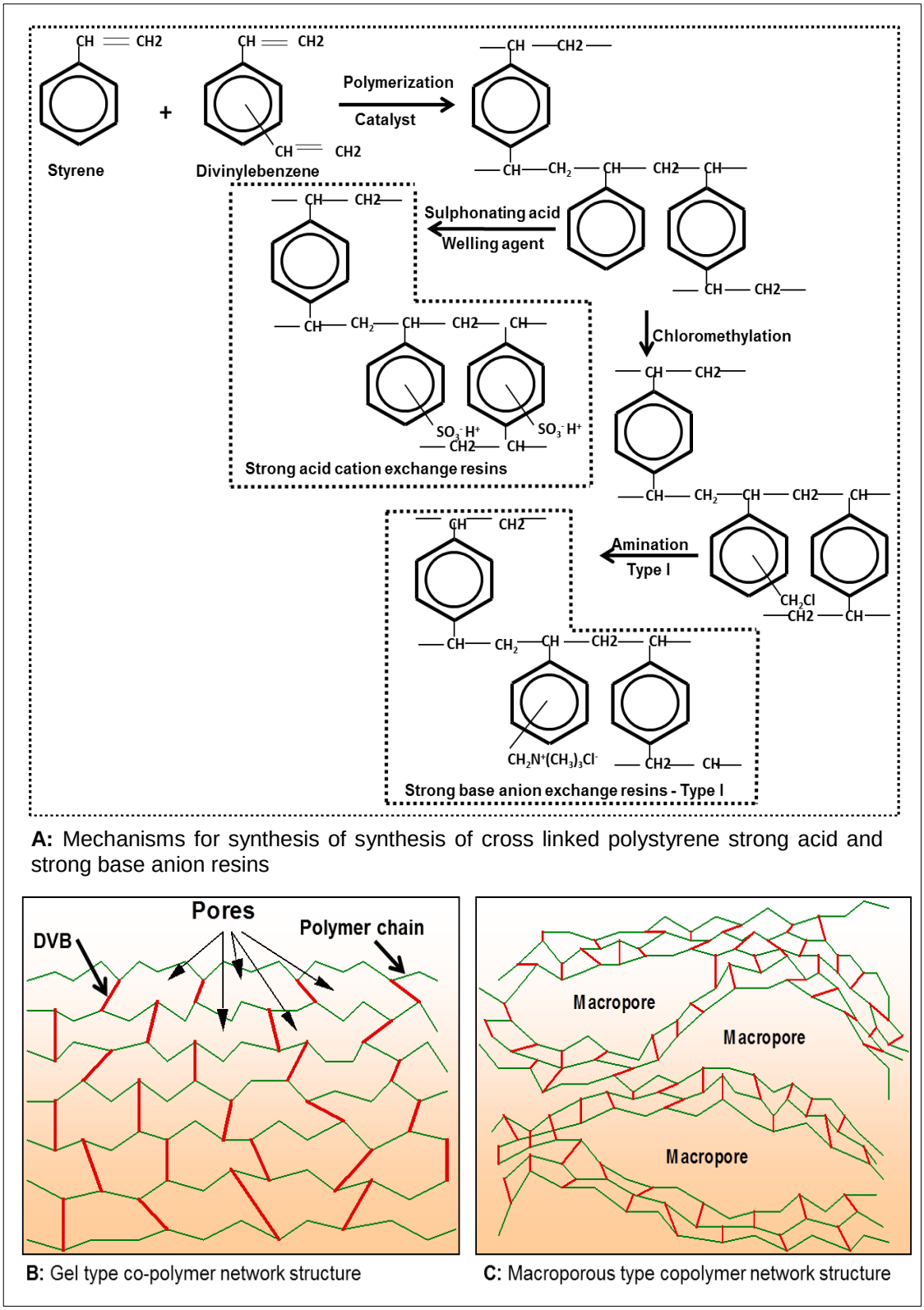

Figure 3: Schematic of styrene-DVB ion exchange resin copolymer network [31]

Strong acid cation exchange resins are based on sulfonic acid functionality which is achieved by a sulfonation process to apply the functional group, $-SO_3^-H^+$ as shown in Figure 3. Approximately one sulfonic acid group is present for each aromatic ring [2,3,25]. Cationic resins are produced in the hydrogen form (H^+) and rinsed as a final step in the manufacturing process to remove residual sulphuric acid and organic sulphur species. Strong base anionic resins are based on quaternary ammonium functionality. DVB crosslinked polymer is reacted in a two-step process; the chloromethylation and amination processes as shown in Figure 3. Anionic resins are produced in the chloride form and regeneration to the desired form ($-OH^-$) may be required for use in the condensate polishing.

2.1.4. Characteristics of ion exchange resins

Ion exchange resin suitability for use in a condensate polishing system is subject to its individual characteristics, the design parameters of the system within which it will operate, the operational philosophy of that particular system, and the resin cost [2,3]. Ion exchange reaction distribution coefficient should be sufficiently favourable towards the incoming ion to make the process feasible. Below are ion exchange resin properties requirements for separate bed condensate polishing [1-3]:

a) **Appropriate porosity:** Porosity ensures that the greater part of the resin is available for ion exchange purpose. It is the property of the resin that allows counter ions to diffuse in and out of the resin bead. It can be determined as the ratio of the volume of pores to the total volume of the resin bead. Resin porosity increases with a decrease in resin apparent density. Porosity of the resins is a function of percentage divinylbenzene and the amount of diluents used during the manufacturing process.

b) **High mechanical stability:** Mechanical stability relates to the ability of resins to handle loads such as high flow rates, deep bed depth and osmotic shock. Ion exchange resins may be subject to abnormal operating conditions from time to time and good ion exchangers should withstand such conditions.

c) **High physical stability:** Physical stability relates to the ability of resins to handle the operating temperature range. Strong acid cation exchange resins can withstand temperatures up to about 105°C whist strong base anion exchange resins can withstand temperatures up to about 60°C. Operating beyond these temperatures may result in resin degradation, loss of functional groups (especially strong base capacity) and shortening of the useful life of resins.

d) **High chemical stability and low organic leachable:** Chemical stability relates to the ability of resins to resist degradation due to heavy metals such as Iron and Copper particulates generated from the Water- Steam cycle due to corrosion. Organic molecules are normally released by new cation resins on installation, and on a low level basis during periods of high condensate temperature operation. Another source of Organics may be make-up water. These molecules have a potential to foul the downstream anion resins, and decomposing at boiler temperatures to form Organic acids, mainly acetate and formate. Because of their acidic character, they may help to provide conditions in which more aggressive agents (e.g. chloride and sulfate) may initiate corrosion. Ion exchange resins with high chemical stability will leach low levels of organics

e) **Rapid ion exchange Kinetics:** Kinetics refers to the rate at which ion exchange reactions occur. Resin kinetics has a great influence on resin performance. Resin bead size, bead surface and influent flow rate and temperature are among the critical parameters to be controlled for high rate of reaction kinetics. Too low ion exchange rate may result in poor quality condensate effluent, whilst too high ion exchange rate may lead to kinetic leakage.

f) **High total capacity:** Total capacity equals number of exchange sites in a mass or volume of resin. Operating capacity is generally more important than total capacity as not all exchange sites may be available for ion exchange. Nevertheless, resins with high total capacity are more likely to have high operating capacity as well.

g) **High operating Capacity:** Operating capacity refers to the number of exchange sites available for ion exchange purpose. As has been mentioned above, the actual operating capacity is usually lower than the total capacity. Operating capacity is affected by total and relative ion concentrations, charge density of ions, flow rate, temperature, pH, regeneration efficiency and equipment design.

h) **Moisture holding Capacity and percentage Cross linkage:** Moisture holding capacity refers to the capacity of ion exchange resin beads to retain water in its fully swollen state. Dry resin beads placed in water take up water and increase in volume. The degree of swelling primarily depends on the percentage cross-linkage. The greater the cross-linkage, the lesser is the swelling. Typical moisture holding capacity for strong acid cation resins and strong base anion resins range is 52-58% (H^+ form) and 66-75% (OH^- form) respectively. Higher percentage cross linkage also increases the mechanical strength of the resins, and resin relative affinity towards the counter ions.

i) **Particle size and particle size distribution:** Measured for specific form of resin, particle size has impact onion exchange kinetics, mixed bed separation, and particulate filtration. Uniformity coefficient indicates particle size distribution or closeness of all beads to the same size. The closer the resin beads are to one another, the more uniform is the particle size, the faster the reaction kinetics, and the lower the pressure drop across the bed.

j) **Low levels of metal impurities:** Metal impurities may be present from the newly manufactured resins. Low levels of metal impurities reduce the potential for accelerated resin degradation and unexpected interactions.

k) **High Selectivity:** Selectivity relates to equilibrium conditions between counter ions in solution and on resin. It varies from ion to ion and to some extent from one resin to another. Ion exchange resins should exhibit high selectivity towards undesirable ions in the influent for better quality effluent.

2.1.5. Theory of condensate polishing

Unlike conventional demineralised water treatment processes which treat water of chemical quality near that of raw waters (typical TDS of 350 mg/L), the primary purpose of condensate polishers is to remove dissolved ionic impurities from steam condensate and make-up water (chemical quality of low to sub µg/L level). The impurities of concern are usually ionic sodium, chloride, sulphate, silica, carbonate/bicarbonate, and organic carbon. Ionic impurities such as calcium, magnesium, potassium, etc. are of equal importance but in the high purity fluids of interest (water - steam cycle), the risk of their contaminants is very low. Equation 2.1 below shows a typical reversible cation exchange reaction involving counter ions A^+ and B^{+z}, where *R* represents the functional group which is covalently bonded to a polymer network or solid phase.

$$\mathbf{zR{-}A^{+} + B^{+z} \leftrightharpoons Rz{-}B^{+z} + zA^{+}} \qquad \textbf{(2.1.)}$$

Earlier researchers on ion exchange reactions of organic exchangers identified the possible rate limiting steps to be coupled diffusion of counter ions in the external solution phase, coupled diffusion of counter ions within the resin, and chemical reaction at the site of the functional group within the resin [11]. According to Raitt and Giannelli [11,22], chemical reaction within the resin in all but a few special cases is very fast and rates of exchange can be interpreted as a function of the two forms of coupled diffusion. The secondary purpose of condensate polishers is filtration of corrosion particulates generated from the water-steam cycle [2,3,8]. In the absence of pre-polishing filters, corrosion particulates are filtered off from the condensate by ion exchange resins [3]. Filtration in deep bed condensate polishers is achieved through depth filtration mechanism [3,22]. Depth filtration is either by particulate bridging within resin pores (mechanical filtration), electrostatic attraction, or both [3,22]. Corrosion particulates are of great concern in power plants, especially in direct dry cooled power plants consisting of large surface area air cooled condensers with mild steel condenser tubing [8]. According to the Electric Power Research Institute (EPRI) [32], condensate polishing offers the following advantages;

eliminate/reduce delays at start-up of units attributable to inappropriate water chemistry, reduce condensate dumping during unit start-up which is often carried out to accelerate the achievement of acceptable condensate quality, reduce use of blowdown on drum boilers, eliminate/reduce the need for chemical cleaning of water - steam cycle, provide protection of water - steam cycle against the effect of impurity ingress incidents, offers the ability to safely use simpler and more effective forms of water treatment on both drum and once-through steam generators, and provide a significant reduction in the rate in which turbine efficiency deteriorates owing to chemical deposition on the blade surface.

2.1.6. Condensate polishing plant configurations

The selection of the appropriate condensate polishing configuration depends on plant operating parameters, mainly pressure and temperature [2,5]. Normally, condensate polishing is not necessary on low pressure boilers such as those operating below 4.1MPa [6]. In these boilers, feed water is treated only to prevent hard scale formation and corrosion in the boiler drum. An optimally operated conventional demineralised water treatment plant can easily achieve this. Furthermore, boiler water salts are kept from the steam phase by control of chemical carryover and by boiler drum blowdown [6]. As pressure increases beyond 4.1MPa, the materials of construction become intolerant of dissolved solids and full flow deep bed/powdex condensate polishing becomes necessary [6]. Listed below are some of the widely used ion exchange condensate polisher configurations [2-4]:

a) Condensate scavenger configuration

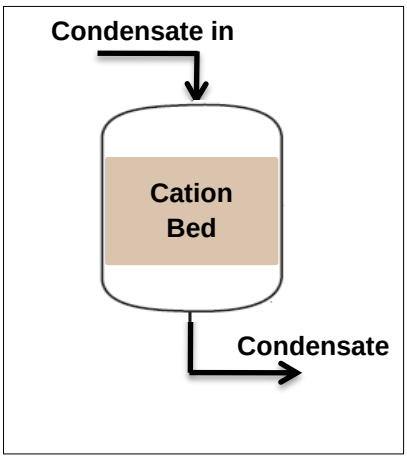

Figure 4: Condensate scavenger configuration

Single cation beds are not used in modern high pressure plant. Mostly found on industrial plants (low to medium pressure boilers) rather than power utility, they are designed mainly to remove corrosion particulate from the condensate. Normally, deep bed of macroporous strong acid cation exchange resin is used as in-depth filter of corrosion products. Some cations such as hardness ions are also interchanged with the cation on the resin. While the H^+-form usage would result in a best neutral effluent, more probably an acid effluent, they are widely operated in the Na^+ form as a condensate softener.

b) Cation/Anion mixed bed configuration

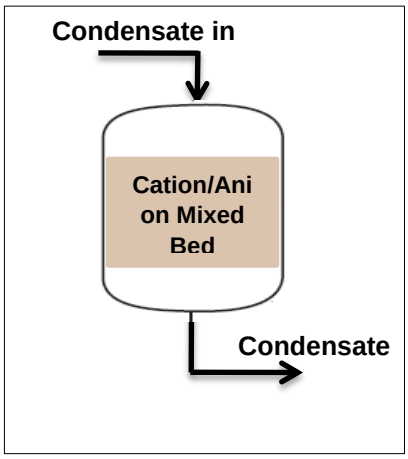

Figure 5: Cation/Anion mixed bed configuration

This is the most common ion exchange configuration used in modern high pressure plants. The system consists of mixed bed of strong acid cation exchange resin and strong base anion exchange resin. It produces very high-quality demineralized water as ion leakage from one resin is quickly removed from the water by the other. Effective condensate polishing and deep-bed, in-depth filtration is accomplished by maintaining the flow rate high enough to prevent channelling and corrosion products from accumulating at the surface (typical flow rate is 120m^3/h). While they are widely operated with cation and anion resins in the H^- and OH^- form respectively, the choice of resin ionic form depends on the chemistry of the circulating water system.

c) Lead cation/Mixed bed configuration

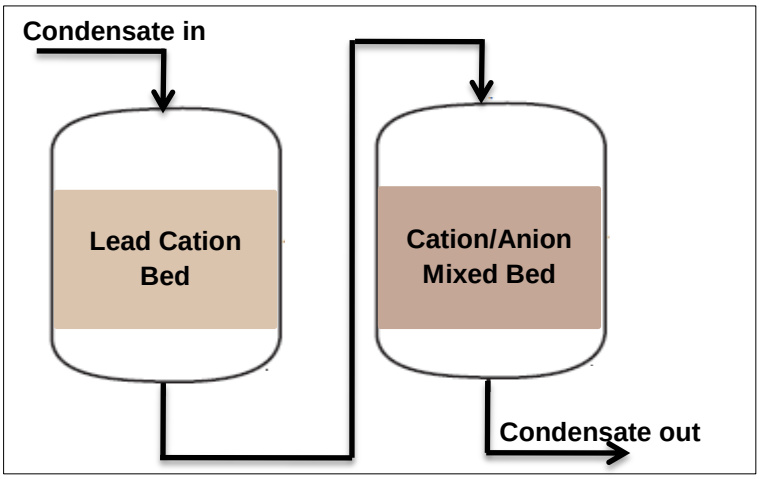

Figure 6: Lead cation resin-mixed bed configuration

In plants where ammonia or other volatile amine is used to adjust feed water pH, the amine carries overhead and transports with the steam. Because the amine is present in substantial amount, when the amine-laden steam condenses it creates a condensate stream with high amine levels. This amine is readily exchanged onto the cation resin during condensate polishing. Eventually, the cation resin becomes exhausted to the amine form, and the amine breaks through into the condensate polisher effluent stream. The lead cation provides a means to remove amines by treating the condensate with a hydrogen form cation resin before it reaches the mixed bed. In this way, corrosion particulate and amine load is removed off the mixed bed, extending their run period.

d) Separated bed configuration

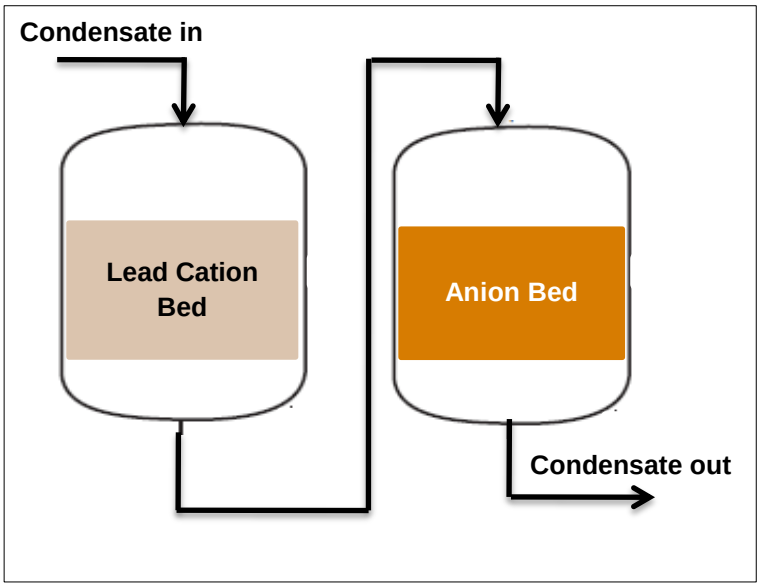

Figure 7: Separate bed configuration

Used in modern high pressure plant, separate bed offers advantages over the mixed bed configuration in that; it eliminate inefficiencies associated with resin separation before regeneration, and eliminate other mixed bed problems such as the partial separation of the mixed beds in service vessels. The use of separate beds of cation and anion resins thus simplifies reliable operation in the ammonium form. However, the operational advantages of separate bed polishers are offset by a reduction in the quality of the polished water when operating in the conventional H^-/OH mode relative to that achievable from mixed beds.

e) Tripol configuration

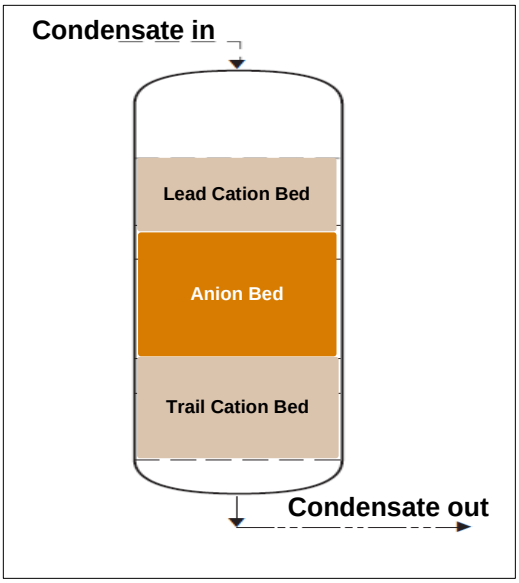

Figure 8: Tripol configuration

This is a single vessel design with compartments that contain separate layers of cation, anion and cation resins. The resins are never mixed, with each resin compartment going to its own external regeneration vessel on exhaustion. This system setup ensures that leakage from the lead cation is polished in the trailing cation resin.

f) Triobed configuration

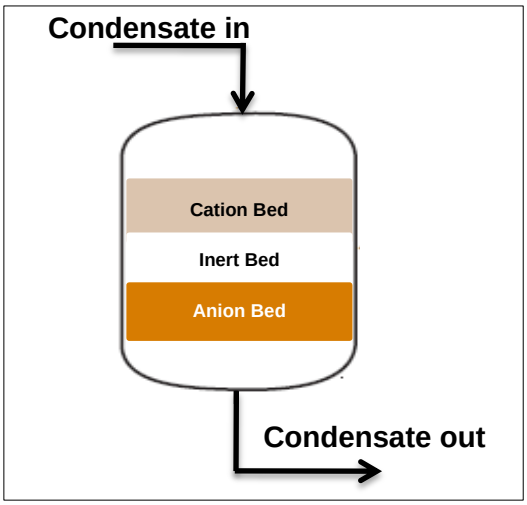

Figure 9: Triobed configuration

This is a single vessel configuration where, in addition to the cation and anion bed, an intermediate layer of inert resin is introduced. The density of anion, cation, and inert resins is such that, when the resins are separated by decompaction it is located between the anion and cation resins. The particle size range of the three resins is designed such that the separation into three layers is virtually perfect. The Triobed process offers advantages in that it does not require any special vessel design, can be used with internal regeneration, and the separation into three layers prevent any contamination of one exchanger by the reagent used to regenerate the other.

Condensate polishers function well at moderate temperatures, 25°C–40 ^{o}C [33]. Operation at elevated temperatures places a strain on ion exchange resins, especially on strong base anion exchange resins. Cation polishers can withstand condensate temperatures of up to about 105 ^{o}C, whilst anion polishers have a 60 ^{o}C limit [2,3,6]. The high ammonia concentration dictates that the cation resin be operated in the ammonium form. At high ammonia concentration, cation bed operating in hydrogen form will exhaust too rapidly for regeneration turn around. Constant operation of condensate polishers at higher than

recommended condensate temperatures also accelerate resin degradation, reducing their useful life.

2.1.7. Ion exchange equilibria

Ion exchange equilibrium has been a subject of interest to many researchers [13,33,34,35,36,37]. Ion exchange equilibrium investigations lead to understanding the behaviour of ion exchange resins of interest, towards ions of interest under specific chemical and physical conditions. This information is critical to Ion Chromatography Scientists and ion exchange based Water Treatment Plant design Engineers and Scientists in order to provide equipment/plants that are fit for purpose. The heterogeneous approach to ion exchange phenomena assumes that the maximum uptake of ions by an ion exchanger is limited only to the number of functional groups in the ion exchanger, and there is no uptake of ions of the same charge sign as the functional group [37]. Furthermore, it is assumed that the amount of solvent in the ion exchanger is independent of the ionic form of the exchanger. A heterogeneous approach to experimental ion exchange data usually consists of thermodynamic models for characterizing aqueous phase thermodynamics and empirical correlation of the non-ideality of the solid solution [37]. According to Søren [37], the assumption of the model holds for the prediction and the correlation of equilibria between ion exchange resins with a high degree of cross linking and aqueous solutions with low to moderate concentrations of ions. The ion exchange equilibrium of reaction 2.1 may be represented in a number of ways, with ion exchange equilibrium isotherm(s) being the most common [38,39,73]. Ion exchange equilibrium isotherm refers to the amount of counter ions in the ion exchanger, and in the external solution, under equilibrium conditions, and at constant temperature. Isotherm data, irrespective of the way it is determined, should be fitted with isotherm models and/or empirical methods to understand the extent and degree of reaction favorability [17]. Previous researchers proposed a number of ion exchange equilibrium characteristic quantities, all of which may be derived from the ion exchange isotherm [38,39]. Selectivity coefficient K_A^B, Thermodynamic equilibrium constant K_T, Distribution

coefficient K_D, and Separation factor $\boldsymbol{\alpha_{A/B}}$ are among the commonly used parameters for characterizing ion exchange equilibria [17, 39]. Although these characteristic quantities may be dissimilar, they all provide quantitative expressions for ion preference by the ion exchange resins. Below is a description of the above equilibrium characteristic properties:

2.1.7.1. Selectivity coefficient, $\mathbf{K_A^B}$

Selectivity coefficient is a practical equilibrium coefficient obtained by the application of the law of mass action to ion exchange reaction and characterizing quantitatively the ability of an ion exchanger to select one of two ions present in the same solution [12,16,40]. Selectivity coefficients are not true constants but vary with test conditions (temperature, ion concentration), resin type, and types of ions [18,37,41]. However, in ion exchange equilibrium studies, it is common to use selectivity coefficient in place of thermodynamic equilibrium constant [31,39,42]. Selectivity coefficient for equation 2.1, based on equilibrium concentrations of counter ions can be expressed according to the following equation [13,43,44,45]:

$$K_A^B = \left(\frac{q_B}{C_A}\right)\left(\frac{C_A}{q_A}\right)^z \qquad \textbf{(2.2)}$$

where;

$$\mathbf{q_B\,(or\ q_A)} = \frac{\mathbf{V\left(C_{initial} - C_{equilibrium}\right)}}{\mathbf{W_{Resin}}} + \mathbf{C'_B\,(or\ C'_A)} \qquad \textbf{(2.2.1)}$$

C_A and C_B (meq/l) are counter ions concentrations in equilibrium solution, q_A and q_B (meq/g) is concentrations of counter ions in the resin phase. $C_{initial}$ and $C_{equilibrium}$ (meq/l) are the initial and equilibrium counter ion concentrations in the solution phase, V (L) is the solution volume, and W_R (g) is the weight of the resin. C'_A and C'_B (meq/l) is the initial counter ions concentrations in the resin phase. The units of resin capacity are meq/g rather than eq/l are chosen to minimize analysis errors associated with volume measurements.

Selectivity coefficient obtained by equation 2.2 is generally not a constant over the whole range of ion exchange isotherm as it is a function of counter ions concentration rather than activities. Alternatively, equation 2.2 can be expressed in terms of equivalent ionic fractions as follows [18,46,72]:

$$\mathbf{K}_{\boldsymbol{A}}^{\boldsymbol{B}} = \left(\frac{\mathbf{X'}_{\boldsymbol{B}}}{\mathbf{X}_{\boldsymbol{B}}}\right)\left(\frac{\mathbf{X}_{\boldsymbol{A}}}{\mathbf{X'}_{\boldsymbol{A}}}\right)^{\boldsymbol{z}} \qquad \textbf{(2.3)}$$

Where:

$$\mathbf{X'_A\,(or\ X'_B)} = \frac{\mathbf{q_A\,(or\ q_B)}}{\mathbf{Q}} \text{ ; and, } \mathbf{X_A\,(or\ X_B)} = \frac{\mathbf{C_A\,(or\ C_B)}}{\mathbf{C_T}} \qquad \textbf{(2.3.1)}$$

$X'_{A/B}$ and $X_{A/B}$ are the equivalent fractions of counter ions in resin and aqueous solution respectively. Q (meq/g) is the total exchange capacity of the resin, and C_T (meq/l) is the total concentration in the solution. On exchange reactions involving counter ions of different valence numbers, K_A^B depends on the counter ions concentration scale of choice and concentration units must be clearly stated [33,40]. Interactions between ions in aqueous solution are so strong such that approximation of replacing activities by molalities is valid only in dilute solutions of less than 0.001 mol/kg total ion concentration, and in practice work activities should be used [47]. To take into account the non-ideal behaviour of the equilibrium solution, equation 2.3 may be corrected for the solution phase activities (γ_X), and molalities (m) in place of mole fraction to read as follows [33]:

$$\mathbf{K'} = \left(\frac{\mathbf{m'}_{\boldsymbol{B}}}{\mathbf{m_B}\gamma_{\mathbf{B}}}\right)\left(\frac{\mathbf{m_A}\gamma_{\mathbf{A}}}{\mathbf{m'}_{\boldsymbol{A}}}\right)^{\boldsymbol{z}} \qquad \textbf{(2.4.)}$$

2.1.7.2. Separation factor, $\alpha_{A/B}$

For ion exchange reactions involving counter-ions of equal charge, selectivity coefficient can be defined by the separation factor, $\alpha_{A/B}$ which is a ratio of the distribution of counter ion B^{+z} between solid and liquid phases (X'_B/X_B) to the ratio of the distribution of counter ion A^+ between phases (X'_A/X_A). However, for exchanging ions of unequal valence the separation factor is not equivalent to the selectivity coefficient. The separation factor for ion B^{+z}against ion A^+can be determined from the following equation [48]:

$$\alpha_A^B = \frac{q_B C_A}{C_B q_A} \qquad \textbf{(2.5.)}$$

And the relationship between selectivity coefficient and separation factor is given by:

$$K_A^B = \alpha_A^B \left(\frac{C_A}{q_A}\right)^{|\pm z|-1} \qquad \textbf{(2.6.)}$$

where C_A is the aqueous phase concentration of the pre-saturation ion in *eq/L*, and q_A is the resin phase concentration of the pre-saturation ion, and *z* is the charge on the ion.

2.1.7.3. Distribution coefficient, K_D

K_D is the distribution coefficient of B^{+z} in equilibrium ion exchange resins and external solution. For a reaction involving100% $R\text{-}A^+$ form resins and a very dilute solution of *AY* containing trace amount of B^{+z}, at equilibrium, $[R\text{-}A^+]$ and $[A^+]$ will not vary significantly from their initial values. If K_D is greater than unity then there is a greater uptake of B^{+z} than A^+ by the ion exchange resins relative to their concentrations in the solution and vice versa. To determine the order of selectivity of $R\text{-}A^+$ towards a series of ions such as B^{+z}, X^{+z} and Y^{+z}, separate ion exchange reactions are conducted using trace amount of ions of interest and K_D computed [11,12]. K_D values provide a useful indication of the selectivity behaviour of resin towards the specified ions [12]. The use of K_D is a special case of

equation 2.4 where the counter ion of interest is present in a trace amount. Values of K_D obtained at concentrations other than trace ones will not be strictly comparable with those determined at trace concentrations of those ions [12].

2.1.7.4. Thermodynamic equilibrium constant, K_T

Equation 2.1 can be described by the law of mass action using the counter ions activities to give thermodynamic equilibrium constant, K_T [23,43]:

$$\mathbf{K}_{\boldsymbol{T}} = \left(\frac{\bar{a}_{\boldsymbol{B}}}{a_{\boldsymbol{B}}}\right)\left(\frac{a_{\boldsymbol{A}}}{\bar{a}_{\boldsymbol{A}}}\right)^{\boldsymbol{z}} = \left(\frac{\gamma'_{\boldsymbol{B}}\mathbf{m}'_{\boldsymbol{B}}}{\gamma_{\boldsymbol{B}}\mathbf{m}_{\boldsymbol{B}}}\right)\left(\frac{\gamma_{\boldsymbol{A}}\mathbf{m}_{\boldsymbol{A}}}{\gamma'_{\boldsymbol{A}}\mathbf{m}'_{\boldsymbol{A}}}\right) \qquad \textbf{(2.7)}$$

and;

$$\mathbf{K}_{\boldsymbol{T}} = \mathbf{K}'\left(\frac{\gamma'_{\boldsymbol{B}}}{\gamma'^{\boldsymbol{Z}}_{\mathbf{A}}}\right) \qquad \textbf{(2.8)}$$

where $\bar{a}_B$, $\bar{a}_A$ and a_A, a_B are the activities of counter ions A^+ and B^{+z} in solid and liquid phases respectively, and $\gamma'_{A/B}$, $\gamma_{A/B}$ and $m'_{A/B}$, $m_{A/B}$ are counter ions activity coefficients and molalities in solid and solution phases respectively. Equation 2.8 shows the correlation between the thermodynamic equilibrium constant, K_T and the corrected selectivity coefficient, K'. The equilibrium constant, K_T is an integral quantity characteristic of the whole isotherm and is a major indicator of the selectivity of resins with respect to counter ions.

K_T determination may be complex in that it requires determination of counter ion activities in both solid and liquid phase. Determination of ionic activities requires knowledge of activity coefficients in both liquid solution and within the resin bead.

2.1.7.5. Solution phase modelling

a) Pitzer model (PT) [35]

The Pitzer equations for determining activity coefficients of particular cation and anion ion in solution are:

$$\ln\gamma'_{A/B} = Z^2_{A/B}F + \sum_a m_a (2B_{Ma} + ZC_{Ma}) + \sum_c m_c (2\phi_{Mc} + \sum_a m_a m_a \psi_{Mca}) + \sum_a \sum_{a'} m_a m_{a'} \psi_{Maa'} + |Z_M| \sum_c \sum_a m_c m_a C_{ca} \quad \textbf{(2.9)}$$

where;

$$F = A_\phi \left[\frac{\sqrt{I}}{1+b\sqrt{I}} + 2/b \ln(1 + b\sqrt{I}\,)\right] + \sum_c \sum_a m_c m_a B'_{ca} + \sum_c \sum_{c'} m_c m_{c'} \phi'_{cc'} + \sum_a \sum_{a'} m_a m_{a'} \phi'_{aa'} \quad \textbf{(2.9.1)}$$

and;

$$Z = \sum_i mi|zi|,\ B^\phi_{ca} = B_{ca} IB'_{ca},\ \text{and}\ \phi^\phi_{cc'} = \phi_{cc'} I\phi'_{cc'} \quad \textbf{(2.9.2)}$$

The subscript M refers to counter ion A or B, *c* is the cation, *a* and *a'* are anions, m*i* is the molality of ion, and z refers to the counter ion charge. F is the quantity defined by the solution ionic strength, *I*, the short-range interaction parameter, B, the interaction between ions of like sign parameter, ϕ, and B' and ϕ' are the ionic strength derivatives of B and ϕ.

b) The Extended Debye-Hückel Equation

The Extended Debye-Hückel Equation is an extension of the Debye-Hückel limiting law to cater for concentrated electrolyte solutions [47,49,72]. The Extended Debye-Hückel Equation is the most frequently applied model and is defined as:

$$-\log_{10}\gamma_i = \frac{Az_i^2\sqrt{I}}{1+Ba_i\sqrt{I}} = \frac{\left((1.825\times10^6)(\varepsilon T)^{-3/2}\right)z_i^2\sqrt{I}}{\left(1+\left(50.3(\varepsilon T)^{-1/2}\right)a_i\sqrt{I}\right)} \quad \textbf{(2.10)}$$

where;

$$\text{Ionic strength},\ I = \frac{1}{2}\sum Ciz^2 \quad \textbf{(2.10.1)}$$

The quantity, $a_i$is an adjustable parameter (angstrom) corresponding to the size of the hydrated ion [49]. The parameter ε is a dielectric constant of water, z_i is the ion charge, Ci ion concentration and, T is the temperature (^oC). Equation 2.10 is applicable in dilute solutions with total ionic strength of < 10^{-1}mol.kg^{-1} [84]. Margules, Van Laar, UNIQUAC are some of the several other expressions that can be found in literature for liquid phase modelling.

2.1.7.6. Resin phase modelling

While activity coefficients of ions in solution can be determined with certainty, activity coefficients determination in solid (resin) phase may be much more complex. Few methods are available in literature for activity coefficient determination in the solid phase.

a) Lokhande et al approach [50]

According to the theory of ionic equilibrium, zero ionic concentration can be regarded as the standard state when the mean activity coefficient becomes unity. However, such standard state cannot be chosen for counter ions in the resin phase as the ion exchange resins will always contain ions to its full exchange capacity. Lokhande *et al* defined the standard state of ion exchange resin to be that of resin completely in univalent ionic form (H^+ - form), and referred the resin at any other composition to the standard state. When plotting the corrected selectivity coefficient versus the equilibrium concentrations of the challenging counter ions in solution, extrapolating such a curve to zero equilibrium concentration of the challenging counter ion in solution give the equilibrium constant in the standard state, K_{std}. Having obtained K_{std}, the activity coefficient ratio $\gamma'_B / \gamma'^{z}_A$ at finite concentration of challenging counter ion in solution can be obtained as the ratio of K_{std}/K'. K_T can then be determined from equation 2.8.

b) The Wilson model

A more complex approach can be followed to estimate the activity coefficients of counter ions in the resin phase. The models of Wilson, Margules, NRTL, etc. are among the

commonly used models solid phase activity coefficients estimation [43]. The Wilson equation was originally formulated to account for non-ideality in vapour-liquid systems, and has been mostly used to define the resin phase activity coefficients [34]. The Wilson equation is defined as:

$$\boldsymbol{Ln\gamma'_i = 1 - Ln\left(\sum_{j=1}^{M} y_j \Lambda_{ij}\right) - \sum_{k=1}^{M}\left(\frac{y_k \Lambda_{ki}}{\sum_{j=1}^{M} y_j \Lambda_{kj}}\right)} \qquad \textbf{(2.11)}$$

where Λ_{ij} and Λ_{ji} are binary interaction temperature-dependent parameters. The interaction parameters of a binary system can also be used for more than two component systems. For a binary *ij* system, equation 2.11 can be simplified to:

$$\boldsymbol{Ln\gamma'_i = -Ln\left(y_i + y_i \Lambda_{ij}\right) + y_i\left[\left(\frac{\Lambda_{ij}}{y_i + y_j \Lambda_{ij}} + \frac{\Lambda_{ji}}{y_j + y_{Bi} \Lambda_{ji}}\right)\right]} \qquad \textbf{(2.12)}$$

Perona [51], extracted values of the interaction parameters from the binary data by substituting equation 2.11 into equation 2.4 which, in their case is defined as equilibrium quotient gives:

$$\boldsymbol{LnK' = LnK_T - z_B\left[1 - Ln(y_B + y_A \Lambda_{B-A}) - \left(\frac{y_B}{y_B + y_A \Lambda_{B-A}} + \frac{y_A \Lambda_{A-B}}{y_A + y_B \Lambda_{A-B}}\right)\right] +}$$

$$\boldsymbol{z_B\left[1 - Ln(y_A + y_B \Lambda_{A-B}) - \left(\frac{y_A}{y_A + y_B \Lambda_{A-B}} + \frac{y_B \Lambda_{B-A}}{y_B + y_A \Lambda_{B-A}}\right)\right]} \qquad \textbf{(2.13)}$$

Equation 2.13 contains three unknown parameters;K_T, Λ_{B-A}, and Λ_{A-B}. According to Addison [34], when more than three data points are available, a search procedure can be used to find the set values of K_T, Λ_{B-A}, and Λ_{A-B} that minimize the sum of the squares of the deviations (R) between experimental corrected selectivity coefficient (equation 2.4) and theoretical corrected selectivity coefficient for all points.

2.1.7.7. Thermodynamic parameters

In order to understand the effect of temperature on ion exchange reactions, thermodynamic parameters such as Gibb's free energy change *ΔG*, enthalpy change *ΔH,* and entropy change *ΔS* can be determined from the following thermodynamic relationship [51].

$$\boldsymbol{\Delta G = \Delta H - T\Delta S} \qquad \textbf{(2.14)}$$

where ΔG is the Gibbs free energy change, ΔH is the enthalpy change, T is the reaction temperature in Kelvins, and ΔS is the entropy of the ion-exchange process. In order to obtain the relation of the selectivity and temperature, the Van't Hoff equation can be used to calculate the thermodynamic parameters. The above thermodynamic parameters can be obtained from the Van't Hoff equation [52]:

$$\mathbf{LnK'} = \left(\frac{\mathbf{\Delta S}}{\mathbf{R}}\right) - \left(\frac{\mathbf{\Delta H}}{\mathbf{RT}}\right) \qquad \textbf{(2.15)}$$

Subscript *T* and *R* have their usual meaning.

2.1.8. Langmuir Isotherm model

Ion exchange equilibria may be modelled using the Langmuir and Freundlich isotherm models [53,54]. Langmuir and Freundlich models are the most commonly used and are widely considered as the bases for studying adsorption characteristics of adsorbent used in water and wastewater [52]. The Langmuir isotherm is valid for monolayer sorption onto a surface with a finite number of identical sites that are homogeneously distributed over the surface of the sorbent [18,46]. The following assumptions were used in the derivation of the Langmuir isotherm model [47,55,56,57,58]:

a) Molecules are adsorbed at a fixed number of well-defined localized sites.

b) Each site can hold one adsorbate molecule.

c) All sites are energetically equivalent.

d) There is no interaction between molecules that adsorbed on adjoining sites.

The non-linear Langmuir isotherm can be represented as follows:

$$q_L = \frac{K_L\, q_{max} Ce}{1 + K_L Ce} \qquad \textbf{(2.16.)}$$

K_L is a constant of the Langmuir isotherm, q_L is the maximum uptake of counter ion on the exchanger adsorbed at equilibrium, *Ce* is the equilibrium concentration of counter ions in solution, and q_{max} is the maximum adsorption capacity of adsorbent. The essential characteristics of the Langmuir isotherm can be expressed by a dimensionless constant called the equilibrium parameter R_L, which is described by the following equation [9,18]:

$$R_L = \frac{1}{1 + K_L C_0} \qquad \textbf{(2.17)}$$

C_o is the initial concentration of counter ion in solution. The value of R_L indicates the type of isotherm. The isotherm is unfavourable when $R_L > 1$, is linear when $R_L = 1$, is favourable when $0 < R_L < 1$, and is irreversible when $R_L = 0$.

2.1.9. Freundlich Isotherm model

The Freundlich isotherm differs from the Langmuir isotherm in that it is based on the assumption that sorption takes place on a heterogeneous surface on which the binding sites are not equivalent or independent [18]. Nonlinear Freundlich isotherm is defined by the following equation [46,52,55]:

$$q_F = K_F C_e^{\,1/n} \qquad \textbf{(2.18)}$$

K_F and 1/n are system specific empirical constants. K_F is an indicator of adsorption capacity whilst *1/n* is a measure of intensity of adsorption. The higher the 1/n value, the more favourable is the adsorption [46,55]. For $n = 1$, the partition between the two phases is independent of the concentration. Generally, $n < 1$ or $1/n < 1$ corresponds to a normal L - type Langmuir isotherm, while $n > 1$ is indicative of a cooperative sorption, which involves strong interaction(s) between the molecules of adsorbate [18].

2.1.10. Langmuir and Freundlich model parameters determination

Following experimental isotherm data determination, the application of isotherm models is necessary to describe data in the universally recognised form. A considerable number of curve fitting tools are available for fitting model equations to experimental data. Following fitting of isotherm model to experimental data, error analysis (goodness of fit) is necessary to determine the isotherm that gives the best fit [55,56]. Linear regression analysis has often been used for this purpose [56]. In recent years, several other error analysis methods have been developed. Outlined below are some of the functions used to measure the goodness of fit of isotherm models to experimental data:

2.1.10.1. The sum of squares, SS

The sum of squares is described by the function [57]:

$$\mathbf{SS} = \sum_{\mathbf{n=1}}^{\mathbf{n}} [\mathbf{q_{exp}} - \mathbf{q_{model}}]^2 \qquad \textbf{(2.19.)}$$

where q_{exp} and q_{model} refers to the experimental and predicted (isotherm) data respectively. “n” is the number of experiments. As a first step of iteration the SS value is calculated based on the initial estimated model parameters. The second iteration involves adjusting model parameters and recalculating SS. This process is repeated until the smallest possible value of SS is obtained.

2.1.10.2. The coefficient of determination, R^2

The coefficient of determination represents the percentage of variability in the dependent variable and is employed to analyse the fitting degree of isotherm and kinetic models with the experimental data [58]. R^2 is a more practical parameter as it gives the proportion of the variance of one variable that is predictable from the other. The coefficient of determination is described by the function [58]:

$$\mathbf{R^2} = \frac{\sum_{\mathbf{n=1}}^{\mathbf{n}}\left[\mathbf{q_{exp} - q_{model}}\right]^{\mathbf{2}}}{\sum_{\mathbf{n=1}}^{\mathbf{n}}\left[\mathbf{q_{exp} - q'_{exp}}\right]^{\mathbf{2}}} \qquad \textbf{(2.20)}$$

where q_{exp}, q_{model} and "n" have the same meaning as in SS. q'_{exp} is the average of experimental data, q_{max}. The coefficient of determination is such that; $0 < R^2 < 1$.

2.1.10.3. Residual root mean square error (RMSE) and the Chi-square test (X^2)

RMSE and the Chi-square test are nonlinear error functions which are used to examine the equilibrium model with optimal magnitude. RMSE and X^2 are given by the following functions [58]:

$$\mathbf{RMSE} = \sqrt{\mathbf{1/(n-1)}\sum_{\mathbf{n=1}}^{\mathbf{n}}[\mathbf{q_{exp} - q_{model}}]^2} \qquad \textbf{(2.21)}$$

And

$$\boldsymbol{X^2} = \sum_{\mathbf{n=1}}^{\mathbf{n}} \frac{\left[\mathbf{q_{exp} - q_{model}}\right]}{\mathbf{q_{exp}}} \qquad \textbf{(2.22)}$$

where q_{exp}, q_{model}, and "n" have the same meaning as in SS and R^2. The small values of RMSE and X^2 indicate the goodness of fit.

A hybrid error function, Marquardt 's percent standard deviation, the average relative error, and the sum of the absolute errors have also been successfully used to determine the best-fitting isotherm model [55,56,59]. Some years ago nonlinear equations would be transformed to linear and be fitted with linear methods. Recently nonlinear curve fitting methods have been mostly used to fit experimental isotherm data in place of the linear methods. Persoff and Thomas [60] employed the non-linear least-squares (NLLS) curve-fitting method for determination of the Michaelis–Menten and Langmuir adsorption isotherm constants from experimental data. They observed that weighted NLLS yielded a more precise and accurate estimation. Similar observations have been reported by other researchers [56,59]. The authors observed that when compared to the nonlinear, the linearized equations generate real problems and errors arising from the complexities and complications for simultaneous transformation of data, leading to the violation of theories behind the isotherms [55,60].

2.1.11. Ion exchange equilibrium isotherm plot

Figure 10 shows a constant temperature equilibrium plot of resin phase equivalent ionic fraction versus the aqueous phase ionic fraction for reaction 2.1. This plot is referred to as the isotherm plot, and values of the separation factor, α_A^B and the selectivity coefficient, K_A^B at point "F" for instance, can be determined as the ratio of area H to area G. Isotherm is said to be favourable (convex to the x-axis) when specie B^{+z} (figure 10, I) is preferred to specie A^+. An "unfavourable" isotherm (concave to the x-axis) indicates that species B^{+z} is less preferred than A^+ (Figure 10,II). In a flow through resin column exhaustion process, favourable isotherms result in sharp breakthroughs when B^{+z} is in the feed and A^+ is on the resin, whereas unfavourable isotherms lead to gradual breakthroughs under these conditions [61].

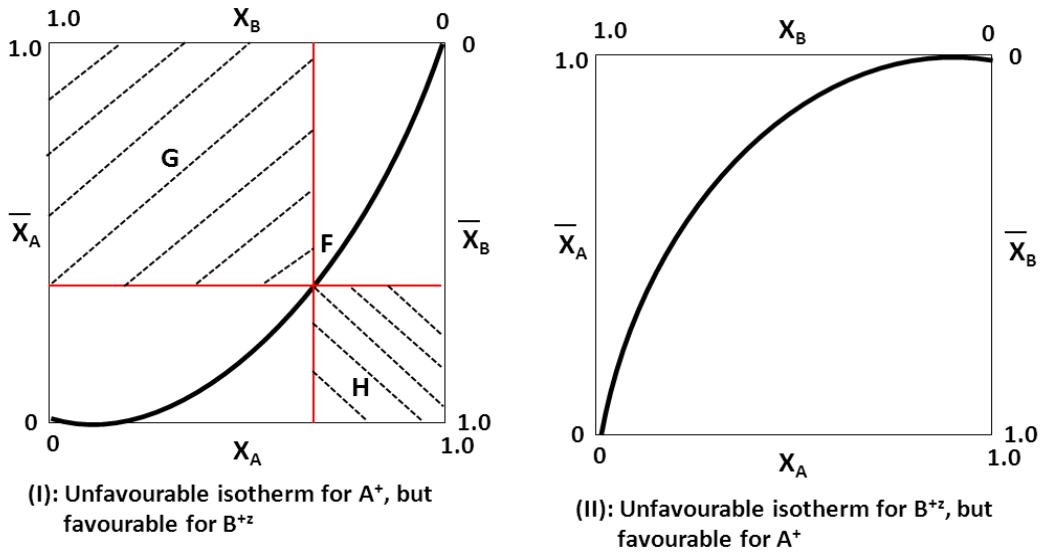

Figure 10: Typical ion exchange equilibrium isotherm plot

3. CHAPTER THREE

3.1. EXPERIMENTAL METHODS

In this section, candidate ion exchange resin capacities, ion exchange equilibrium rate, as well as the equilibrium isotherms were determined. The equilibrium rate provided the time estimate for ion exchange reactions to reach equilibrium, hence the duration of the reactions under investigation.

3.1.1. Materials

3.1.1.1. Reagents

Table 1 shows a list of chemical solutions used in this study. These chemical solutions were prepared from analytical grade chemicals purchased from Merck. Individual salt solutions were prepared separately and carefully mixed to obtain a solution of desired counter ion concentration. Deionized water with specific conductivity of ≤ 0.06 µS/cm was used as solvent.

Table 1: List of chemicals

Chemical solutions	Concentration	Function
H_2SO_4	1.0N	Cation resin regeneration
NaOH	0.1N	Standard titrant
Na_2CO_3	0.50N	For standardising H_2SO_4 solutions
NaCl	0.50N	Served as eluent to cation resin column
Na^+(aq) (as NaCl and Na_2SO_4)	1258 - 1.0µg/L	Served as electrolyte test solution

NH_4^+(aq) (as NH_3/NH_4OH)	25%	For pH adjustment
Methyl orange indicator	-	Served as indicator for H_2SO_4 standardisation against Na_2CO_3
Phenolphthalein indicator	-	Served as indicator acid-base titration

3.1.1.2. Glassware

All glassware used in this work were of class A grade, and prior to use were washed with dilute nitric acid solution (1%) followed by rinsing with deionized water to remove traces of impurities.

3.1.1.3. Analytical instrumentation

Figure 11 to 14 shows instruments/equipment used in this work. Magnetic stirrer hotplates from STUART Scientific were used to carry out the reactions. The 700 series ICP-OES from Agilent technologies was used to analyse the concentrations of sodium in solution, and SWAN AMI Inspector (portable specific conductivity instrument) was used to monitor specific conductivity (measured at 25^oC) of deionised or UPW water.



Figure 11: Filtration apparatus



Figure 12: Experimental setup for ion exchange reactions

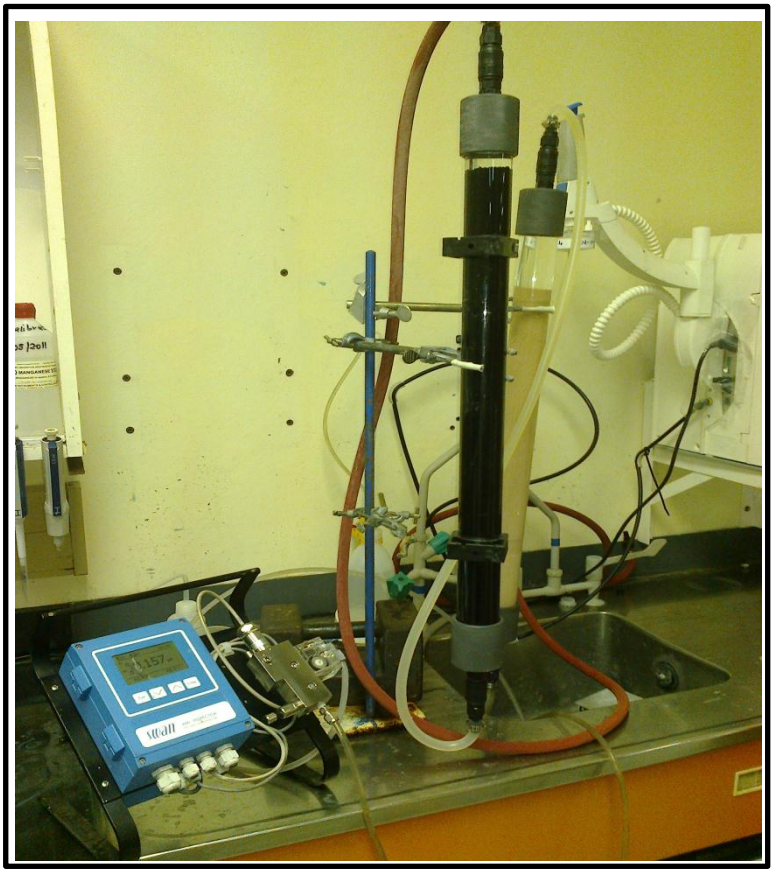

Figure 13: Set up for UPW production

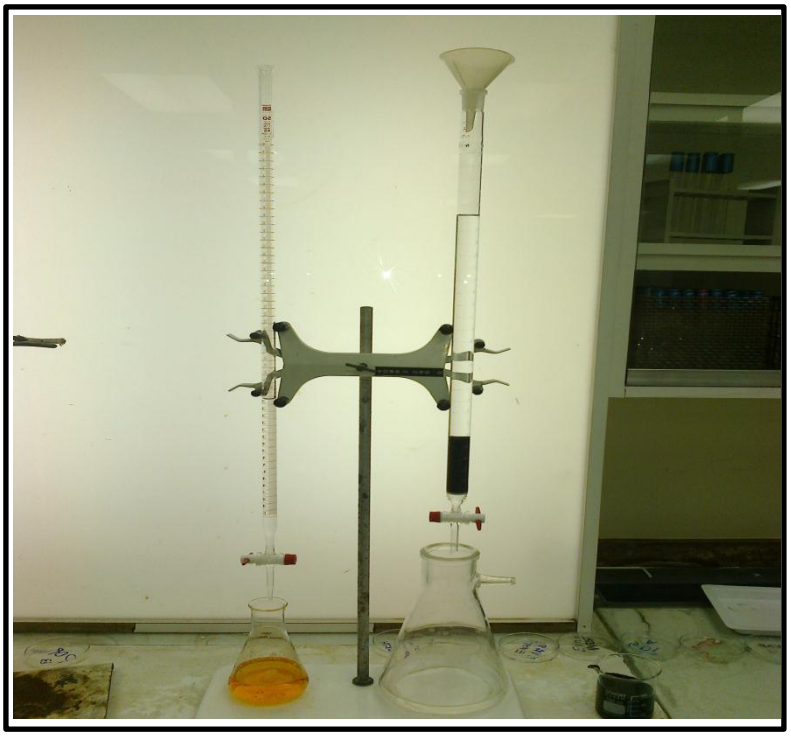

Figure 14: Experimental setup for exchange capacity measurements

3.1.2. Candidate ion exchange resins

Table 2 shows properties and specification of candidate strong acid cation exchange resins used in this study. This is a combination of macroporous, and gel type resins. The resins were chosen based on their chemical and physical properties, which meet the requirements for use in condensate polishing process.

Table 2: Typical ion exchange resin physical and chemical properties

Strong Acid Cation Exchange Resins				
Resin type / Properties	**Ambersep 252 H**	**Amberjet 1600 H**	**SGC 650 H**	**PPC 150 H**
Matrix	Styrene-DVB copolymer	Styrene-DVB copolymer	Styrene-DVB copolymer	Styrene-DVB copolymer
Functional group	$-SO_3^-$	$-SO_3^-$	$-SO_3^-$	$-SO_3^-$
Physical form	Light grey beads	Dark amber translucent beads	Spherical beads	Spherical beads
Ionic form (as shipped)	H^+ (99% min)	H^+ (99% min)	H^+ form	H^+ form
Total exchange capacity	≥ 1.65 eq/L (H^+ form)	≥ 2.4eq/L (H^+ form)	≥ 2.0eq/L (H^+ form)	≥ 1.8eq/L (Na^+ form)
Moisture holding capacity	52-58% (H^+ form)	37-43% (H^+ form)	46-50% (H^+ form)	54-59% (H^+ form)
Specific gravity	1.18-1.22 g/mL (H^+ form)	-	1.21g/mL (H^+ form)	1.18g/mL
Shipping weight	755g/L	840g/L	770-790g/L	740-775g/L

Harmonic mean size	0.90-1.90mm	0.600-0.700mm	650±50µm	300-1200µm
Uniform coefficient	≤1.4	≤1.2	1.1-1.2	≤1.7

3.1.3. Methods

3.1.3.1. Ion exchange capacity measurements

Strong acid cation exchange resins were supplied in H^+ form. The resins were regenerated prior to testing to remove/lower any impurity levels (e.g. water soluble organics). As a first step to ion exchange capacity determination, about 100 g of each resin type was hydrated by equilibrating with equal amount of UPW in a 250 mL volumetric flask, for a period exceeding 30 minutes. The hydrated resins were transferred to a Buchner funnel containing a 0.45 µm filter paper. The funnel was placed on the dewatering apparatus (see Figure 11), and the vacuum adjusted to 40±5 mm Hg below atmospheric pressure to remove excess water from the sample. The ion exchange capacity of hydrated resin samples was determined by a column method [37,73]. The column was prepared in a burette, 140 mL in length provided with a fritted glass wool at the bottom. A known amount of hydrated resin, 15 g ± 0.5 g were transferred to a 50 ml graduated cylinder and the resin minimum tapped volume measured by carefully tapping the cylinder on a rubber surface to compact the resin. The resin were then converted to H^+ form, by placing the resin sample in a column, and passing 1000 mL of H_2SO_4 solution (1.0 N) through the column.

After conversion, the resins were rinsed with 1000 mL of UPW. This was followed by passing 1000 mL of NaCl solution (0.5 N) through the column to elute the hydrogen ions. Exactly 1000 mL of the effluent was collected in a 1000 mL volumetric flask and 100 mL of the effluent transferred to a conical flask. The quantity of hydrogen ions was determined by titration with NaOH solution (0.2N). 100 mL of 0.5 N NaCl influent blank

was also titrated for hydrogen ion concentration. The experimental exchange capacity was calculated from the following equations [74]:

$$\mathbf{Ex.\ Cap.H-form\ (meq/g)} = \frac{\mathbf{10 \times N_{NaOH\ (eq/l)}\left(V_{regen,NaOH\ (ml)} - V_{Blank,NaOH\ (ml)}\right)}}{\mathbf{W_{moist\ (g)}}} \qquad \textbf{(3.1)}$$

3.1.3.2. Equilibrium rate determination

3 x 15.0 ± 0.5 g of resin samples were contacted with 100 mL of sodium ion solution (2.0µg/L) in separate tightly sealed 250 mL Scotch bottles, at room temperature. The bottles were put on magnetic stirrer hot plates, and the mixing speed adjusted such that the resins were in suspension. When the required mixing speed was achieved, the ion exchange reactions were timed, and the reactions proceed for a maximum period of two hours. One Scotch bottle was removed after every 30 minutes, resin filtered off and filtrate analysed for sodium ion concentration. The concentration was trended as a function of time, and the time where a constant ion concentration in solution was observed was assumed to be a point of equilibrium.

3.1.3.3. Equilibrium isotherms determination

a) RH^+—Na^+ system with Cl^- and SO_4^{2-} co-ions (no pH adjustment)

A 15.0 ± 0.5 g/100 ml mixture of conditioned cation exchange resin and dilute Na^+ solution (1.258 mg/L, 0.5000 mg/L, 0.001700 mg/L, and 0.001100 mg/L) prepared from a dilute solutions of NaCl and Na_2SO_4 were equilibrated in tightly sealed 250 mL Scotch bottles, placed in magnetic stirrer hot plate under constant mixing, at temperature range; 50°C, 60°C, 70°C, 80°C, and 90°C, until equilibrium was reached (as determined in section 3.1.2.3.). The equilibrium reaction for this system was:

$$\mathbf{R{-}H^+ + Na^+ \rightleftarrows R{-}Na^+ + H^+} \qquad \textbf{(3.2)}$$

On reaching equilibrium, the resins were filtered off, and the filtrate analysed for Na^+ by inductively coupled plasma–optical emission spectroscopy. Three sets of 15.0 ± 0.500 g per 100 mL were tested for each temperature range under study to ensure results reliability and consistency.

b) RH+—Na+ system with Cl-, SO42-, as co-ions at variable pH

The test conditions were similar to that of the above binary system. However, sample pH was conditioned using NH_3/NH_4^+ solution. The tests were carried out at pH; 9.6, 9.8, and 10. On reaching equilibrium, the resin were filtered off, and the filtrate analysed for Na^+ the same way as in (a).

3.1.3.4. Configuring Excel Spreadsheet for Langmuir and Freundlich Models

A trial and error approach was applied to obtain the isotherm model parameters. This method was based on the optimization routine to maximize the coefficient of determination, R^2 between the experimental data and isotherms in the solver add-in with Microsoft Excel. This process was based on the method of nonlinear least squares regression for fitting of non-linear equations to the experimental data. Error analysis or goodness of fit was spread sheet based model efficiency (R^2), which is considered to be the best overall indicator of model fit [57,58,60]. The default settings of MS Excel built-in Solver functions were appropriate for the current situation (and normally for most other situations as well). The most relevant settings to the current situation were:

1) **Max time:** it is the amount of time in seconds that the Solver was allowed to run the iteration process before stopping. The default value is set at 100 s.
2) **Iterations:** It is the number of iterations that the Solver carried out the calculation and provided the optimal solution before stopping. The default value is set at 100 s.
3) **Constrained precision:** it is a measure of the preciseness of the calculated values to meet a target or satisfies a lower or upper bound. The default value is 0.000001. The higher the precision, the more time is taken to reach a solution.

4) **Integer optimality:** This option is appropriate only to problems with integer constraints. The percent value by which the target cell of a solution will fulfil the integer constraints and it can differ from the true optimal value; however, it still be considered acceptable. A lower tolerance tends to slow up the solution process and the default value is set at 5.

To execute non-linear regression analysis using the Langmuir and Freundlich isotherm models, the following procedure was formulated:

1) The experimental data was inserted in two columns onto a Spreadsheet; column B containing the equilibrium counter ion concentration, Ce, mg/l, and column C containing the equilibrium counter ion concentration in the solid phase, qe, mg/g
2) Labels; q_{max} or 1/n and K_L or K_F were entered in cells D02 to D03 to depict the contents of the adjacent cells (E02 and E03).
3) The objective cell I12 was set to maximum by changing variable cells D02 and D03, subject to constrains; D02 and D03 ≥ 0
4) The Langmuir or Freundlich equation was inserted in column D06 to D10, which gave the predicted values of q_e (q_L and q_F) for the corresponding experimental equilibrium concentration, C_e and q_e.
5) The mean value of q_e for experimental equilibrium isotherm was calculated from the data at column C11.
6) The residual sum of squares, RSS and total sum of squires, TSS of the experimental and predicted data was measured in column E11 and F11. The value of R^2 was determined by equation 2.20

4. CHAPTER FOUR

4.1. RESULTS AND DISCUSSION

4.1.1. Exchange capacity

The experimental procedure for exchange capacity determination is outlined in Chapter three. Table 3 below shows the exchange capacities for candidate ion exchange resins calculated from the measured experimental data using equation 3.1. As expected, the measured exchange capacities were found to be lower than the total exchange capacity as reported by the resin manufacturer. The total exchange capacity is a measure of the total number of ionizable site present in the resin, whereas the measured exchange capacity or operating capacity is a measure of the available sites the resin has for ion exchange purposes. Practically, not all functional groups are available to take part in the ion exchange process; hence the measured (operating) exchange capacity is lower than the total exchange capacity [2,3,22].

Table 3: Ion exchange capacities of candidate resins

Resin type	Measured exchange capacity, Eq/L	Reference exchange capacity (total), Eq/L [62,63,64,65]
Ambersep 252 H	1.52 (H^+ form)	≥1.65 eq/L (H^+ form)
Amberjet 1600 H	2.12 (H^+ form)	≥2.4 eq/L (H^+ form)
SGC 650 H	1.52 (H^+ form)	≥2.0 eq/L (H^+ form)
PPC 150 H	1.55 (H^+ form)	≥1.8 eq/L (Na^+ form)

The measured exchange capacity is a function of many factors such as the total exchange capacity, the level of ion exchange resin regeneration or resin composition (regeneration efficiency), the composition of electrolyte solution being treated, the resin bead size, the charge density of ions, flow rate, reaction temperature and pH, equipment design, etc [20]. According to Table 2, the measured exchange capacity for Ambersep 252 H was found to be atleast 7% lower than that measured by the resin manufacturer (1.69 eq/L) [66]. We couldn't find literature for other types of resins, hence no comparison was made. Amberjet 1600 H are gel type ion exchange resins characterised by its highest total exchange capacity when compared to macroporous type resins (Ambersep 252 Hand PPC 150 H. This was evident as its measured exchange capacity was found to be higher than those of macroporous resins. Another gel type resin SGC 650 H, however, showed lower measured exchange capacity when compared to macroporous type resins even though its total exchange capacity is higher than that of macroporous resins. This can be attributed to the loss of exchange capacity on the resin sample used

4.1.2. Optimum contact time

Figure 15 shows the effect of contact time on the exchange of Na^+ ions by Ambersep 252 H from the solution concentration of 2.0 µg/L at room temperature. The trend shows that the amount of Na^+ in solution decreases with contact time. The concentration of Na^+ in solution decreased from 2.0 µg/L to 0.037 µg/L as measured in the first 30 minute. There was a steady decrease in the concentration of Na^+ in solution after 60 minute, and it remained almost constant from 90 to 120 minutes with only a decrease in equilibrium solution concentration of 2×10^{-4} µg/L which, in this work was considered trivial. The high exchange rate during the first 30 minutes can be attributed to the high concentration of Na^+ in solution and high number of available exchange sites. The Na^+ concentration in solution and exchange sites in resin gradually decreased with contact time leading to decreasing exchange rate. Therefore a reaction period of 1hr 30 min was considered sufficient for a state of equilibrium to be established. Although there is no published data on similar tests for the resin under study, the 1hr 30 min period appeared to be in

agreement with that of similar studies of comparable resins [13]. In this work, all exchange reactions were allowed to proceed for a maximum of 3 hours.

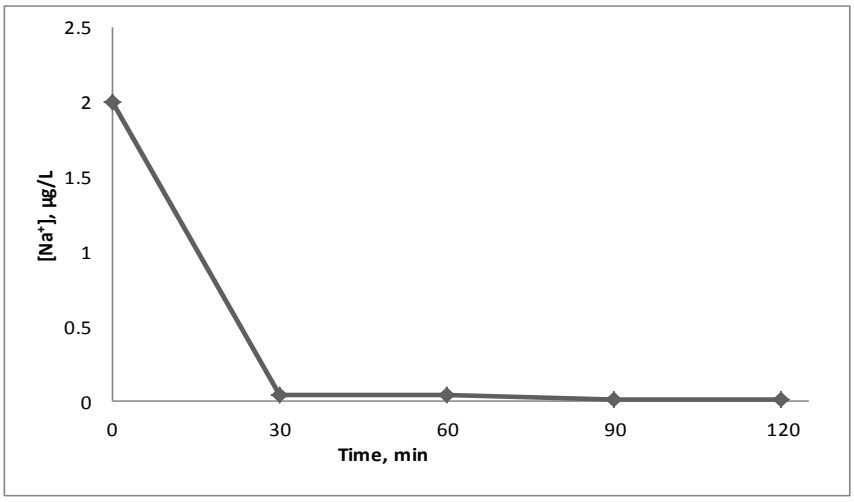

Figure 15: Removal of Na^+ ions from solution by Ambersep 252 H as a function of contact time at 25°C, C_{in} = 2.0 µg/L

4.1.3. Ion exchange equilibria

4.1.3.1. The Langmuir and Freundlich non-linear isotherm models

The experimental data of Na^+/RH^+ exchange reactions at reaction temperature; 50°C, 60°C, 70°C, 80°C, and 90°C was used to compute the constants of Langmuir and Freundlich models by equation 2.16 and 2.18 respectively. Table 4 shows the Langmuir and Freundlich model parameter values computed using an iterative approach on Microsoft Excel (based on the "SOLVER" function). The Langmuir constant, K_L represents the adsorption bond energy (L/g) [66]. Figure 16 shows the variation of K_L with reaction temperature. The magnitude of the bond energy was found to be dependent on reaction temperature as the K_L values decreased with increasing reaction temperature. Catterjee et al [67], in their study of the removal of nitrate from aqueous solutions by chitosan hydrogel beads observed a similar trend. The K_L values were also dependent on the type of ion exchange resins used and decreased according to the following order:

Amberjet 1600 H > SGC 650 H > PPC 150 H > Ambersep 252 H

The K_L values obtained from Amberjet 1600 H were much higher when compared to others (64.1–16.4 L/g), with Ambersep 252 H showing the least K_L values. This observation was unique in that, the gel type ion exchange resins (Amberjet 1600 H and SGC 650 H) showed stronger bond energy when compared to macroporous type (PPC 150 H and Ambersep 252 H). Apart from high exchange capacity, one other characteristic of gel type resins is smaller pore size when compared to macroporous resins. According to Dabrowski [68], adsorbents with limited space of micropores are associated with strong adsorption field as molecules adsorbing in micropores do not form adsorption layers, but fill up micropores in respect of volume according to the mechanism of micropore filling. With all resin type, K_L values were highest at reactions carried out at 50 °C, and lowest at 90 °C. The q_{max} (mg/g) also varied with ion exchange resins. The q_{max} for Ambersep 252 H was almost independent of reaction temperature with the exception of that of reactions carried out at 50 °C. q_{max} of reactions carried out using other resin type were affected by reaction temperature as they showed a decreasing trend. PPC 150 H had the highest q_{max} values with Ambersep 252 H having the least.

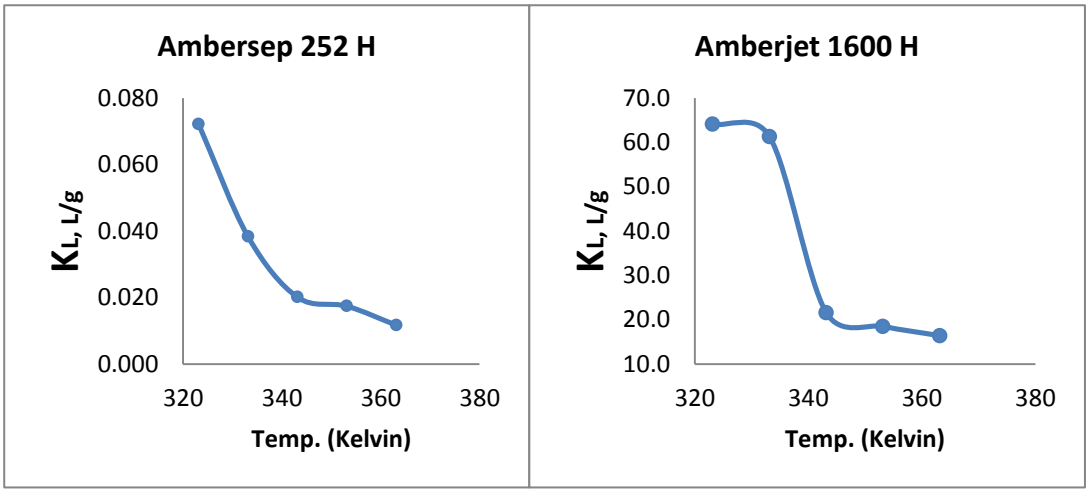

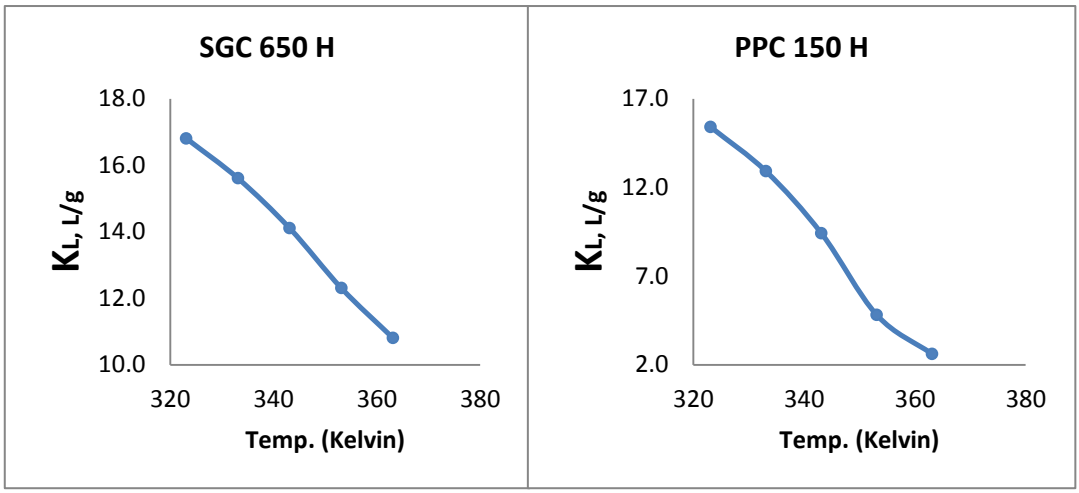

Figure 16: The variation of Langmuir constant, K_L with reaction temperature

The Freundlich constant, K_F values obtained from reactions involving Amberjet 1600 H, SGC 650 H, and PPC 150 H were similar (7.76 L/mg) across the reaction temperature range, but differed from those obtained using Ambersep 252 H. According to Coles and Young [69], values of K_F depend on the value of 1/n (where n is the measure of the magnitude of adsorption), and K_F parameters are only comparable when their 1/n parameters are comparable. The 1/n values of Amberjet 1600 H, SGC 650 H, and PPC 150 H were comparable per reaction temperature (with a maximum difference of 0.008). The 1/n values obtained from Ambersep 252 H were too high when compared to others. The 1/n appeared to be dependent on reaction temperature as they increased slightly with reaction temperature.

Table 4: Constants for equilibrium isotherm models for exchange reactions involving; Ambersep 252 H, Amberjet 1600 H, SGC 650 H, and PPC 150 H resins

Resin type	Ambersep 252 H												
Ion	Temperature	Parameter	Units	Langmuir Model Parameters					Parameter	Units	Freundlich Model Parameters				
				Concentration, mg/L							Concentration, mg/L				
Na^+	°C	-	-	0.001100	0.0001700	0.1033	0.5000	1.258	-	-	0.001100	0.0001700	0.1033	0.5000	1.258
	50	K_L	L/g	0.0721					K_F	L/mg	0.266				
		q_{max}	Mg/g	3.48					1/n	-	2.79				
		R_L	-	1.00	1.0	0.99	0.97	0.92	-	-	-				
		R^2	-	0.7311					R^2	-	0.9047				
	60	K_L	L/g	0.0383					K_F	L/mg	0.371				
		q_{max}	Mg/g	3.90					1/n	-	3.34				
		R_L	-	1.00	1.0	1.0	0.98	0.95	-	-	-				
		R^2	-	0.7609					R^2	-	0.9995				
	70	K_L	L/g	0.0201					K_F	L/mg	0.371				
		q_{max}	Mg/g	3.90					1/n	-	3.85				
		R_L	-	1.00	1.0	1.0	0.99	0.98	-	-	-				

		R^2	-	0.4806					R^2	-	0.7566					
	80	K_L	L/g	0.0174					K_F	L/mg	0.270					
		q_{max}	Mg/g	3.90					1/n	-	3.89					
		R_L	-	1.00	1.0	1.0	0.99	0.98	-	-	-					
		R^2	-	0.4558					R^2	-	0.6782					
	90	K_L	L/g	0.0117					K_F	L/mg	0.335					
		q_{max}	Mg/g	3.91					1/n	-	4.68					
		R_L	-	1.0	1.0	1.0	1.0	0.99	-	-	-					
		R^2	-	0.5464					R^2	-	0.9793					
Resin type	**Amberjet 1600 H**															
Ion	Temperature	Parameter	Units	Langmuir Model Parameters Concentration, mg/L					Parameter	Units	Freundlich Model Parameters Concentration, mg/L					
	°C	-	-	0.001100	0.0001700	0.1033	0.5000	1.258	-	-	0.001100	0.0001700	0.1033	0.5000	1.258	
Na^+	50	K_L	L/g	64.1					K_F	L/mg	7.76					
		q_{max}	Mg/g	4.45					1/n	-	1.30					
		R_L	-	0.93	0.90	0.13	0.030	0.012	-	-	-					
		R^2	-	0.6656					R^2	-	0.7262					
	60	K_L	L/g	61.3					K_F	L/mg	7.76					
		q_{max}	Mg/g	3.21					1/n	-	1.36					
		R_L	-	0.94	0.91	0.14	0.031	0.013	-	-	-					
		R^2	-	0.9452					R^2	-	0.9868					
	70	K_L	L/g	21.6					K_F	L/mg	7.76					
		q_{max}	Mg/g	8.31					1/n	-	1.37					
		R_L	-	0.98	0.97	0.31	0.085	0.036	-	-	-					
		R^2	-	0.9004					R^2	-	0.9642					
	80	K_L	L/g	18.5					K_F	L/mg	7.76					
		q_{max}	Mg/g	3.07					1/n	-	1.52					
		R_L	-	0.98	0.97	0.340	0.097	0.041	-	-	-					
		R^2	-	0.6779					R^2	-	0.7487					
	90	K_L	L/g	16.4					K_F	L/mg	7.76					
		q_{max}	Mg/g	2.01					1/n	-	1.64					
		R_L	-	0.98	0.97	0.37	0.11	0.046	-	-	-					
		R^2	-	0.9122					R^2	-	0.9851					
Resin type	**SGC 650 H**															
Ion	Temperature	Parameter	Units	Langmuir Model Parameters Concentration, mg/L					Parameter	Units	Freundlich Model Parameters Concentration, mg/L					
	°C	-	-	0.001100	0.0001700	0.1033	0.5000	1.258	-	-	0.001100	0.0001700	0.1033	0.5000	1.258	
Na^+	50	K_L	L/g	16.8					K_F	L/mg	7.76					
		q_{max}	Mg/g	10.4					1/n	-	1.36					
		R_L	-	0.98	0.97	0.36	0.11	0.045	-	-	-					
		R^2	-	0.7886					R^2	-	0.8811					
	60	K_L	L/g	15.6					K_F	L/mg	7.76					
		q_{max}	Mg/g	8.6					1/n	-	1.40					
		R_L	-	0.98	0.97	0.38	0.11	0.048	-	-	-					
		R^2	-	0.6902					R^2	-	0.7108					
	70	K_L	L/g	14.1					K_F	L/mg	7.76					
		q_{max}	Mg/g	7.7					1/n	-	1.43					
		R_L	-	0.99	0.98	0.410	0.12	0.054	-	-	-					
		R^2	-	0.7660					R^2	-	0.8606					
	80	K_L	L/g	12.3					K_F	L/mg	7.76					
		q_{max}	Mg/g	5.62					1/n	-	1.48					
		R_L	-	0.99	0.98	0.44	0.14	0.061	-	-	-					
		R^2	-	0.5483					R^2	-	0.6517					
	90	K_L	L/g	10.8					K_F	L/mg	7.76					
		q_{max}	Mg/g	4.02					1/n	-	1.57					
		R_L	-	0.99	0.98	0.47	0.16	0.068	-	-	-					
		R^2	-	0.7336					R^2	-	0.8629					
Resin type	**PPC 150 H**															
Ion	Temperature	Parameter	Units	Langmuir Model Parameters Concentration, mg/L					Parameter	Units	Freundlich Model Parameters Concentration, mg/L					
	°C	-	-	0.001100	0.0001700	0.1033	0.5000	1.258	-	-	0.001100	0.0001700	0.1033	0.5000	1.258	
	50	K_L	L/g	15.4					K_F	L/mg	7.76					
		q_{max}	Mg/g	17.7					1/n	-	1.31					
		R_L	-	0.98	0.98	0.39	0.12	0.049	-	-	-					
		R^2	-	0.9275					R^2	-	0.9696					
	60	K_L	L/g	12.9					K_F	L/mg	7.76					
		q_{max}	Mg/g	16.2					1/n	-	1.34					
		R_L	-	0.99	0.98	0.43	0.13	0.058	-	-	-					
		R^2	-	0.6947					R^2	-	0.8120					
		K_L	L/g	9.4					K_F	L/mg	7.76					

Na^+	70	q_{max}	Mg/g	14.4					1/n	-	1.38
		R_L	-	0.99	0.98	0.51	0.18	0.078	-	-	-
		R^2	-	0.4627					R^2	-	0.5608
	80	K_L	L/g	4.8					K_F	L/mg	7.76
		q_{max}	Mg/g	12.6					1/n	-	1.51
		R_L	-	0.99	0.99	0.67	0.29	0.14	-	-	-
		R^2	-	0.5885					R^2	-	0.7121
	90	K_L	L/g	2.6					K_F	L/mg	7.76
		q_{max}	Mg/g	12					1/n	-	1.65
		R_L	-	0.99	0.99	0.79	0.44	0.24	-	-	-
		R^2	-	0.9221					R^2	-	0.9919

Figure 17a-d shows a plot of the experimental and predicted q_e (mg/g) versus C_e (mg/L). At lower initial Na^+ solution concentrations (0.011–0.1033 mg/L), the experimental data followed almost a linear isotherm. A sharp increase in q_e was observed as initial Na^+ solution concentration increased from 0.5 mg/L to 1.258 mg/L, indicating an increase in Na^+ uptake by resins at higher Na^+ solution concentration. Although this was the case, the isotherms did not reach a plateau, indicating that the resins were not entirely converted to the R–Na^+ form. According to the R^2 values, the experimental data, especially data generated using Ambersep 252 H and SGC 650 H could not well be fitted with the Langmuir model as all R^2 values were less than 0.9. Better fits however were observed on reactions carried out at; 60°C, 70°C, and 90°C involving Amberjet 1600 H, and at; 50°C and 90°C involving PPC 150 H. On the other hand the Freundlich model provided better fits for reactions carried out at 50°C, 60°C, 90°C involving Ambersep 252 H, 60°C, 70°C, 90°C for Amberjet 1600 H, and at; 50°C and 90°C for PPC 150 H. All R^2 values for reactions involving SGC 650 H were less than 0.9.

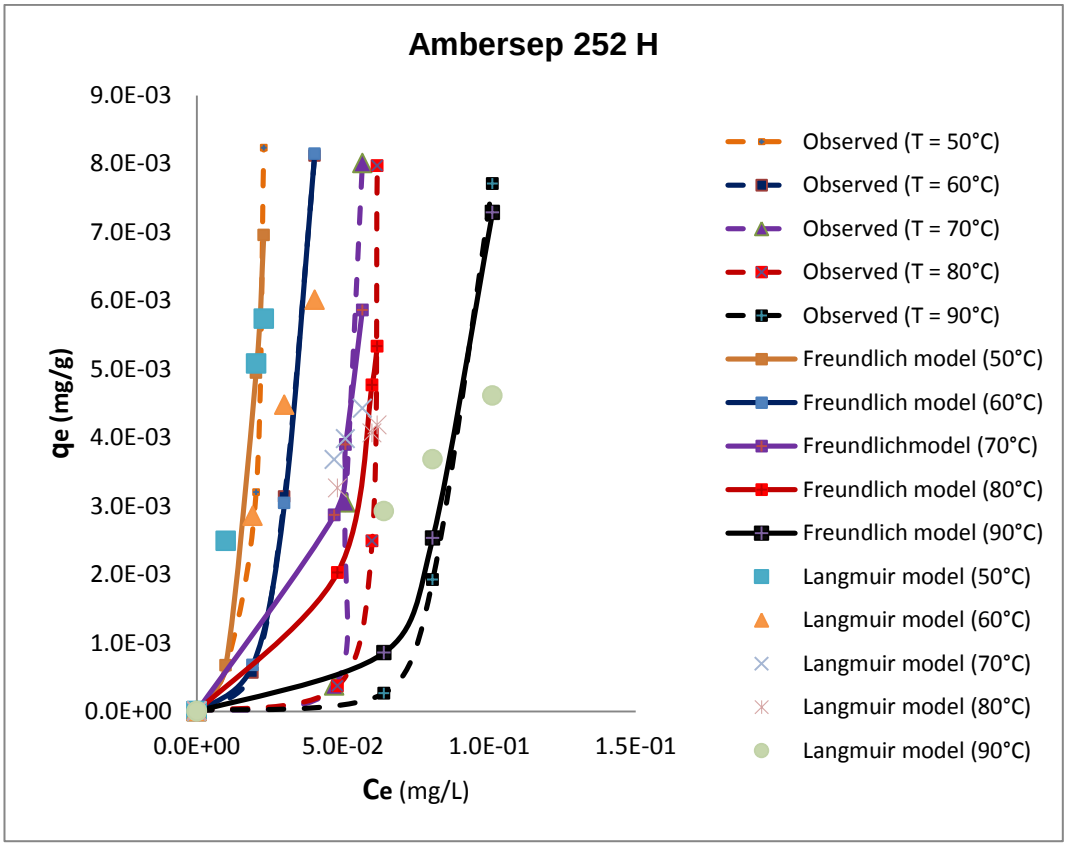
Ambersep 252 H
9.0E-03
8.0E-03
7.0E-03
6.0E-03
5.0E-03
4.0E-03
3.0E-03
2.0E-03
1.0E-03
0.0E+00
qe (mg/g)
0.0E+00
5.0E-02
1.0E-01
1.5E-01
Ce (mg/L)
Observed (T = 50°C)
Observed (T = 60°C)
Observed (T = 70°C)
Observed (T = 80°C)
Observed (T = 90°C)
Freundlich model (50°C)
Freundlich model (60°C)
Freundlichmodel (70°C)
Freundlich model (80°C)
Freundlich model (90°C)
Langmuir model (50°C)
Langmuir model (60°C)
Langmuir model (70°C)
Langmuir model (80°C)
Langmuir model (90°C)

(a)

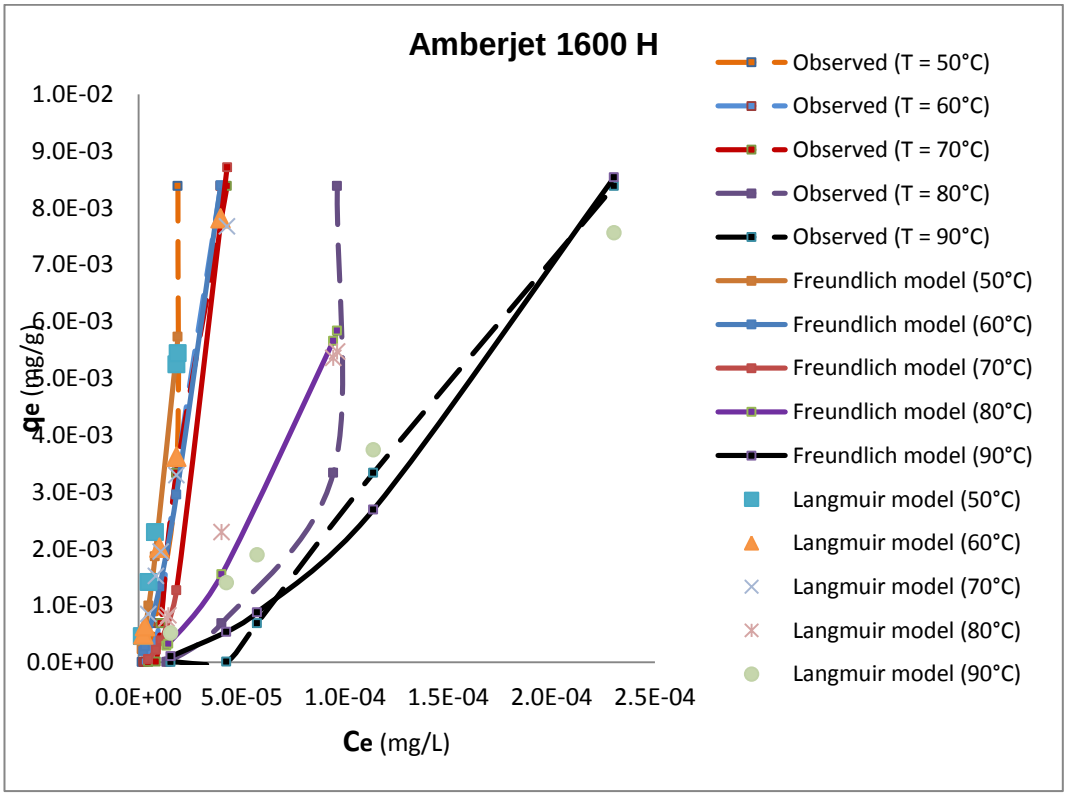
Amberjet 1600 H
1.0E-02
9.0E-03
8.0E-03
7.0E-03
6.0E-03
5.0E-03
4.0E-03
3.0E-03
2.0E-03
1.0E-03
0.0E+00
qe (mg/g)
0.0E+00
5.0E-05
1.0E-04
1.5E-04
2.0E-04
2.5E-04
Ce (mg/L)
Observed (T = 50°C)
Observed (T = 60°C)
Observed (T = 70°C)
Observed (T = 80°C)
Observed (T = 90°C)
Freundlich model (50°C)
Freundlich model (60°C)
Freundlich model (70°C)
Freundlich model (80°C)
Freundlich model (90°C)
Langmuir model (50°C)
Langmuir model (60°C)
Langmuir model (70°C)
Langmuir model (80°C)
Langmuir model (90°C)

(b)

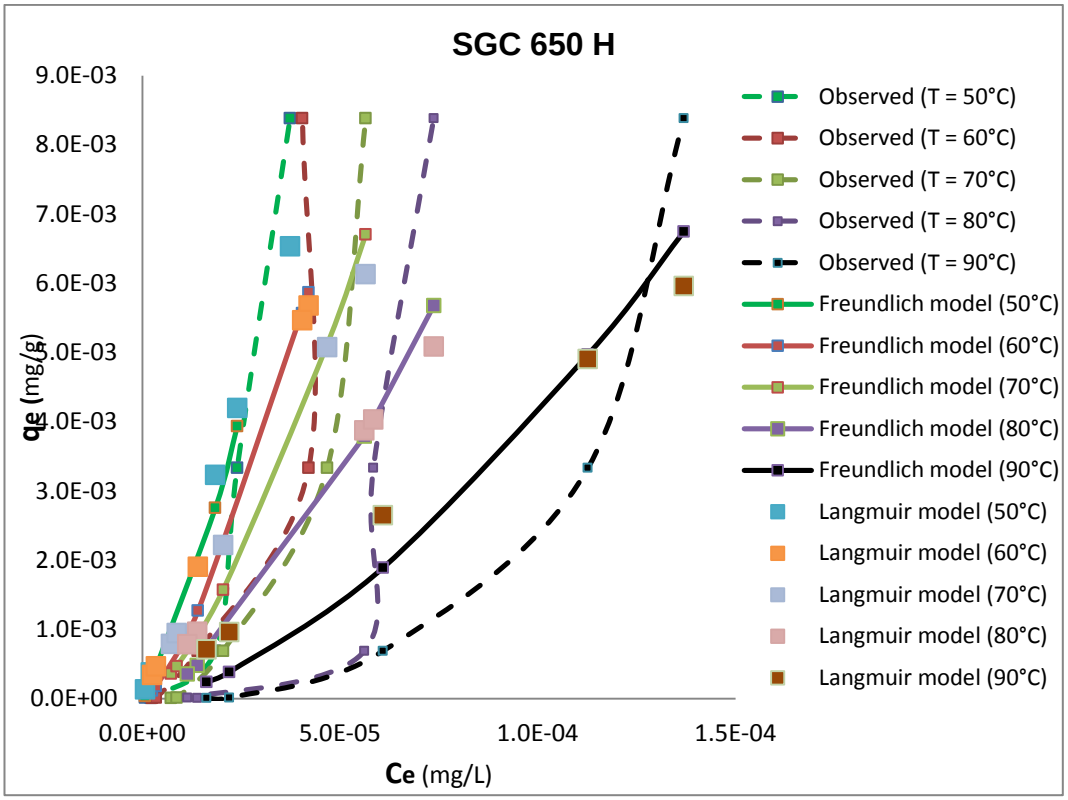

(c)

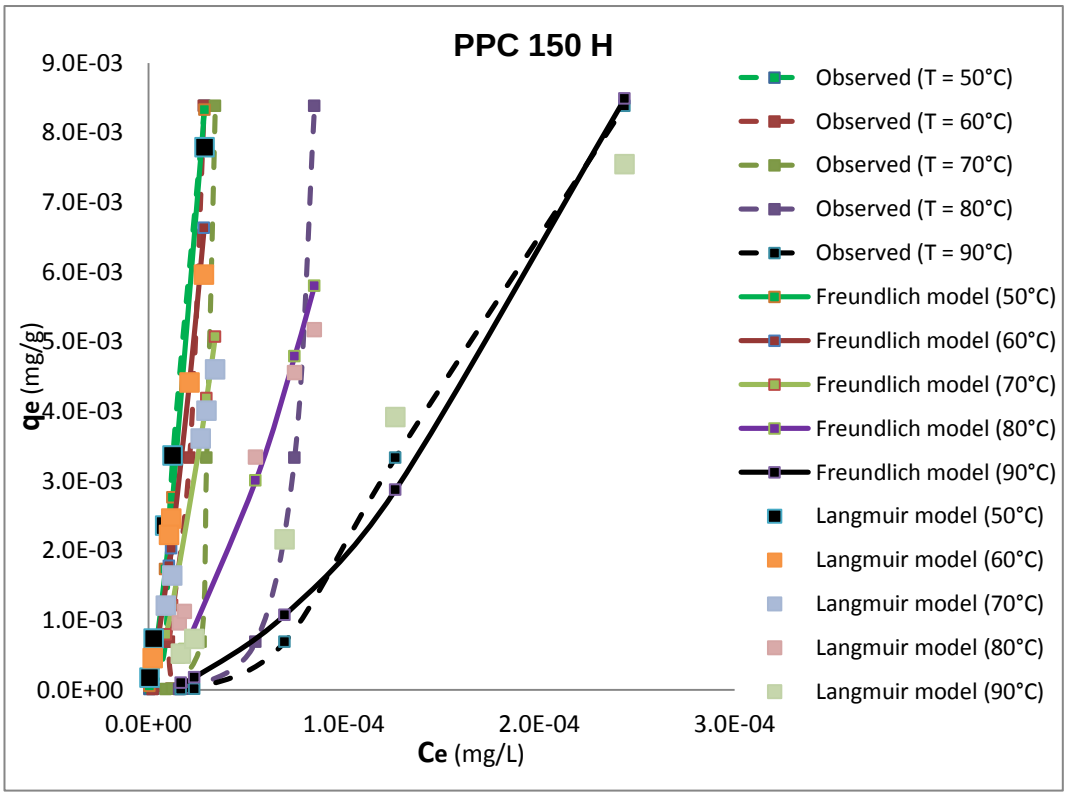

(d)

Figure 17: Experimental and predicted ion exchange equilibria for Na^+/RH^+ reactions at varying reaction temperatures using resin type; (a) ambersep 252 H , (b) amberjet 1600 H, (c) SGC 650 H, and (d) PPC 150 H

The essential characteristic of the Langmuir isotherm is the dimensionless separation factor or equilibrium parameter, R_L which is defined by equation 2.17. The R_L values are presented in Table 4, and Figure 18a-d shows a plot of R_L against initial concentration of Na^+ in solution, C_o (mg/L). R_L is a function of K_L and C_o, and since K_L decreased with increasing reaction temperature, R_L increased. Likewise, R_L decreased with increasing initial solution concentration, C_o which indicates that reactions carried out at higher C_o were more favourable than others. The increase in the initial Na^+ concentration in solution, together with the availability of the exchange sites in the resins favours the exchange process. The decrease in R_L with increasing C_o can be attributed to this effect. The earlier decline in R_L shows that the reactions were more favourable at higher initial solution concentrations. Whilst the later indicate that the exchange reaction was less favourable at higher reaction temperatures. The R_L values for Ambersep 252 H were all but those obtained at higher initial solution concentrations equal to one, giving rise to a linear plot of R_L versus C_o. they were also highest when compared with other R_L values which was a sign of least performance by the Ambersep 252 H. The R_L values were lowest in reactions carried out at 50°C, which indicated that the reactions carried out at this temperature were more favourable than the others. These observations were also in agreement with experimental data.

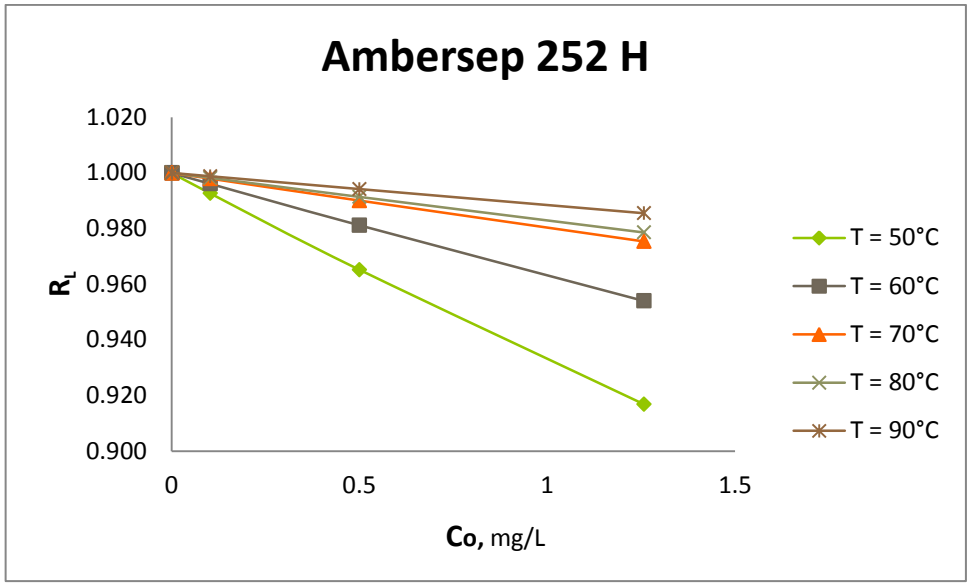
Ambersep 252 H
1.020
1.000
0.980
0.960
0.940
0.920
0.900
R_L
0
0.5
1
1.5
Co, mg/L
T = 50°C
T = 60°C
T = 70°C
T = 80°C
T = 90°C

(a)

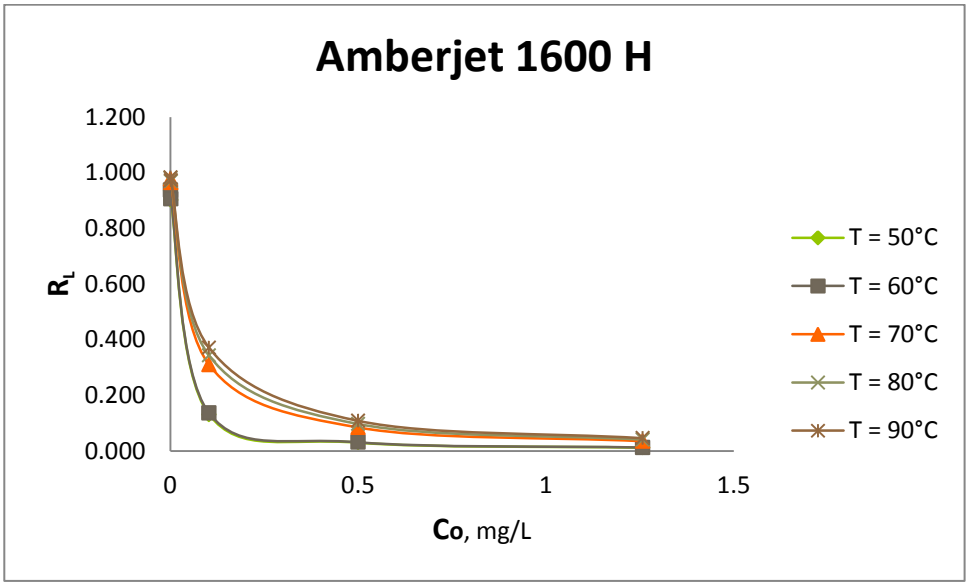
Amberjet 1600 H
1.200
1.000
0.800
0.600
0.400
0.200
0.000
R_L
0
0.5
1
1.5
Co, mg/L
T = 50°C
T = 60°C
T = 70°C
T = 80°C
T = 90°C

(b)

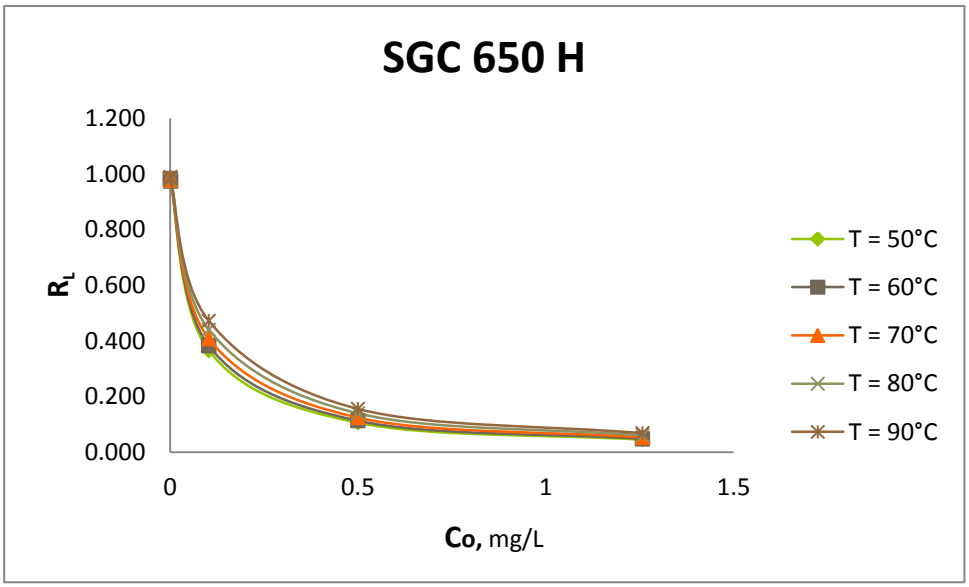

(c)

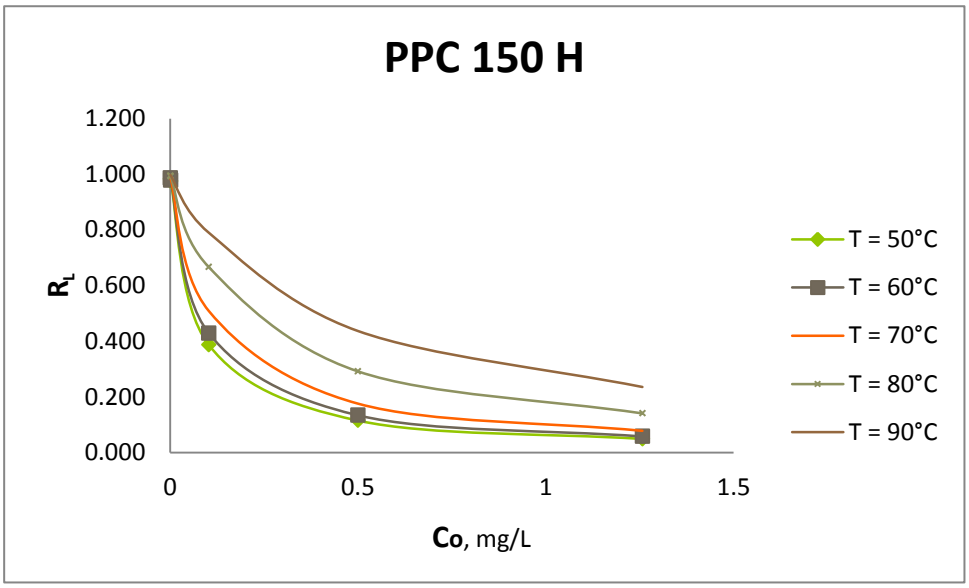

(d)

Figure 18: Separation factor for the Na^+/RH^+ exchange reaction and varying initial solution concentration and reaction temperature

4.1.1.1. Selectivity coefficient, $K_{H^+}^{Na^+}$

The selectivity coefficient values for the Na^+/RH^+ exchange reaction at different reaction temperatures and varying initial solution concentrations are presented in Table 5. A considerable uptake of Na^+ from the solution by all resin types was observed across the studied reaction temperature range. Na^+ on resin, q_{Na+} per initial solution concentration was at its maximum at 50°C. A decrease in q_{Na+} was observed with increasing reaction temperature. This, in turn resulted in a decrease in the selectivity coefficient. The observation was consistent throughout the tests and is contrary to that of work of similar reactions carried out at lower temperatures (although not for similar ion exchange resins and solution concentration levels) [13]. Bonner and Pruett however observed a similar behaviour when studying the temperature effect on uni-univalent exchange reactions [70]. There is about 10 times increase in the dissociation of water as temperature increase from 50°C to 90°C [71]. As the temperature increases the viscosity of water decreases, and the diffusion coefficient increases. As water dissociate, the concentration of H^+ increases, which then compete with Na^+ for the exchange site (H^+ displaces some of the Na^+ already present in the resin). The decrease in selectivity coefficient with rise in reaction temperature may be attributed to this effect. Elevated temperatures also increase the rate of ion exchange, however due to water ionisation effect, this results in an increase in Na^+ release by the resin [3]. Although the Na^+ uptake by ion exchange resins was satisfactory, examination of Table 5 shows that across the solution concentrations and temperature range studied, on average Amberjet 1600 H, performed better followed by SGC 650 H, and PPC 150 H. Both Amberjet 1600 H and SGC 650 H are gel type resins and their superiority may be attributed to their large surface area resin bed.

Table 5: Selectivity coefficients for the Na^+/RH^+ reaction at varying initial solution concentration and reaction temperatures

Common Parameters		Selectivity Coefficient, K_H^{Na}			
Initial Conc.	Temperature	Ambersep 252 H	Amberjet 1600 H	SGC 650 H	PPC 150 H
mg/L	°C	-	-	-	-
0.001100	50	2.30×10^{-3}	1.86×10^{-3}	1.92×10^{-3}	6.54×10^{-3}
0.001700		3.26×10^{-3}	1.44×10^{-3}	1.30×10^{-2}	3.69×10^{-3}
0.1033		2.87×10^{-3}	$3.30 \times 10^{+00}$	$1.96 \times 10^{+00}$	$4.26 \times 10^{+00}$
0.5000		2.71×10^{-2}	$3.38 \times 10^{+1}$	$3.54 \times 10^{+1}$	$7.01 \times 10^{+1}$
1.258		2.18×10^{-1}	$2.06 \times 10^{+2}$	$1.44 \times 10^{+2}$	$1.91 \times 10^{+2}$
0.001100	60	1.29×10^{-3}	1.20×10^{-3}	1.63×10^{-3}	1.92×10^{-3}
0.001700		8.36×10^{-4}	2.21×10^{-3}	2.84×10^{-3}	8.43×10^{-4}
0.1033		1.21×10^{-3}	$2.59 \times 10^{+00}$	$2.57 \times 10^{+00}$	$3.48 \times 10^{+00}$
0.5000		2.41×10^{-2}	$3.38 \times 10^{+1}$	$2.02 \times 10^{+1}$	$4.12 \times 10^{+1}$
1.258		1.20×10^{-1}	$9.89 \times 10^{+1}$	$1.33 \times 10^{+2}$	$1.93 \times 10^{+2}$
0.001100	70	4.02×10^{-4}	6.31×10^{-4}	5.61×10^{-4}	4.61×10^{-4}
0.001700		4.13×10^{-4}	8.37×10^{-4}	1.12×10^{-3}	8.11×10^{-4}
0.1033		2.20×10^{-4}	$2.44 \times 10^{+00}$	$1.77 \times 10^{+00}$	$1.38 \times 10^{+00}$
0.5000		1.32×10^{-2}	$3.38 \times 10^{+1}$	$1.82 \times 10^{+1}$	$2.91 \times 10^{+1}$
1.258		8.33×10^{-2}	$9.17 \times 10^{+1}$	$9.52 \times 10^{+1}$	$1.61 \times 10^{+2}$

0.001100	80	2.86×10^{-4}	2.16×10^{-4}	2.88×10^{-4}	2.59×10^{-4}
0.001700		1.88×10^{-4}	4.87×10^{-4}	8.52×10^{-4}	5.31×10^{-4}
0.1033		2.07×10^{-4}	6.58×10^{-1}	6.46×10^{-1}	6.74×10^{-1}
0.5000		8.95×10^{-3}	$6.59 \times 10^{+00}$	$1.45 \times 10^{+1}$	$1.16 \times 10^{+1}$
1.258		7.58×10^{-2}	$4.09 \times 10^{+1}$	$7.30 \times 10^{+1}$	$6.46 \times 10^{+1}$
0.001100	90	2.21×10^{-4}	1.86×10^{-4}	2.46×10^{-4}	2.44×10^{-4}
0.001700		1.31×10^{-4}	1.61×10^{-4}	4.35×10^{-4}	4.14×10^{-4}
0.1033		7.89×10^{-5}	4.62×10^{-1}	5.96×10^{-1}	5.31×10^{-1}
0.5000		4.90×10^{-3}	$5.47 \times 10^{+00}$	$7.54 \times 10^{+00}$	$6.86 \times 10^{+00}$
1.258		4.32×10^{-2}	$1.71 \times 10^{+1}$	$3.93 \times 10^{+1}$	$2.25 \times 10^{+1}$

4.1.1.2. Thermodynamic parameters

For different concentrations of Na^+ ions in solution at a given reaction temperature, the corrected selectivity coefficient, K^l was calculated using equation 2.4. Table 6 shows the average value of K^l. The selectivity coefficient and corrected selectivity coefficients per initial counter ion concentration, across the reaction temperature range were plotted against the equilibrium counter ion concentration in solution, C_e, as shown in Figure 19a-d. As expected, the corrected selectivity coefficients were far from the values of selectivity coefficients. The magnitude of deviation indicates the influence of electrolytes on ion exchange resin selectivity which is unaccounted when using the uncorrected selectivity coefficient.

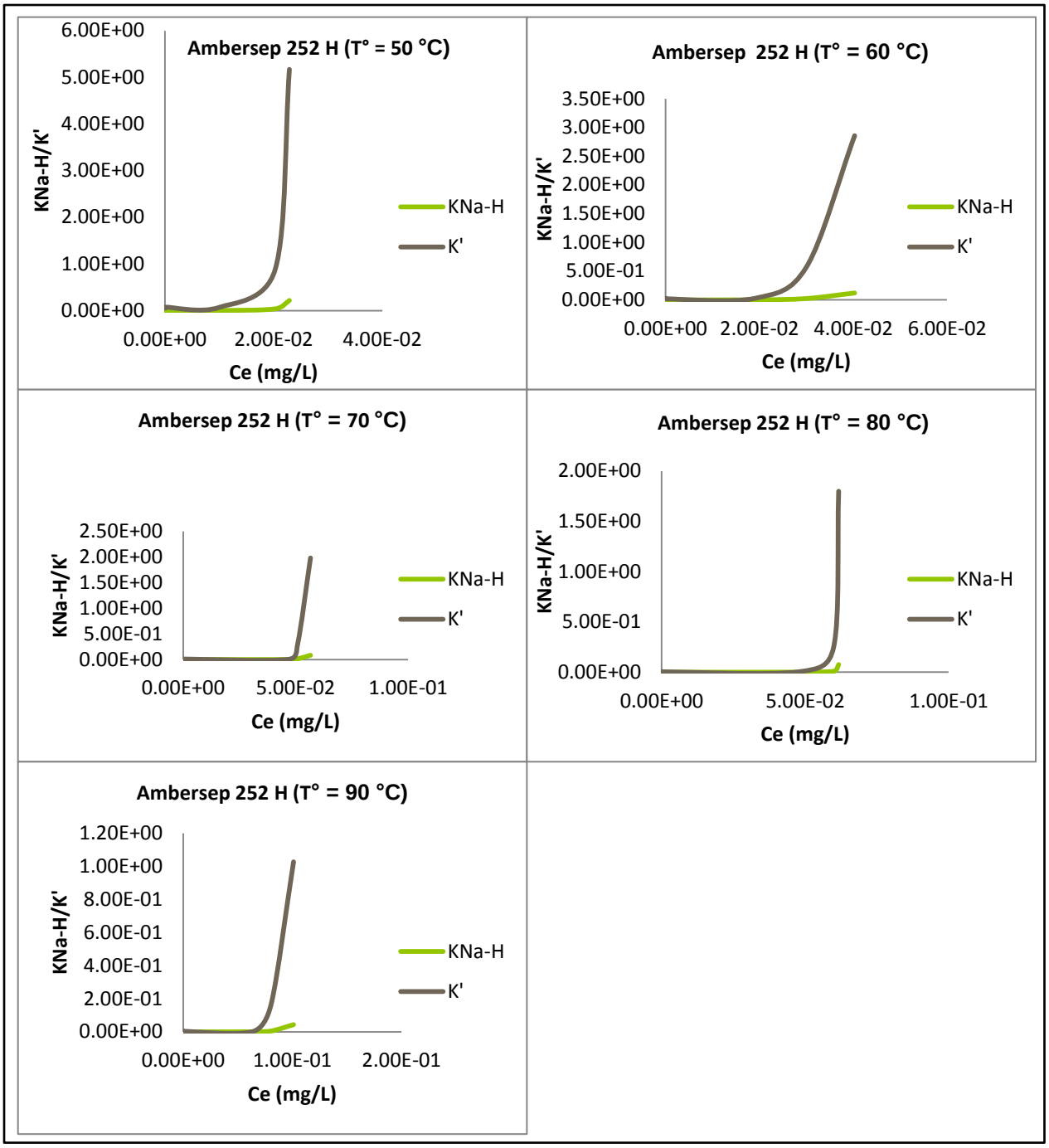
Ambersep 252 H (T° = 50 °C)
KNa-H/K'
6.00E+00
5.00E+00
4.00E+00
3.00E+00
2.00E+00
1.00E+00
0.00E+00
0.00E+00
2.00E-02
4.00E-02
Ce (mg/L)
KNa-H
K'
Ambersep 252 H (T° = 60 °C)
KNa-H/K'
3.50E+00
3.00E+00
2.50E+00
2.00E+00
1.50E+00
1.00E+00
5.00E-01
0.00E+00
0.00E+00
2.00E-02
4.00E-02
6.00E-02
Ce (mg/L)
KNa-H
K'
Ambersep 252 H (T° = 70 °C)
KNa-H/K'
2.50E+00
2.00E+00
1.50E+00
1.00E+00
5.00E-01
0.00E+00
0.00E+00
5.00E-02
1.00E-01
Ce (mg/L)
KNa-H
K'
Ambersep 252 H (T° = 80 °C)
KNa-H/K'
2.00E+00
1.50E+00
1.00E+00
5.00E-01
0.00E+00
0.00E+00
5.00E-02
1.00E-01
Ce (mg/L)
KNa-H
K'
Ambersep 252 H (T° = 90 °C)
KNa-H/K'
1.20E+00
1.00E+00
8.00E-01
6.00E-01
4.00E-01
2.00E-01
0.00E+00
0.00E+00
1.00E-01
2.00E-01
Ce (mg/L)
KNa-H
K'

(a)

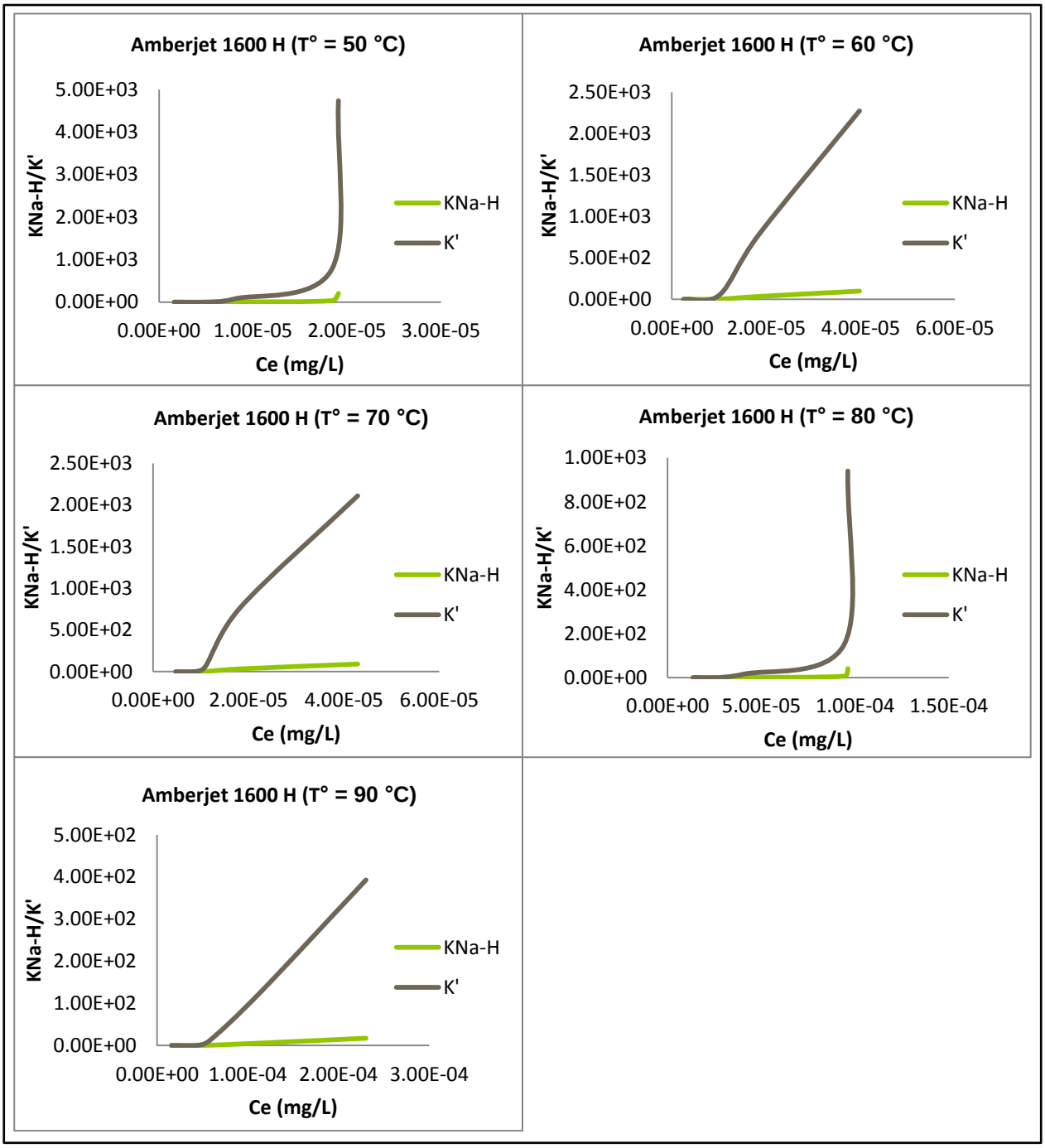
Amberjet 1600 H (T° = 50 °C)
KNa-H/K'
5.00E+03
4.00E+03
3.00E+03
2.00E+03
1.00E+03
0.00E+00
0.00E+00 1.00E-05 2.00E-05 3.00E-05
Ce (mg/L)
KNa-H
K'
Amberjet 1600 H (T° = 60 °C)
KNa-H/K'
2.50E+03
2.00E+03
1.50E+03
1.00E+03
5.00E+02
0.00E+00
0.00E+00 2.00E-05 4.00E-05 6.00E-05
Ce (mg/L)
KNa-H
K'
Amberjet 1600 H (T° = 70 °C)
KNa-H/K'
2.50E+03
2.00E+03
1.50E+03
1.00E+03
5.00E+02
0.00E+00
0.00E+00 2.00E-05 4.00E-05 6.00E-05
Ce (mg/L)
KNa-H
K'
Amberjet 1600 H (T° = 80 °C)
KNa-H/K'
1.00E+03
8.00E+02
6.00E+02
4.00E+02
2.00E+02
0.00E+00
0.00E+00 5.00E-05 1.00E-04 1.50E-04
Ce (mg/L)
KNa-H
K'
Amberjet 1600 H (T° = 90 °C)
KNa-H/K'
5.00E+02
4.00E+02
3.00E+02
2.00E+02
1.00E+02
0.00E+00
0.00E+00 1.00E-04 2.00E-04 3.00E-04
Ce (mg/L)
KNa-H
K'

(b)

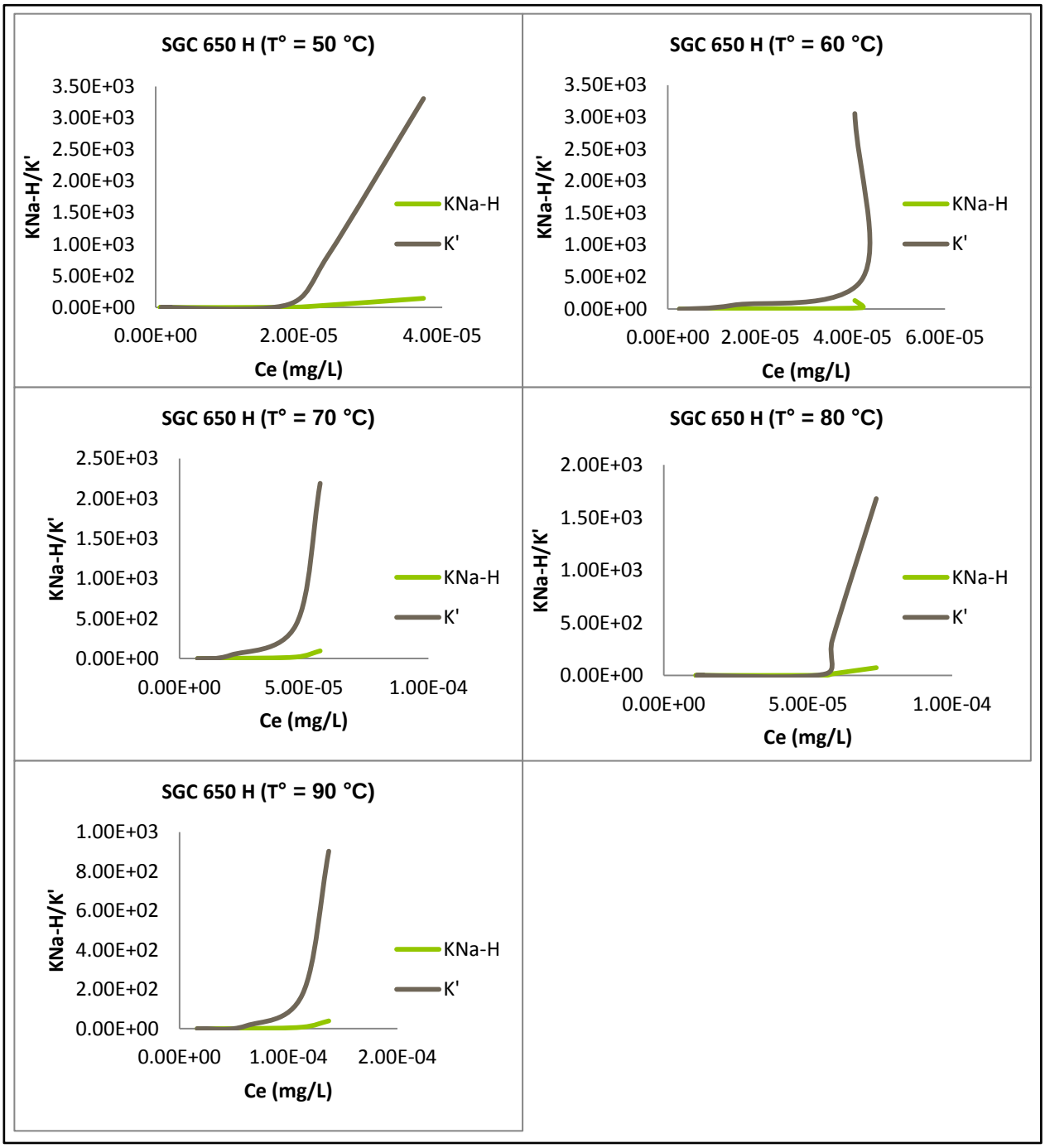
SGC 650 H (T° = 50 °C)
KNa-H/K'
3.50E+03
3.00E+03
2.50E+03
2.00E+03
1.50E+03
1.00E+03
5.00E+02
0.00E+00
0.00E+00
2.00E-05
4.00E-05
Ce (mg/L)
KNa-H
K'
SGC 650 H (T° = 60 °C)
KNa-H/K'
3.50E+03
3.00E+03
2.50E+03
2.00E+03
1.50E+03
1.00E+03
5.00E+02
0.00E+00
0.00E+00
2.00E-05
4.00E-05
6.00E-05
Ce (mg/L)
KNa-H
K'
SGC 650 H (T° = 70 °C)
KNa-H/K'
2.50E+03
2.00E+03
1.50E+03
1.00E+03
5.00E+02
0.00E+00
0.00E+00
5.00E-05
1.00E-04
Ce (mg/L)
KNa-H
K'
SGC 650 H (T° = 80 °C)
KNa-H/K'
2.00E+03
1.50E+03
1.00E+03
5.00E+02
0.00E+00
0.00E+00
5.00E-05
1.00E-04
Ce (mg/L)
KNa-H
K'
SGC 650 H (T° = 90 °C)
KNa-H/K'
1.00E+03
8.00E+02
6.00E+02
4.00E+02
2.00E+02
0.00E+00
0.00E+00
1.00E-04
2.00E-04
Ce (mg/L)
KNa-H
K'

(c)

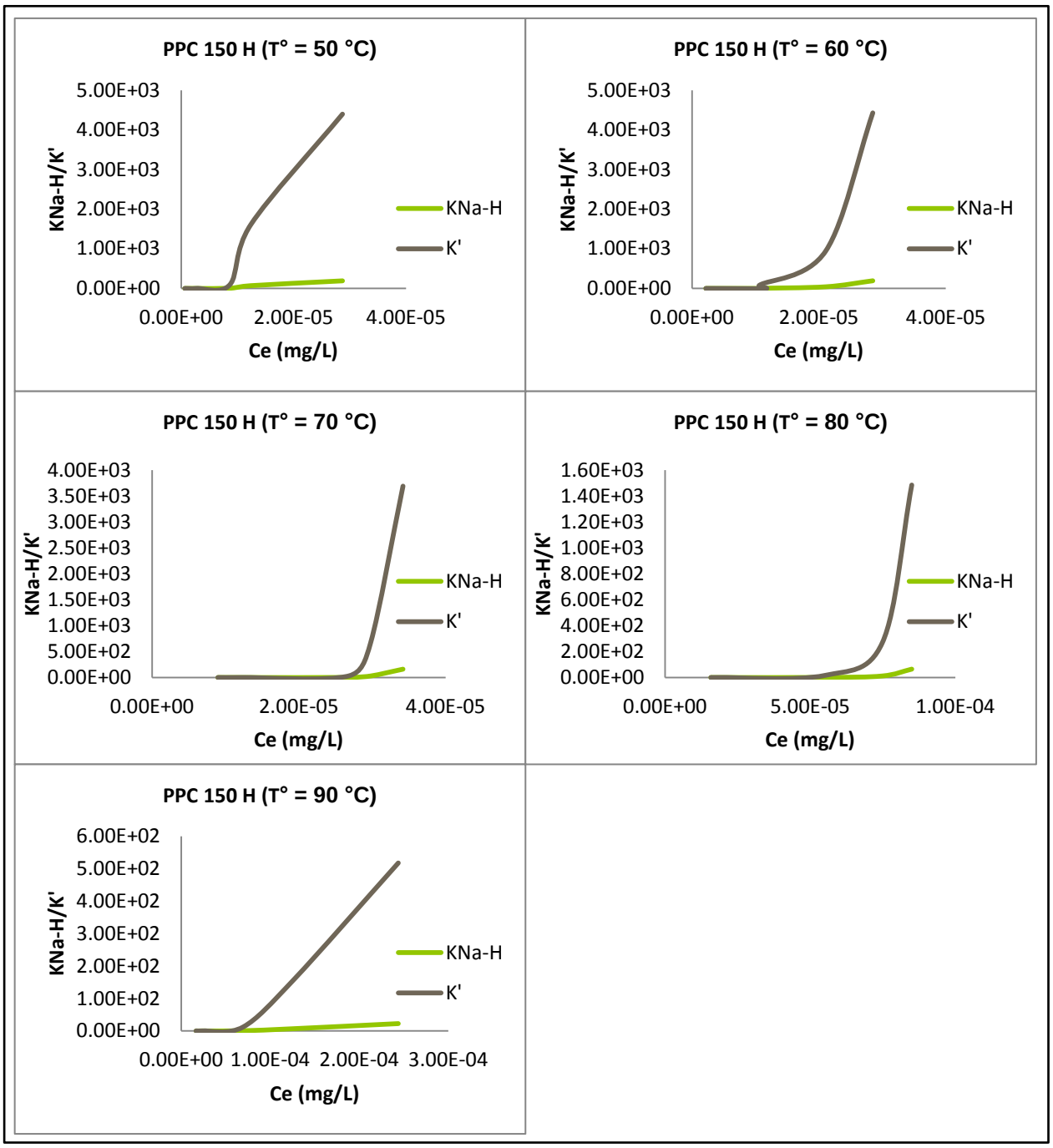

(d)

Figure 19: Variation of selectivity and corrected selectivity coefficients with initial counter ion solution and temperature

Table 6: Equilibrium and Thermodynamic parameters generated using; (a) Ambersep 252 H, Amberjet 1600 H, and; (b) SGC 650 H, PPC 150 H

Ambersep 252 H						Amberjet 1600 H			
In. Conc.	**Temp.**	**K^l**	**ΔG**	**ΔS**	**ΔH**	**K^l**	**ΔG**	**ΔS**	**ΔH**
mg/L	**Kelvin**	**-**	**kJ/mol**	**kJ/mol.K**	**kJ/mol.K**	**-**	**kJ/mol**	**kJ/mol.K**	**kJ/mol.K**
0.001100	323.15	4.41×10^{-02}	7.846	-0.2010	-57.17	1.50×10^{-1}	3.909	-0.2734	-84.44
	333.15	3.76×10^{-02}	9.858			4.41×10^{-2}	6.643		
	343.15	1.29×10^{-02}	11.87			1.06×10^{-2}	9.377		
	353.15	6.62×10^{-03}	13.88			5.96×10^{-3}	12.11		
	363.15	5.63×10^{-03}	15.89			5.61×10^{-3}	14.84		
0.001700	323.15	7.49×10^{-02}	7.624	-0.2641	-77.72	3.31×10^{-02}	7.499	-0.1987	-56.71
	333.15	1.93×10^{-02}	10.26			5.08×10^{-02}	9.486		
	343.15	9.53×10^{-03}	12.91			1.93×10^{-02}	11.47		
	353.15	4.33×10^{-03}	15.54			1.12×10^{-02}	13.46		
	363.15	3.02×10^{-03}	18.18			3.70×10^{-03}	15.44		
0.1033	323.15	6.73×10^{-02}	7.426	-0.2949	-87.87	$7.59 \times 10^{+01}$	0.02854	-0.1589	-51.32
	333.15	2.84×10^{-02}	10.38			$5.95 \times 10^{+01}$	1.618		
	343.15	5.14×10^{-03}	13.32			$5.61 \times 10^{+01}$	3.206		
	353.15	4.83×10^{-03}	16.27			$1.51 \times 10^{+01}$	4.796		
	363.15	1.84×10^{-03}	19.22			$1.06 \times 10^{+01}$	6.384		
		8.78×10^{-01}					-18.92		

0.5000	323.15		0.4192	-0.1261	-40.33	$7.77 \times 10^{+02}$		-0.0986	-50.79
	333.15	5.69×10^{-01}	1.680			$7.77 \times 10^{+02}$	-17.94		
	343.15	3.06×10^{-01}	2.941			$7.77 \times 10^{+02}$	-16.96		
	353.15	2.49×10^{-01}	4.202			$1.52 \times 10^{+02}$	-15.97		
	363.15	1.69×10^{-01}	5.463			$1.26 \times 10^{+02}$	-14.98		
1.258	323.15	$5.17 \times 10^{+00}$	-4.217	-0.09860	-36.08	$4.74 \times 10^{+03}$	-22.94	-0.1050	-56.87
	333.15	$2.86 \times 10^{+00}$	-3.231			$2.27 \times 10^{+03}$	-21.88		
	343.15	$1.98 \times 10^{+00}$	-2.245			$2.11 \times 10^{+03}$	-20.84		
	353.15	$1.80 \times 10^{+00}$	-1.259			$9.40 \times 10^{+02}$	-19.78		
	363.15	$1.03 \times 10^{+00}$	-0.2734			$3.93 \times 10^{+02}$	-18.74		
SGC 650 H						**PPC 150 H**			
In. Conc	**Temp.**	**K^I**	**ΔG**	**ΔS**	**ΔH**	**K^I**	**ΔG**	**ΔS**	**ΔH**
mg/L	**Kelvin**	**-**	**kJ/mol**	**kJ/mol.K**	**kJ/mol.K**	**-**	**kJ/mol**	**kJ/mol.K**	**kJ/mol.K**
0.001100	323.15	4.41×10^{-02}	8.159	-0.1974	-55.63	1.50×10^{-01}	5.808	-0.2794	-84.48
	333.15	3.76×10^{-02}	10.13			4.41×10^{-02}	8.602		
	343.15	1.29×10^{-02}	12.11			1.06×10^{-02}	11.39		
	353.15	6.62×10^{-03}	14.08			5.96×10^{-03}	14.19		
	363.15	5.65×10^{-03}	16.06			5.61×10^{-03}	16.98		
	323.15	3.00×10^{-01}	4.018			8.49×10^{-02}	7.543		

0.001700	333.15	6.53×10^{-02}	6.579	-0.2561	-78.74	1.94×10^{-02}	9.255	-0.1712	-47.78
	343.15	2.57×10^{-02}	9.141			1.87×10^{-02}	10.96		
	353.15	1.96×10^{-02}	11.70			1.22×10^{-02}	12.68		
	363.15	1.00×10^{-02}	14.26			9.53×10^{-03}	14.39		
0.1033	323.15	$4.52 \times 10^{+01}$	-13.67	-0.3400	-123.6	$9.81 \times 10^{+01}$	-12.72	-0.1361	-56.70
	333.15	$5.92 \times 10^{+01}$	-10.27			$8.02 \times 10^{+01}$	-11.36		
	343.15	$4.08 \times 10^{+01}$	-6.872			$3.17 \times 10^{+01}$	-9.998		
	353.15	$1.49 \times 10^{+01}$	-3.474			$1.55 \times 10^{+01}$	-8.638		
	363.15	$1.37 \times 10^{+01}$	-0.0710			$1.22 \times 10^{+01}$	-7.276		
0.5000	323.15	$8.15 \times 10^{+02}$	-22.94	-0.5720	-207.8	$1.61 \times 10^{+03}$	-20.13	-0.1154	-57.44
	333.15	$4.65 \times 10^{+02}$	-17.22			$9.47 \times 10^{+02}$	-18.97		
	343.15	$4.18 \times 10^{+02}$	-11.51			$6.70 \times 10^{+02}$	-17.82		
	353.15	$3.35 \times 10^{+02}$	-5.788			$2.67 \times 10^{+02}$	-16.66		
	363.15	$1.73 \times 10^{+02}$	-0.06884			$1.58 \times 10^{+02}$	-15.51		
1.258	323.15	$3.31 \times 10^{+03}$	-22.29	-0.02660	-30.88	$4.40 \times 10^{+03}$	-23.64	-0.08630	-51.52
	333.15	$3.06 \times 10^{+03}$	-22.02			$4.43 \times 10^{+03}$	-22.77		
	343.15	$2.19 \times 10^{+03}$	-21.76			$3.69 \times 10^{+03}$	-21.92		
	353.15	$1.68 \times 10^{+03}$	-21.49			$1.49 \times 10^{+03}$	-21.05		
	363.15	$9.03 \times 10^{+02}$	-21.22			$5.18 \times 10^{+02}$	-20.19		

K^{l} was used to construct the Van't Hoff plot. The thermodynamic parameters, ΔH (kJ/mol) and ΔS (kJ/mol) were calculated from the slope and intercept of the Van't Hoff plot (K^{l} vs 1/T, obtained by equation. 2.15) respectively. Values of ΔG (kJ/mol) were determined from equation 2.14. Figure 20 shows the Van't Hoff plots and the thermodynamic

parameters are listed in Table 6. The R^2 values in the plot of LnK^{l} *vs*. 1/*T* in Figure 20 (G), (H), (I), (M), (N), (Q), and (T) were not high enough (R^2< 0.9), which altered the trend of the temperature effect. The R^2 values in other plots were satisfactory showing a better fit of the corrected selectivity coefficient to the Van't Hoff equation (R^2 > 0.9). The enthalpy change, ΔH was negative which reveals that energy was released as ion exchange reaction precedes, hence the exothermic reaction [13]. The entropy, ΔS was also negative corresponding to a decrease in the degree of freedom of the system. Since ΔS is associated with order-disorder changes in a reaction, it was observed on reactions carried out with Amberjet 1600 H and PPC 150 H that when the cationic property of the solution increases (by increasing Na^+ concentration), the system became more disordered (ΔS became less negative), which can be attributed to the high levels of released H^+ ions. A similar trend however could not be observed with other reactions, but could only be observed when comparing the lower and upper ends of initial Na^+ solution concentrations. The Gibbs free energy change, ΔG was generally positive with the exception of some reactions as can be seen in Table 6. ΔG increased with increasing reaction temperature which proved that elevated reaction temperatures favour the reverse reaction.

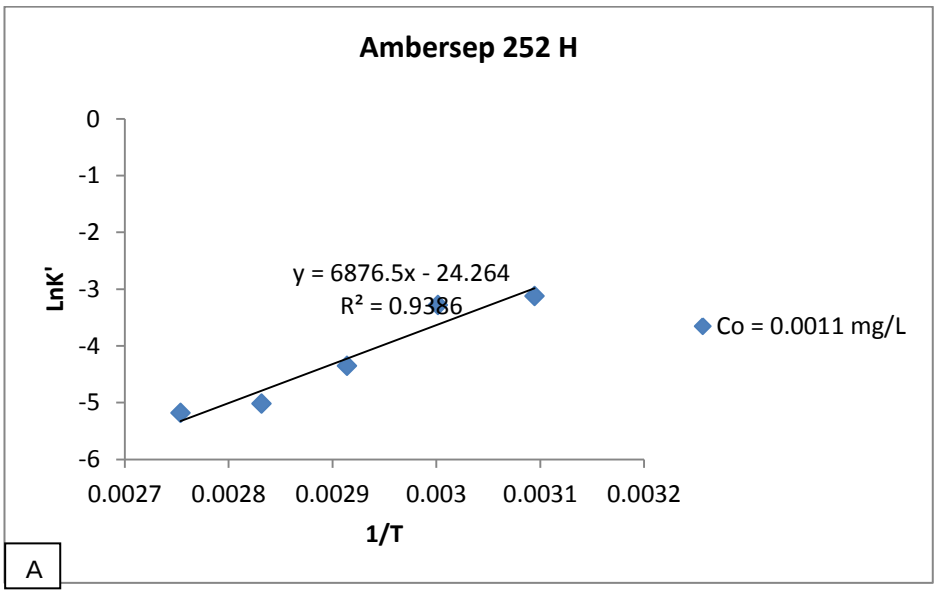

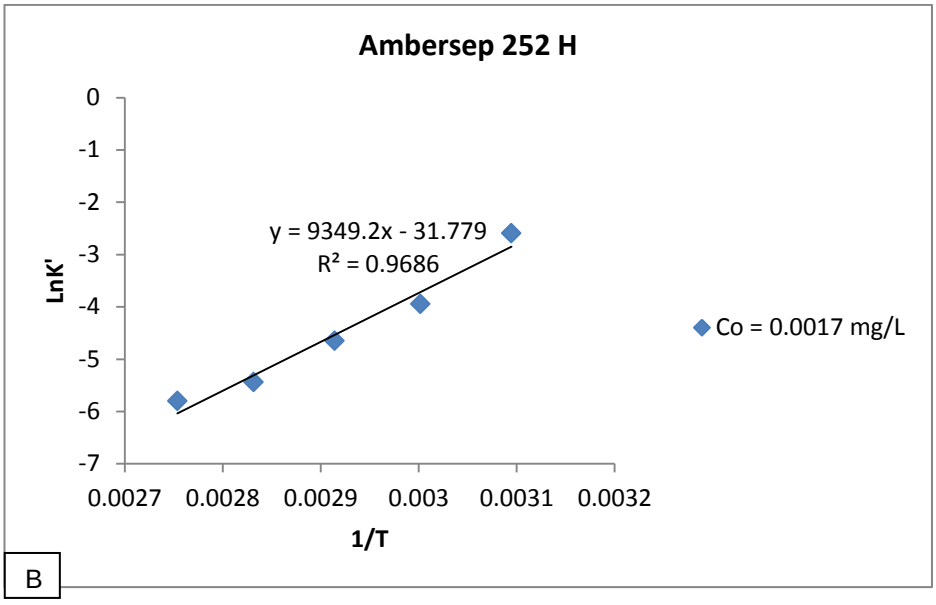
Ambersep 252 H
0
-1
-2
-3
-4
-5
-6
-7
LnK'
y = 9349.2x - 31.779
R² = 0.9686
0.0027
0.0028
0.0029
0.003
0.0031
0.0032
1/T
Co = 0.0017 mg/L

B

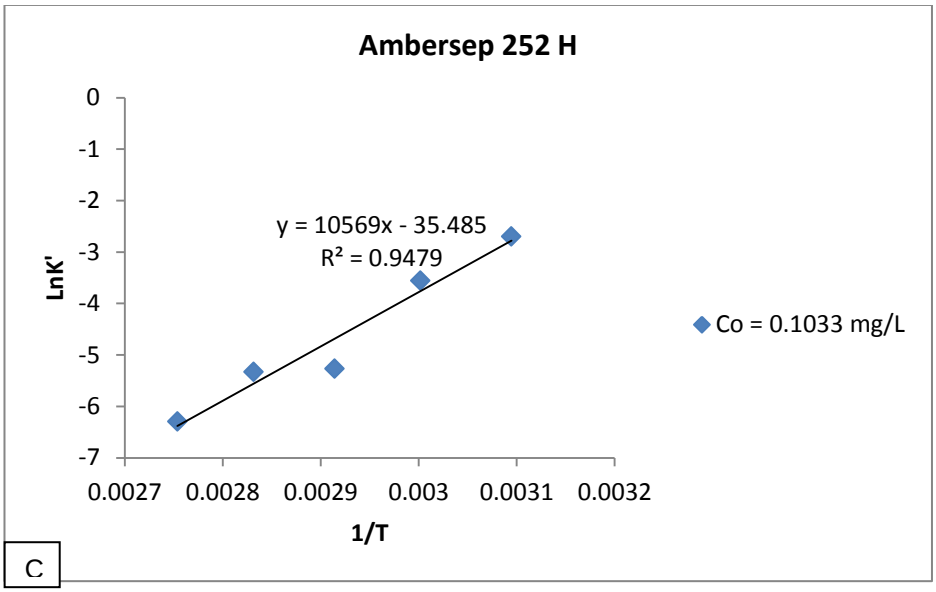
Ambersep 252 H
0
-1
-2
-3
-4
-5
-6
-7
LnK'
y = 10569x - 35.485
R² = 0.9479
0.0027
0.0028
0.0029
0.003
0.0031
0.0032
1/T
Co = 0.1033 mg/L

C

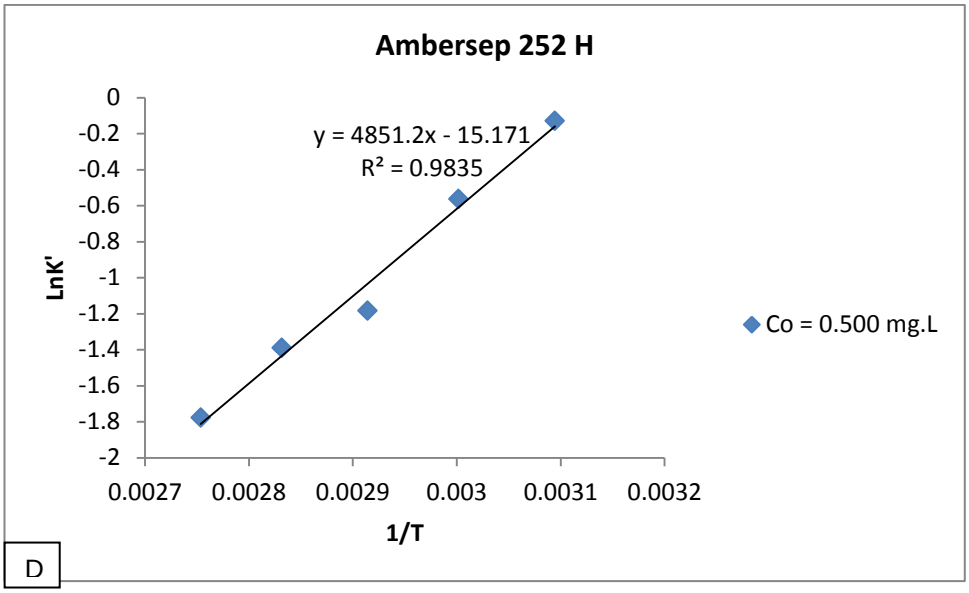
Ambersep 252 H
y = 4851.2x - 15.171
R² = 0.9835
LnK'
1/T
0
-0.2
-0.4
-0.6
-0.8
-1
-1.2
-1.4
-1.6
-1.8
-2
0.0027
0.0028
0.0029
0.003
0.0031
0.0032
Co = 0.500 mg.L

D

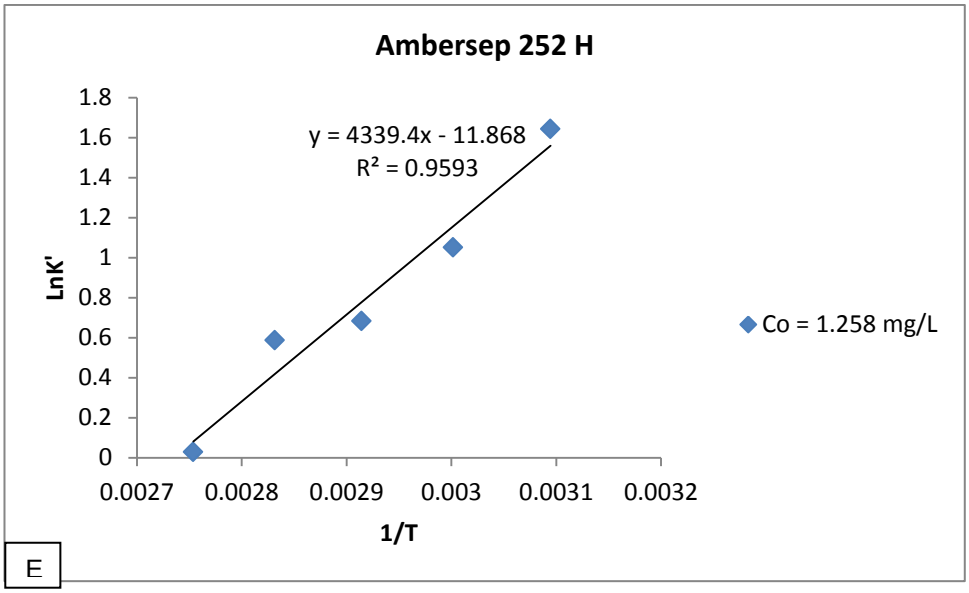
Ambersep 252 H
y = 4339.4x - 11.868
R² = 0.9593
LnK'
1/T
1.8
1.6
1.4
1.2
1
0.8
0.6
0.4
0.2
0
0.0027
0.0028
0.0029
0.003
0.0031
0.0032
Co = 1.258 mg/L

E

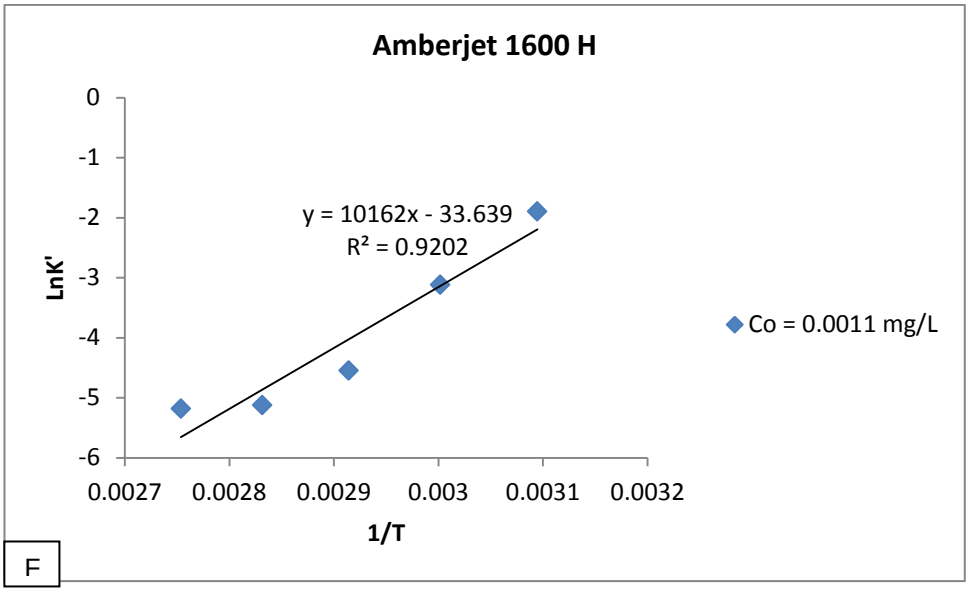
Amberjet 1600 H
0
-1
-2
-3
-4
-5
-6
LnK'
y = 10162x - 33.639
R² = 0.9202
0.0027
0.0028
0.0029
0.003
0.0031
0.0032
1/T
Co = 0.0011 mg/L

F

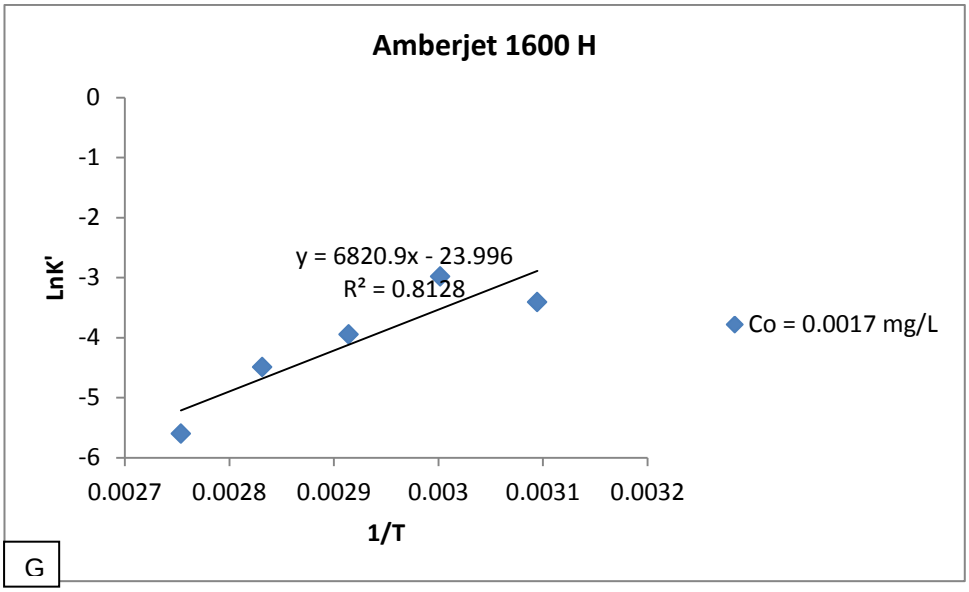
Amberjet 1600 H
0
-1
-2
-3
-4
-5
-6
LnK'
y = 6820.9x - 23.996
R² = 0.8128
0.0027
0.0028
0.0029
0.003
0.0031
0.0032
1/T
Co = 0.0017 mg/L

G

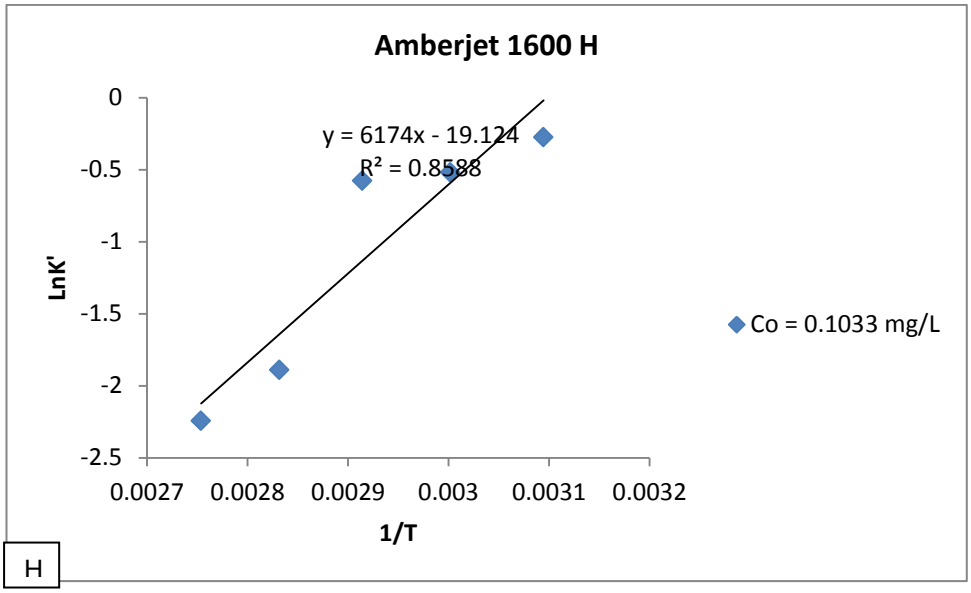
Amberjet 1600 H
y = 6174x - 19.124
R² = 0.8588
0
-0.5
-1
-1.5
-2
-2.5
LnK'
0.0027
0.0028
0.0029
0.003
0.0031
0.0032
1/T
Co = 0.1033 mg/L

H

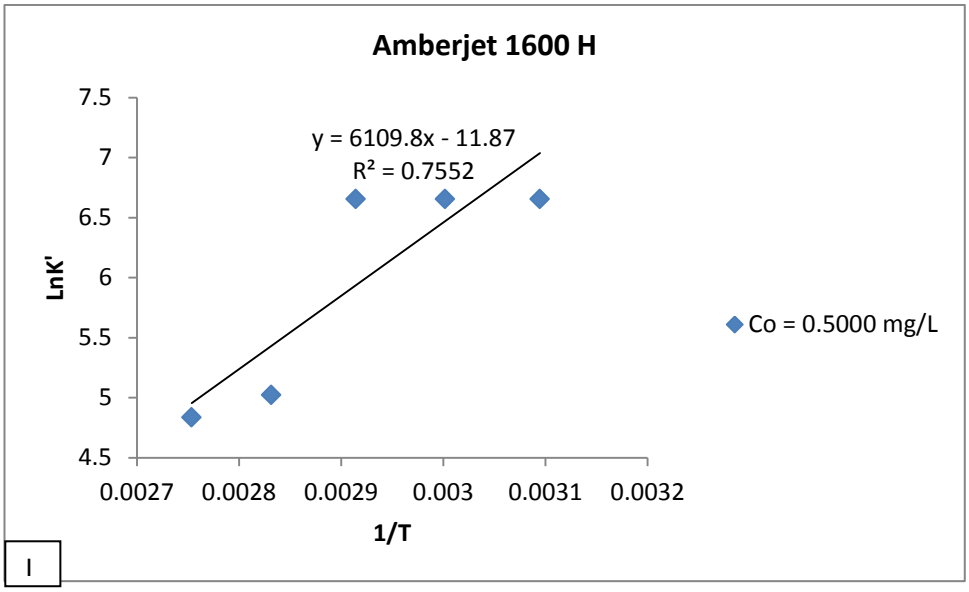
Amberjet 1600 H
y = 6109.8x - 11.87
R² = 0.7552
7.5
7
6.5
6
5.5
5
4.5
LnK'
0.0027
0.0028
0.0029
0.003
0.0031
0.0032
1/T
Co = 0.5000 mg/L

I

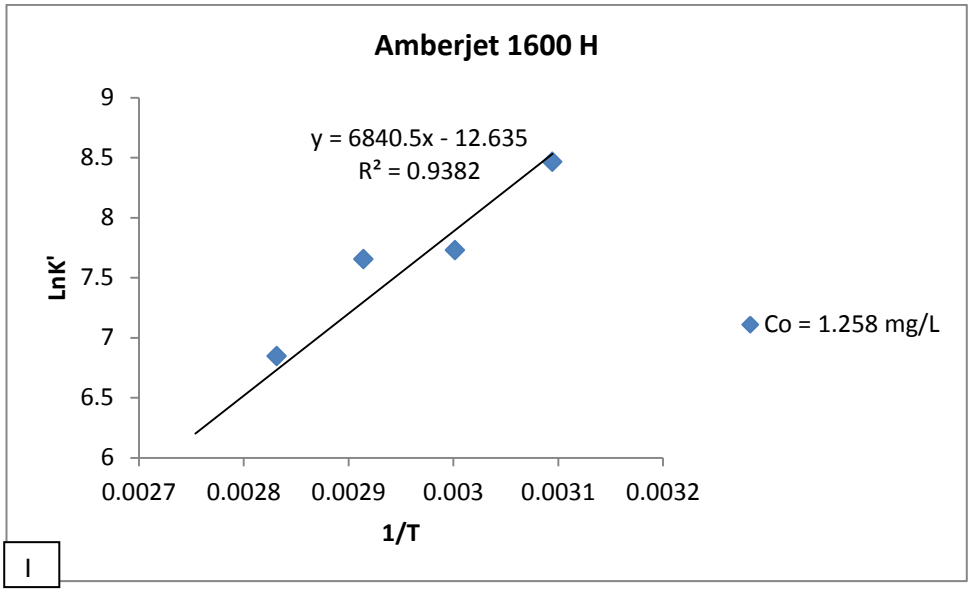
Amberjet 1600 H
y = 6840.5x - 12.635
R² = 0.9382
LnK'
1/T
Co = 1.258 mg/L

I

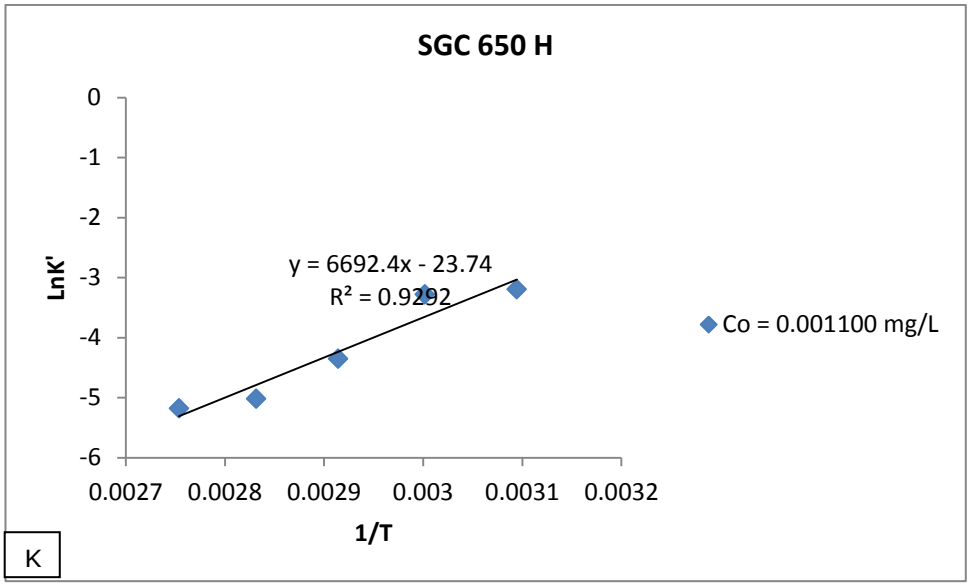
SGC 650 H
y = 6692.4x - 23.74
R² = 0.9292
LnK'
1/T
Co = 0.001100 mg/L

K

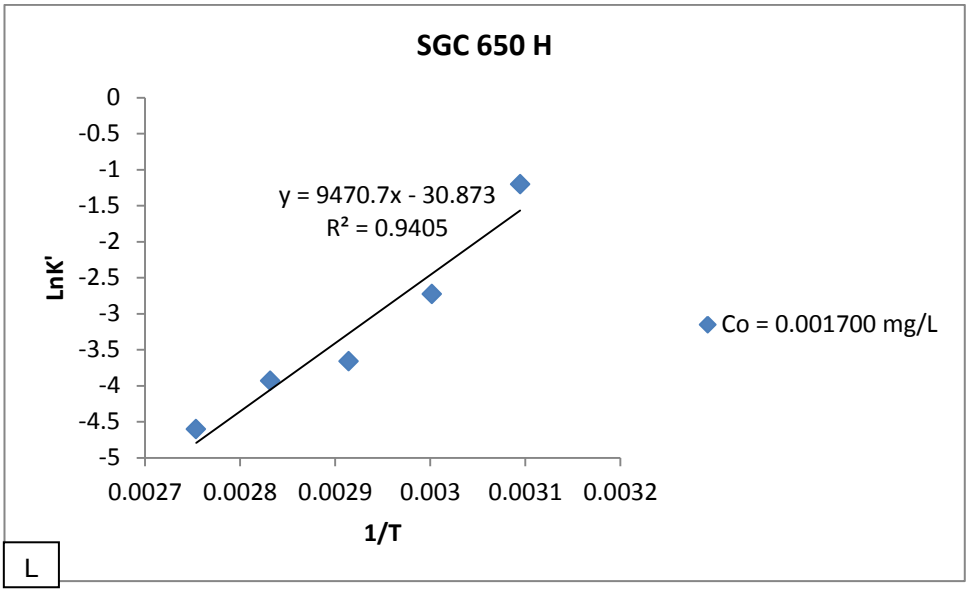
SGC 650 H
0
-0.5
-1
-1.5
-2
-2.5
-3
-3.5
-4
-4.5
-5
LnK'
y = 9470.7x - 30.873
R² = 0.9405
0.0027
0.0028
0.0029
0.003
0.0031
0.0032
1/T
Co = 0.001700 mg/L

L

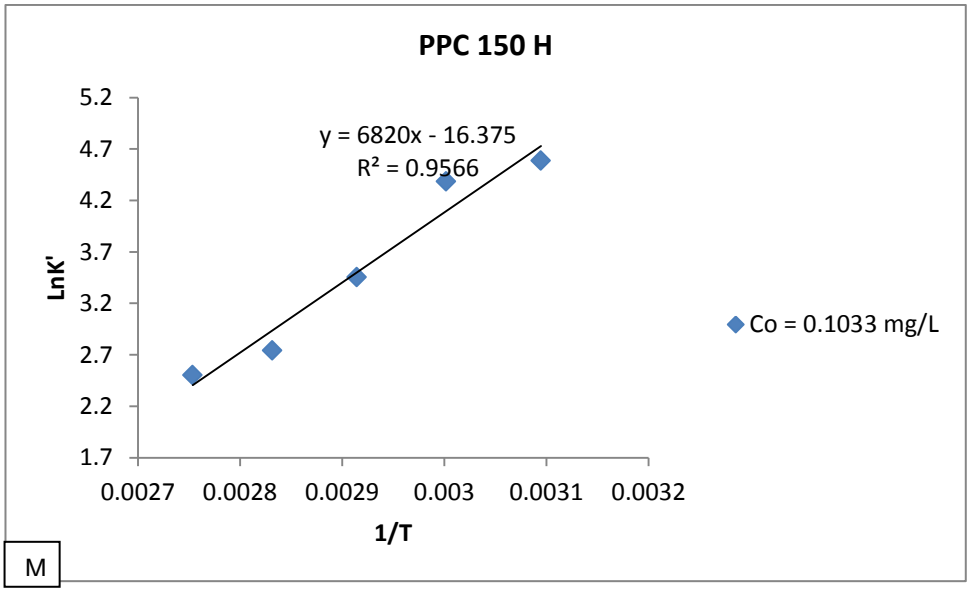
PPC 150 H
5.2
4.7
4.2
3.7
3.2
2.7
2.2
1.7
LnK'
y = 6820x - 16.375
R² = 0.9566
0.0027
0.0028
0.0029
0.003
0.0031
0.0032
1/T
Co = 0.1033 mg/L

M

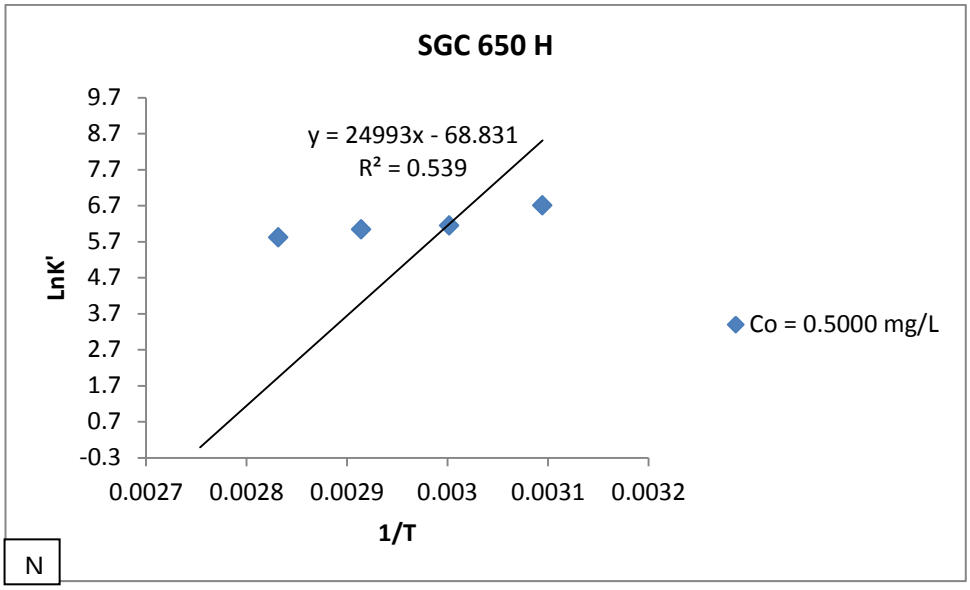
SGC 650 H
y = 24993x - 68.831
R² = 0.539
LnK'
9.7
8.7
7.7
6.7
5.7
4.7
3.7
2.7
1.7
0.7
-0.3
0.0027
0.0028
0.0029
0.003
0.0031
0.0032
1/T
Co = 0.5000 mg/L

N

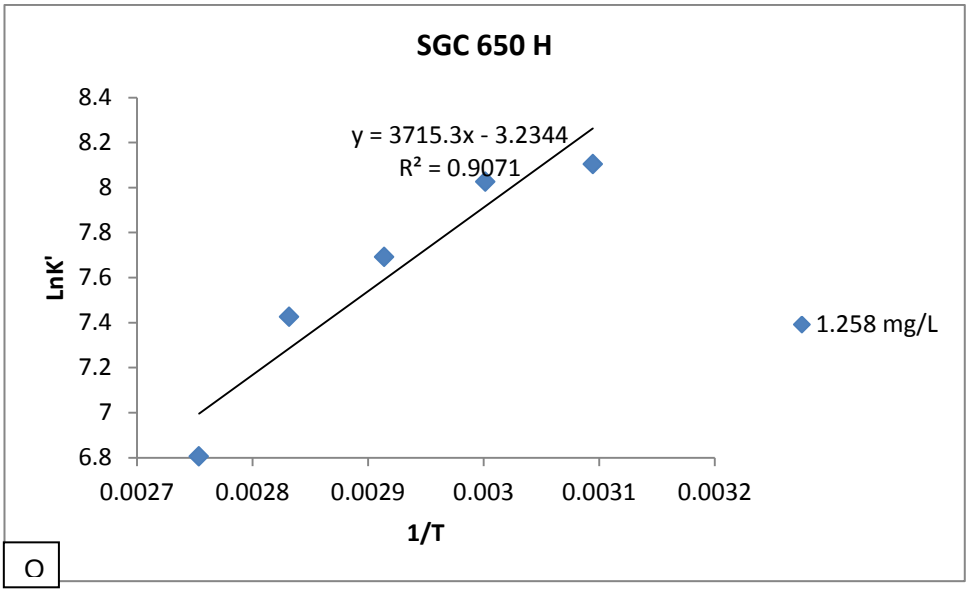
SGC 650 H
y = 3715.3x - 3.2344
R² = 0.9071
LnK'
8.4
8.2
8
7.8
7.6
7.4
7.2
7
6.8
0.0027
0.0028
0.0029
0.003
0.0031
0.0032
1/T
1.258 mg/L

O

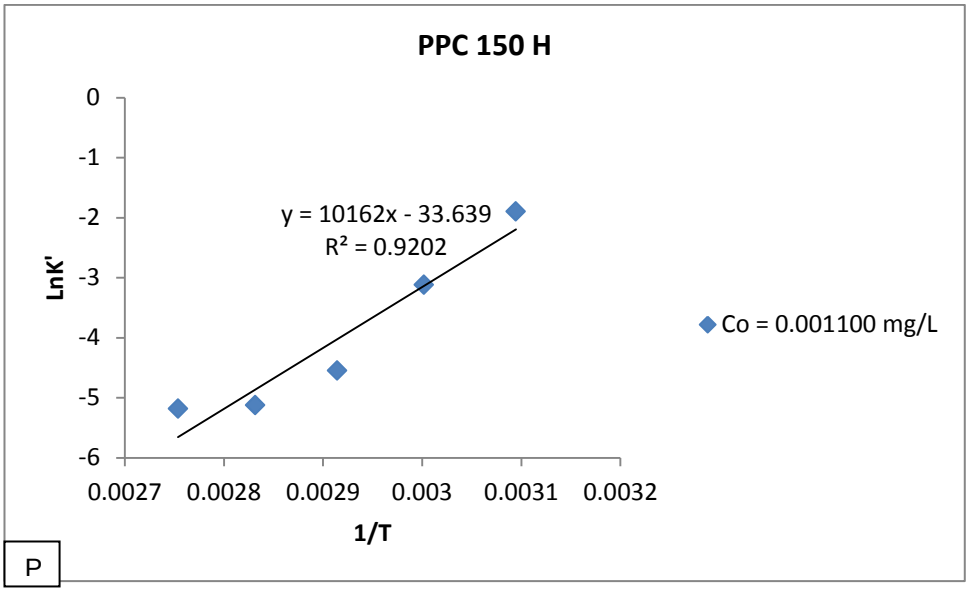
PPC 150 H
y = 10162x - 33.639
R² = 0.9202
LnK'
1/T
0
-1
-2
-3
-4
-5
-6
0.0027
0.0028
0.0029
0.003
0.0031
0.0032
Co = 0.001100 mg/L

P

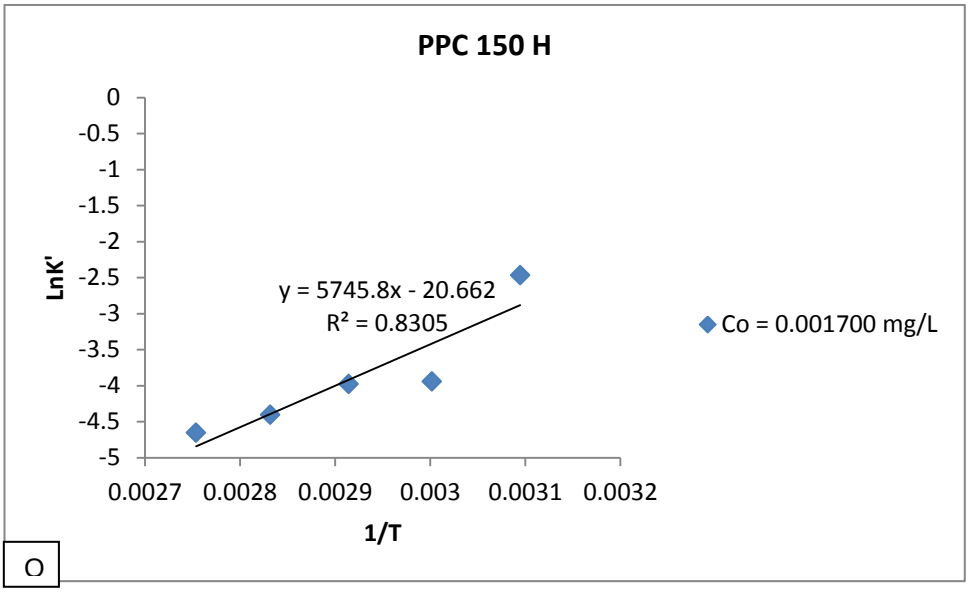
PPC 150 H
y = 5745.8x - 20.662
R² = 0.8305
LnK'
1/T
0
-0.5
-1
-1.5
-2
-2.5
-3
-3.5
-4
-4.5
-5
0.0027
0.0028
0.0029
0.003
0.0031
0.0032
Co = 0.001700 mg/L

O

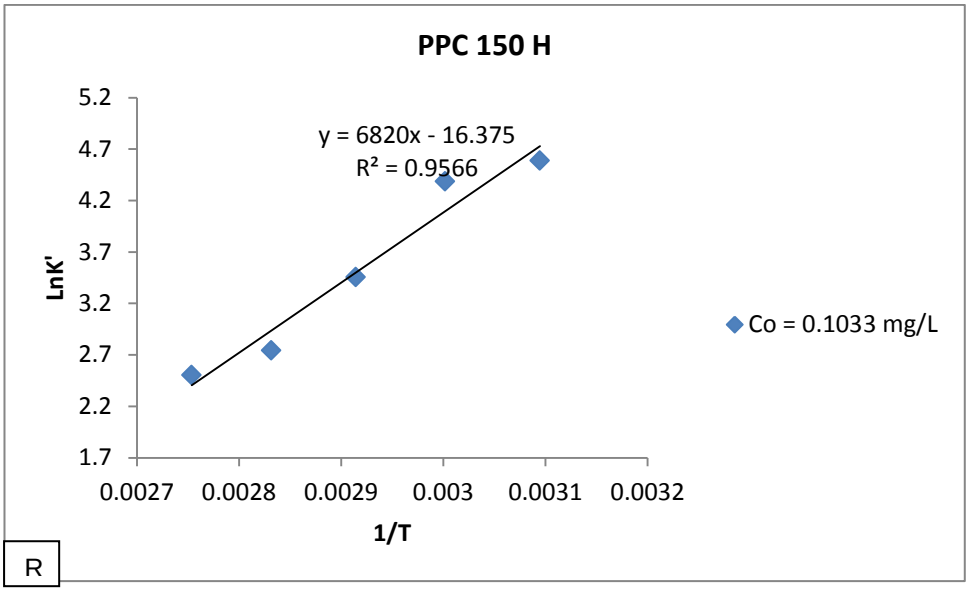
PPC 150 H
y = 6820x - 16.375
R² = 0.9566
LnK'
5.2
4.7
4.2
3.7
3.2
2.7
2.2
1.7
0.0027
0.0028
0.0029
0.003
0.0031
0.0032
1/T
Co = 0.1033 mg/L

R

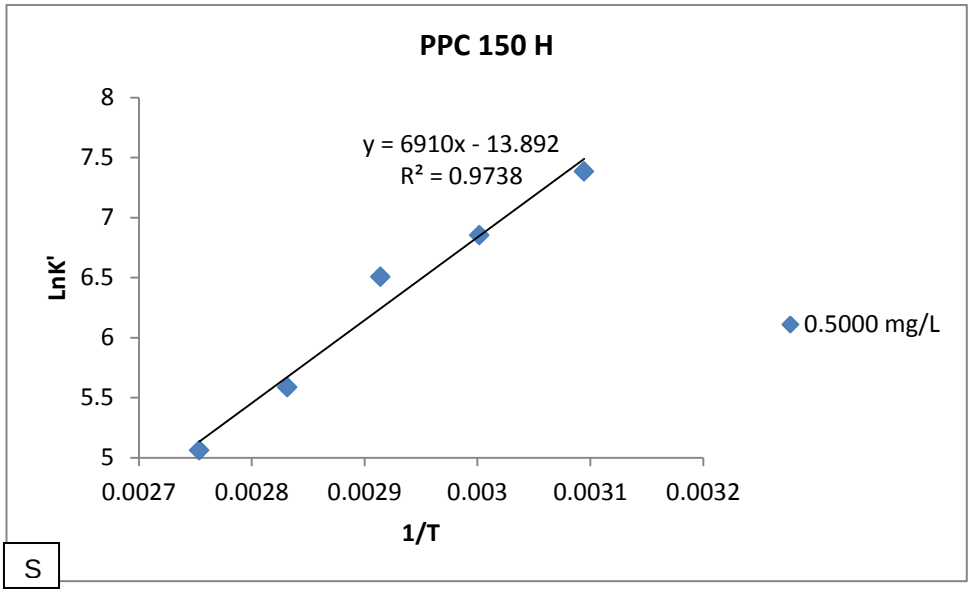
PPC 150 H
y = 6910x - 13.892
R² = 0.9738
LnK'
8
7.5
7
6.5
6
5.5
5
0.0027
0.0028
0.0029
0.003
0.0031
0.0032
1/T
0.5000 mg/L

S

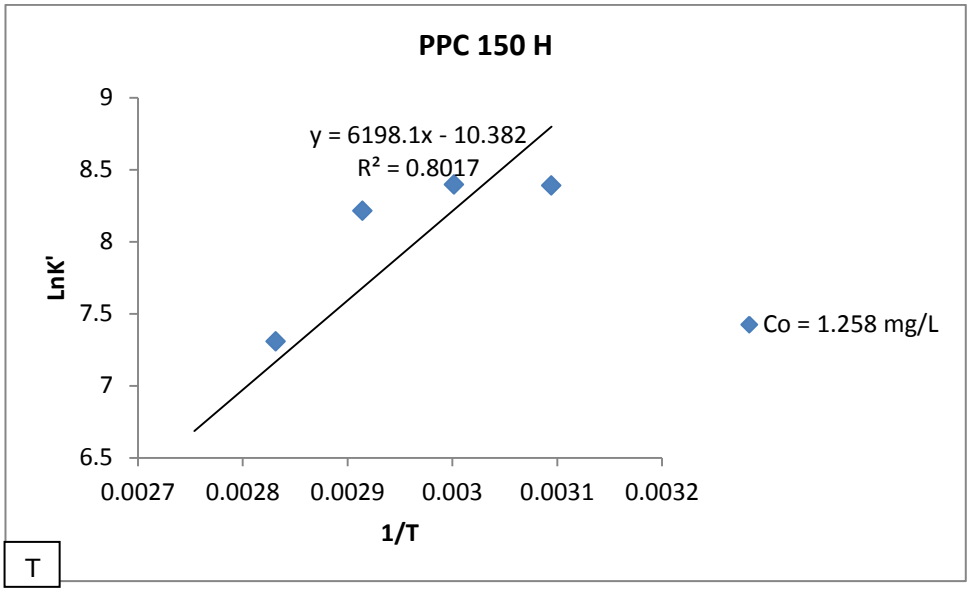

Figure 20: The Van't Hoff plots for Na^+/RH^+ exchange reactions

4.1.4. The pH effect

Figure 21 shows the effect of pH on the exchange of Na^+ by ion exchange resins for reaction carried out at C_o = 0.001100 mg/L (additional data is shown in Table 7). Na^+ uptake from solution was found to decrease with an increase in solution pH. The use of ammonia solution to alter the test solution pH to a desired pH introduced a second counter ion NH_4^+ which reacted with the resin through ion exchange according to the following equation:

$$R{-}H^+ + NH_4^+ \rightleftarrows R{-}NH_4^+ + H^+ \qquad (5.1)$$

Ammonia concentration during the tests was varied from about 2.3 mg/L, 5.0 mg/L, and 12 mg/L which were necessary to bring test solution pH to 9.6, 9.8, and 10 respectively. These were too high concentrations to compete with a sodium ion concentration ranging from 0.001100 mg/L to 1.258 mg/L. The equilibrium concentration of NH_4^+ in solution was not measured due to a delay in the installation and commissioning of the ammonia analyser. An alternative to analysis of NH_4^+ in equilibrium solution would have been to

compute it based on the measured exchange capacity and equilibrium Na^+ concentration in solution. However, this method was not considered as it was expected that not the entire remaining exchange capacity would have been occupied by NH_4^+, as some would have been still occupied by H^+ whose concentration in solution was increased by the water ionization effect. Although the competition reaction between the two counter ions was expected, however it was the magnitude of the differences in selectivity coefficient, $K_{\mathrm{Na}}^{\mathrm{NH}_4^+}$ at elevated reaction temperatures that was of interest. Not being able to measure equilibrium NH_4^+ concentration in solution made it impossible to compute, $\mathrm{K}_{\mathrm{Na}}^{\mathrm{NH}_4^+}$.

However, the decrease in the equilibrium Na^+ concentration in solution after pH conditioning when compared to that obtained in chapter four was evidence of competition reaction and magnitude of the effect of pH on the Na^+/RH^+ exchange reaction. For instance, on reactions carried out using Ambersep 252 H, there was a drop in equilibrium sodium on resin (q_e) of 1.91 x 10^{-9} mg/g to 2.43 x 10^{-8} mg/g, and 1.63 x 10^{-4} mg/g to 6.42 x 10^{-4} mg/g across the pH range (9.6 – 10) for reactions carried out at 50°C using initial solution concentrations of 0.001100 mg/L and 1.258 mg/L respectively, And a drop of 8.58 x 10^{-9} mg/g to 9.57 x 10^{-8} mg/g and 2.55 x 10^{-4} mg/g to 1.86 x 10^{-3} mg/g for reactions carried out at 90 °C for the same initial solution concentrations. A similar trend was observed with other reactions as well.

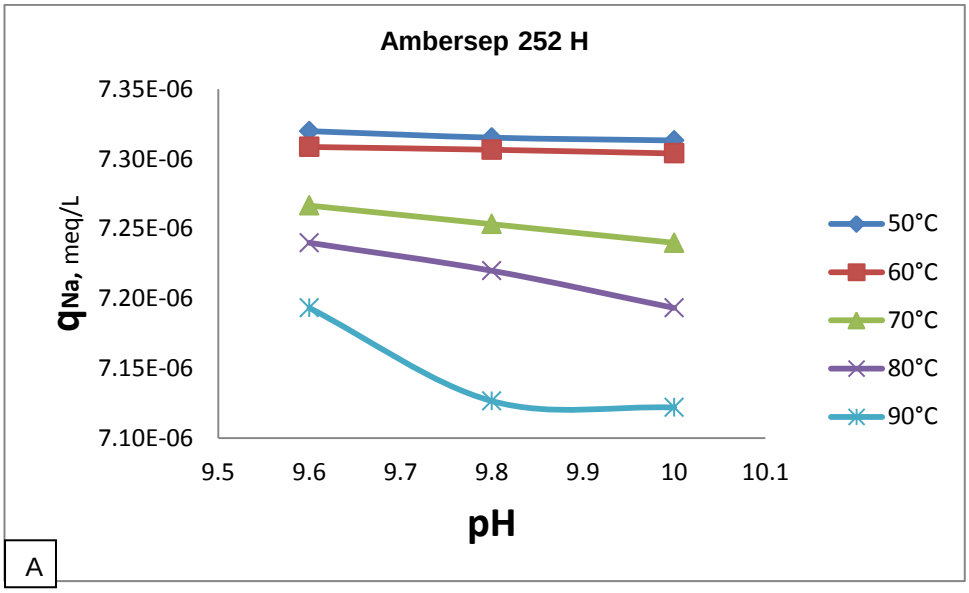
Ambersep 252 H
7.35E-06
7.30E-06
7.25E-06
7.20E-06
7.15E-06
7.10E-06
qNa, meq/L
9.5
9.6
9.7
9.8
9.9
10
10.1
pH
50°C
60°C
70°C
80°C
90°C

A

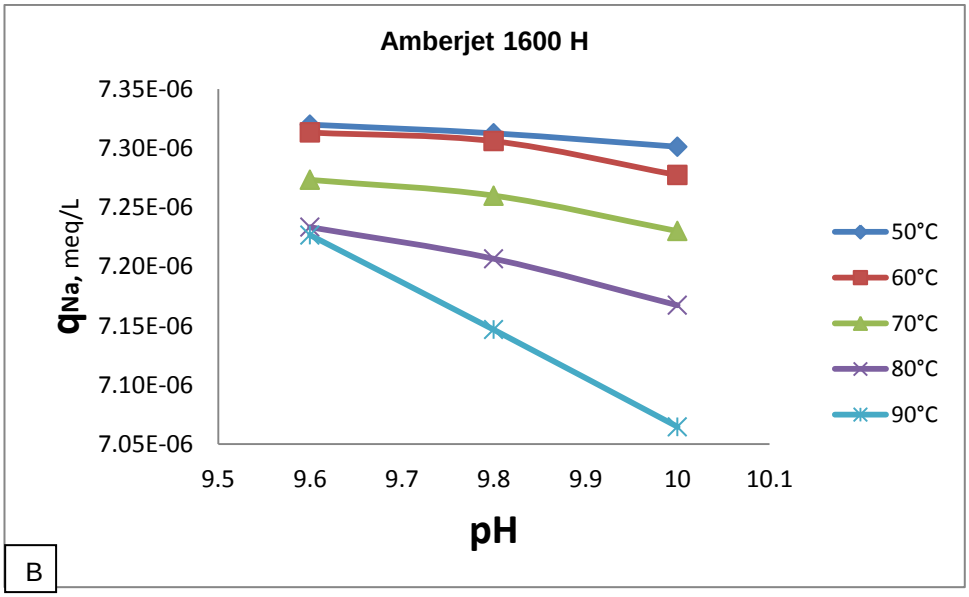
Amberjet 1600 H
7.35E-06
7.30E-06
7.25E-06
7.20E-06
7.15E-06
7.10E-06
7.05E-06
qNa, meq/L
9.5
9.6
9.7
9.8
9.9
10
10.1
pH
50°C
60°C
70°C
80°C
90°C

B

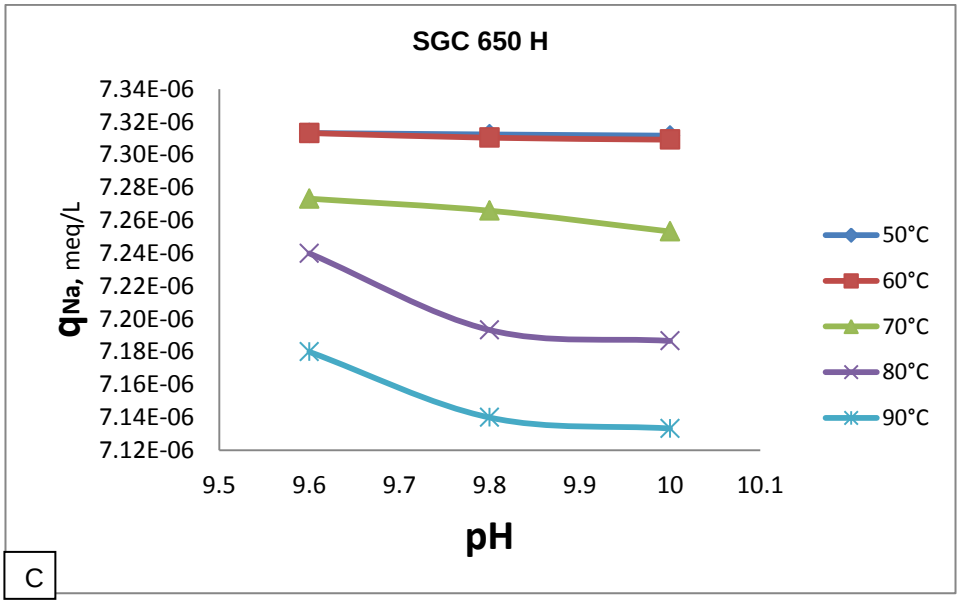

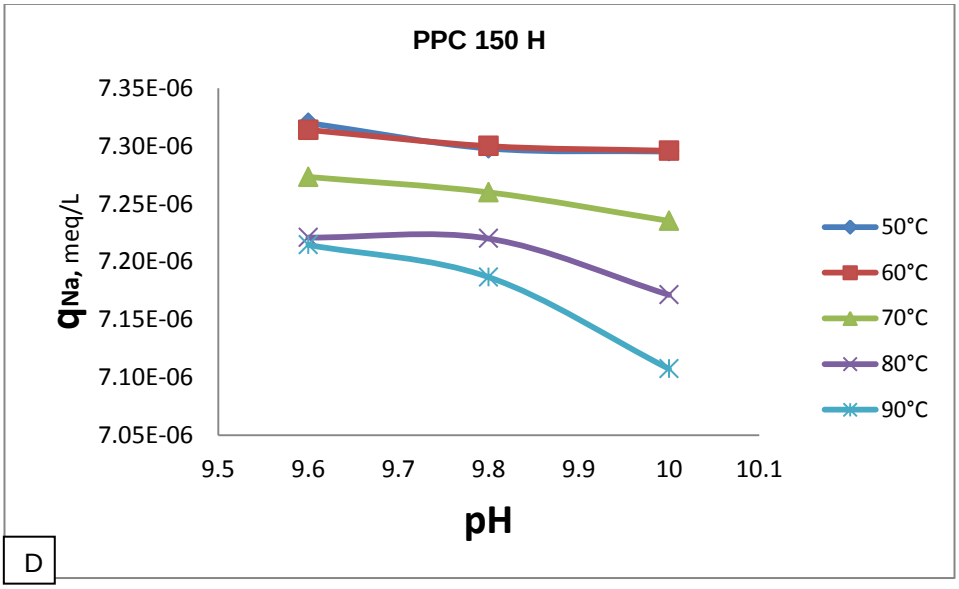

Figure 21: The effect of pH on Na^+ exchange by candidate ion exchange resins at varying reaction temperature (C_o = 0.001100 mg/L)

The equilibrium quotient was used to define the selectivity coefficient under the influence of pH. The magnitude of the equilibrium quotient differs from that of the selectivity coefficient or corrected selectivity coefficient as ionic fraction ($X_{Na/H}$) in solid phase were used in place of q_e (mg/g) or molarity (M) [51]. The liquid phase activity coefficients were factored and computed the same way as in Chapter Four.

$$\Lambda_{Na-H} = \frac{X_{Na}.\gamma_H C_H}{\gamma_{Na} C_{Na}.X_H.} \qquad (5.1)$$

The experimental data displayed in Figure 22 suggest that pH influenced the equilibrium of the exchange of sodium on ion exchange resins at a given initial solution concentration (additional data is shown in Table 8-11). The temperature influence was also in agreement with the results reported in Chapter Four. The equilibrium quotient increased across the initial solution concentration and was highest for reactions carried out at 1.258 mg/L. This further served as evidence of the observed increase in Na^+ uptake by ion exchange resins with increasing initial solution concentration reported in Chapter Four. The equilibrium quotient decreased across the pH range per initial solution concentration, indicating the pH effect.

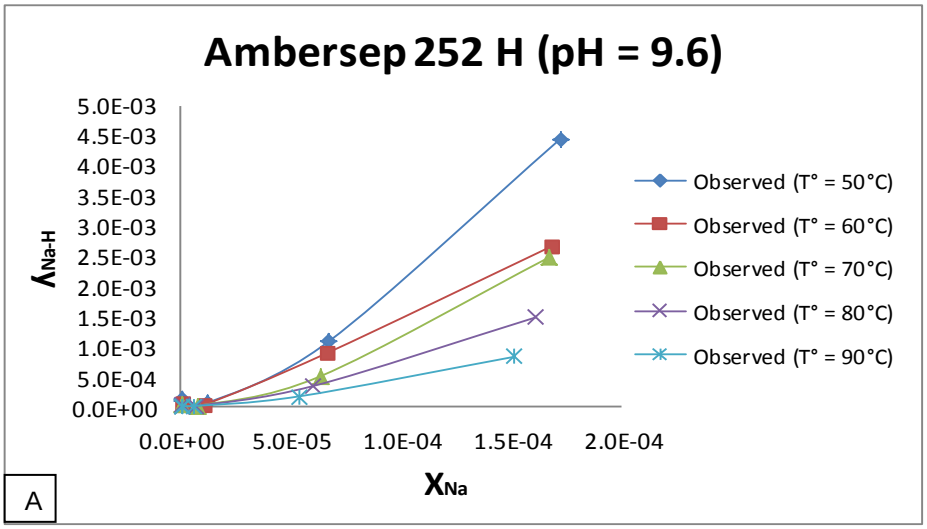

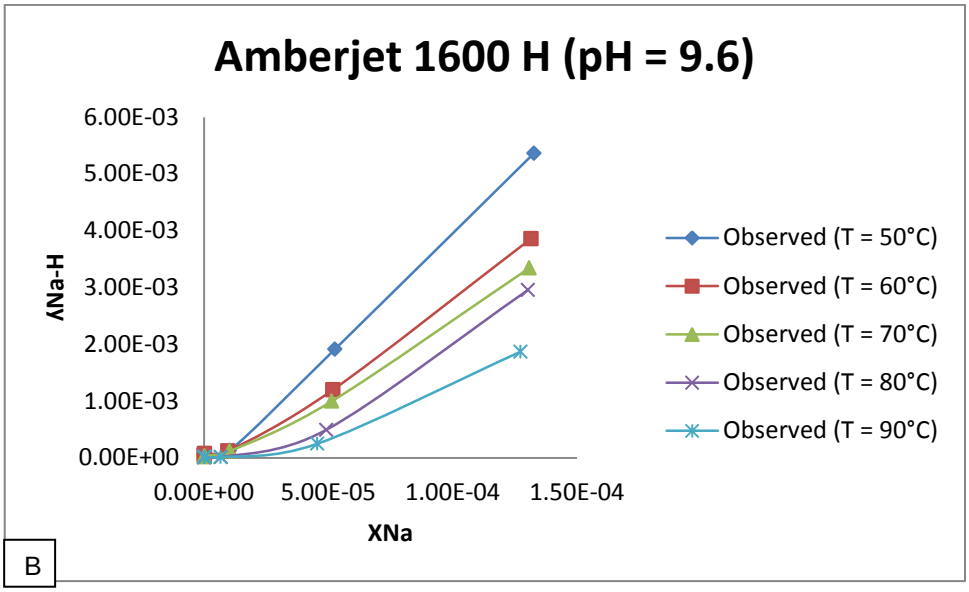
Amberjet 1600 H (pH = 9.6)
6.00E-03
5.00E-03
4.00E-03
3.00E-03
2.00E-03
1.00E-03
0.00E+00
ΔNa-H
0.00E+00
5.00E-05
1.00E-04
1.50E-04
XNa
Observed (T = 50°C)
Observed (T = 60°C)
Observed (T = 70°C)
Observed (T = 80°C)
Observed (T = 90°C)

B

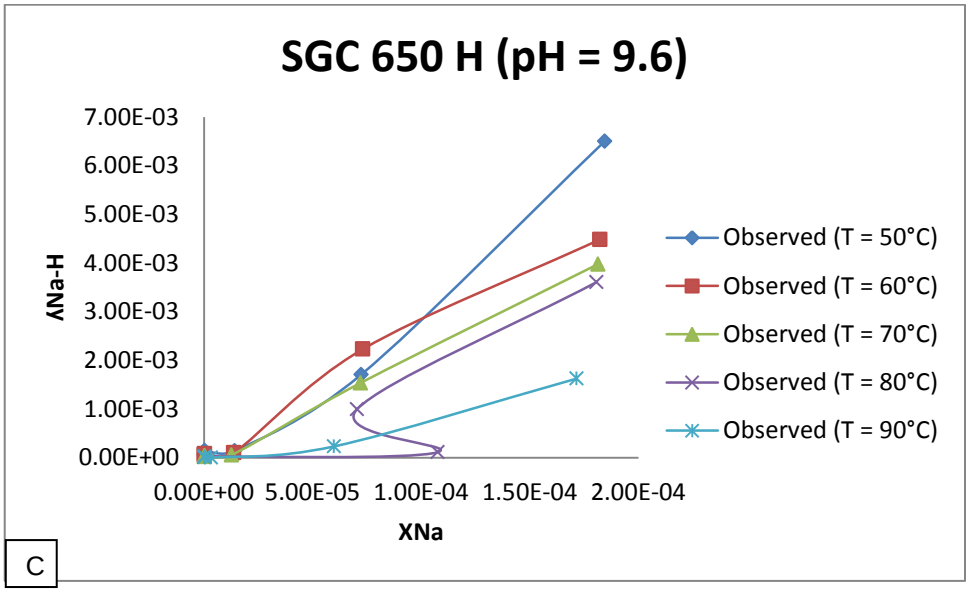
SGC 650 H (pH = 9.6)
7.00E-03
6.00E-03
5.00E-03
4.00E-03
3.00E-03
2.00E-03
1.00E-03
0.00E+00
ΔNa-H
0.00E+00
5.00E-05
1.00E-04
1.50E-04
2.00E-04
XNa
Observed (T = 50°C)
Observed (T = 60°C)
Observed (T = 70°C)
Observed (T = 80°C)
Observed (T = 90°C)

C

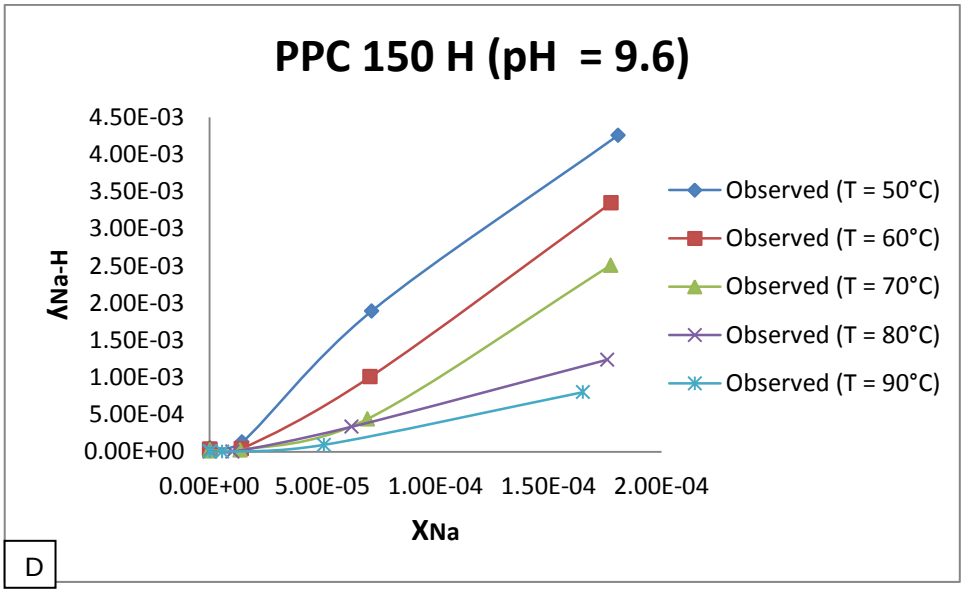

Figure 22: The effect of pH on Na^+ exchange by candidate ion exchange resins at varying reaction temperature

5. CHAPTER FIVE

5.1. CONCLUSION

Ion exchange equilibria tests were conducted at varying Na^+ solution concentration and reaction temperature using strong acid cation exchange resins Ambersep 252 H, Amberjet 1600 H, SGC 650 H, and PPC 150 H. The exchange capacity measurements and time required for ion exchange reactions to reach equilibria were comparable to that found in literature. The Langmuir constant, K_L was found to be dependent on reaction temperature, with gel type resins showing higher K_L than macroporous type. K_L was highest at reactions carried out at 50°C. This, together with the increase in R_L with reaction temperature was proof of the poor exchange reaction observed at reactions carried out at temperatures greater than 50°C. A “good fit” of isotherm models to experimental data was only observed with reactions carried out at certain reaction temperatures and selected candidate ion exchange resins. The selectivity coefficients, corrected selectivity coefficients, and thermodynamic parameters were determined from the experimental data. According to the results, the following conclusions can be made:

1) The selectivity and corrected selectivity coefficient decreased with increasing reaction temperature, implying poor uptake of Na^+ from solution by all types of ion exchange resins. On average, Amberjet 1600 H performed better followed by SGC 650 H, and PPC 150 H.
2) The thermodynamic parameters of the ion-exchange process were calculated. The ion exchange equilibria of Na^+/RH^+ were found to be exothermic processes.
3) The positive ΔG values indicated that the reverse reaction is spontaneous, whilst the negative ΔG indicates that the forward reaction is spontaneous.

There was a decrease in the equilibrium Na^+ concentration in solution after pH conditioning, and the difference was considerable when compared with that obtained from reactions without pH conditioning.

The equilibrium quotient increased with the increasing initial solution concentration and as it was highest for reactions carried out at 1.258 mg/L.

The equilibrium quotient decreased across the pH range, per initial solution concentration, indicating the pH effect.

The equilibrium and thermodynamic data obtained in this work will be of considerable use in understanding the behaviour of ion exchange reactions for Na^+/RH^+ systems operated at elevated temperatures.

5.2. RECOMMENDATION

The equilibrium as well as the isotherm model parameters were deduced from the experimental data gathered using a Batch method. It is recommended that a similar study be conducted using a Dynamic method and be extended to anion exchange reactions. All tests parameters should match those of the actual condensate polishing process. This can be realised if a trial is conducted in the plant, in parallel with the actual condensate polishing unit.

The author also recommends that a study on novel ion exchangers be conducted. Such a study should seek to synthesise ion exchangers with improved physicochemical properties when compared with those already available. The potential ion exchange resins would be those that can offer excellent exchange rate not only at moderate temperatures but also at elevated reaction temperatures and pH, and have longer shelf-life.

5.3. REFERENCES

1. EPRI. *Condensate Polishing Performance Assessment: Use of Separate Bed Single Vessel Designs*. Electric Power Research Institute, EPRI TR1014130, 2008.
2. EPRI. *Condensate Polishing Training Manual*. Electric Power Research Institute, EPRI TR1004933, 2004.
3. F.M. Cutler. *Condensate polishing training program: Condensate polishing in fossil units*. Proceedings: Eskom international conference on power plant Chemistry and Process water treatment, Johannesburg, South Africa, 2001.
4. R.N. Robinson and L.A. Chapple. *Operation of the world's largest Tripol condensate polishing vessel at Stanwell power station (Queensland) Australia*. Ion exch. Dev. Applica. Royal Socie. Chem.1996, Cambridge, UK.
5. T.H. McCloskey and R.B. Dooley. *Turbine steam path damage: Theory and Practice*. Turbine Fundamentals, Vol. 1, EPRI (1999), 17-5–17-9.
6. DOWEX. *Ion exchange resin: A guide to condensate polishing*. Dow liquid separations, 2003, 03-04.
7. A.L. Tavares and R. A. Applegate. *Condensate polishing for nuclear and super critical power plants for the 21st Century*. Power Plant Chemistry, Vol. 11, No. 3, 2009, pp. 01-10.
8. J.D. Aspden and G.W. Lock. *Condensate polishing at a 6×665 MW dry cooled power plant*. Proceedings: Eighth International Conference on Cycle Chemistry in Fossil and Combined Cycle Plants with Heat Recovery Steam Generators, 2006, Calgary, Alberta Canada.
9. R.S. Juang, and L.D. Shiau. *Ion exchange equilibria of metal chelates of ethylene diamine tetra-acetic acid (EDTA) with Amberlite IRA-68*. Ind. Eng. Chem. Res., Vol. 37, No. 2, 1998, pp. 555–560.
10. L. Khezami, R. Capart. *Removal of Chromium (VI) from aqueous solution by activated carbons: Kinetic and equilibrium studies*. J. Hazard. Mater., Vol. 123, 2005, pp. 223-231.

11. J.L. Valverde, A. De Lucas, M. Carmona, M. Gonzalez, and J.F. Rodriguez. *Model for the determination of diffusion coefficients of heterovalent ions in macroporous ion exchange resins by the zero length column method*. Chem. Eng. Sci., Vol. 60, 2005, pp. 5836–5844.
12. www.iupac.org/publications/pac/25/4/0797/pdf/. Retrieved on 2015/11/07
13. P. Singare, R. M. Lokhande, and N. Samant. *Studies of Uni-Univalent Ion Exchange Reactions Using Strongly Acidic Cation Exchange Resin Amberlite IR-120*. Nat. Sci., Vol.01, 2009, pp. 124-128.
14. M.M. Valenta, K.E. Parker, and E.M. Pierce. *Tc-99 Ion exchange resin testing*. PNNL 19681, 2010.
15. M. Petrova, M. Guique, L. Venault, P. Moisy, and P. Heseman. *Anion selectivity in ion exchange reactions with surface functionalised ionosilicas*. Phys. Chem. Chem. Phys., Vol. 17, 2015, pp. 10182-10188.
16. P.U. Singare, R.S. Lokhande, and S.Y. Pimple. *Study of uni-bivalent ion exchange reactions using strongly acidic cation exchange resin Duolite ARC 9353*. R. J. Chem., Vol.2, 2009, pp. 75-80.
17. N.S. Yousef, S. Darwish, T.M. Zewail, and Y.A. Tawail. *Mass transfer study of heavy metal removal by ion exchange in batch conical air spouting bed*. J. Chem. Eng. Process Technol., Vol. 4, No. 6, 2013, pp. 4-6
18. Z. Aksu, U. Açıkel, E. Kabasakal, and S. Tezer. *Equilibrium modelling of individual and simultaneous biosorption of chromium(VI) and nickel(II) onto dried activated sludge.* Wat. Res., Vol. 36, 2002, pp. 3063-3073.
19. M. Grahn. *Development of a novel zeolite coated ATR-FTIR sensor.* MSc. Thesis. Luleå University of Technology, 2004, Sweden.
20. T.S. Najim, S.A. Farhan, and R.M. Dadoosh. *New solid extractor for separation of Cadmium (II) based on agricultural waste*. Basrah J. Sci. Vol.30, No. 01, 2012, pp. 66-78.
21. Z. Ma, R.D. *Whitley, and N.H. Wang. Pore and surface diffusion in multicomponent adsorption and chromatography systems*. AIChE J., Vol. 42, 1996, pp. 1244.

22. G. Limousin, J.-P. Gaudet, L. Charlet, S. Szenknect, V. Barthe`s, and M. Krimissa. *Sorption isotherms: A review on physical bases, modelling and measurement*. Applied Geochem., Vol. 22, 2007, pp. 249–275.
23. DOWEX. *Ion Exchange Resins: A Practical Handbook for Engineers and Chemists.* Dow Liquid Separations, 2005.
24. W. Miller, C. Castagna, and A. Pieper. *Understanding ion exchange resins for water treatment systems*. GE water and process technologies, TP1050N, 2009, pp. 1-3.
25. O. Okay. *Macroporous copolymer networks*. Prog. Polym. Sci., Vol. 25, 2000, pp. 711-779.
26. J. Falke. *Condensate polishers in separate bed configuration*. Proceedings: 5th EPRI international conference on Fossil Plant Cycle Chemistry. Electric Power Research Institute, TR108459, 1997, Palo Alto.
27. http://www.soci.org/~/media/Files/Conference%20Downloads/2012/IEX%20Intro%20Water%20Sept%202012/Marc_Slagt_resin. Retrieved on 2015/12/07.
28. B. Hoffman and J.D. Aspden. *Critical aspects of ion exchange resin performance in high temperature condensate polishing applications*. Proceedings: 8th international conference on Cycle Chemistry in fossil and combined Cycle plants with heat recovery steam generators, 2006, Calgary, Aberta Canada.
29. D.C. Sherrington. *Preparation, structure and morphology of polymer supports*. Chem. Commun., 1998, pp. 2275–2286.
30. http://dardel.info/IX/resin_structure.html. retrieved on 2013/12/04.
31. S. Alexandratos. Ion exchange resins: *A retrospective from industrial and engineering chemistry research*. Ind. Eng. Chem. Res. Vol. 48, 2009, pp. 388-398
32. EPRI. *Condensate Polishing Guidelines for Fossil Plants.* Electric Power Research Institute, EPRI 1010181, 2006.
33. A. Marton. *Classification and characterization of stationary phases for liquid Chromatography Part II*. Pure Appl. Chem., Vol. 69, No. 7, 1997, pp. 1481–1487.
34. P.A. Addison. *A study of ion exchange equilibrium*. PhD Thesis, University of Canterbury Christ Church, New Zealand, 1990.

35. J.L. Valverde, A. de Lucas, M. Gonza´ lez, and J. F. Rodrı´guez. *Equilibrium Data for the Exchange of $Cu^{2+,}$ Cd^{2+}, and Zn^{2+}Ions for H^{+} on the Cationic Exchanger Amberlite IR-120*. J. Chem. Eng. Data, Vol. 47, 2002, pp. 613-617.

36. M. Berber-Mendoza, R. Ramos, P. Davila, L. Rubio, and R.M. Guerrero-Coronado. *Comparison of isotherms for the ion exchange of Pb(II)from aqueous solution onto homo-ionic clinoptilolite*. J. Colloid and Int. Sci., Vol. 301, 2006, pp. 40–45.

37. S.G. Christensen. *Thermodynamics of Aqueous Electrolyte Solutions –Application to Ion Exchange Systems*. PhD Thesis. Technical University of Denmark, Department of Chemical engineering, 2005.

38. S. Kumar and S. Jain. *History, introduction, and kinetics of ion exchange materials*. J. Chem. Vol. 2013, 2013, pp. 1-13.

39. Yu-Chung Kuan. *Acid extraction of heavy metals from sludge facilitated by ion exchange*. MSc. Thesis. Graduate School of Tatung University. 2006.

40. C.E. Harland. *Ion exchange: Theory and Practice.* The Royal Soc. Of Chem., Cambridge, 1994.

41. EPRI. *Condensate polishing guidelines: Ammonium form operation*. Electric Power Research Institute, EPRI 1004322, 2001.

42. B.N. Yalala. *Ion exchange resins and functional fibres: A comparative study for the treatment of brine waste water*. MSc thesis, University of Western Cape, South Africa. Nov. 2009.

43. J. Aniceto, S. Cardoso, T. Faria, P. Lito, and C. Silva. *Modelling ion exchange equilibrium: Analysis of exchanger phase non-ideality*. Desalination, Vol. 290, 2012, pp. 43-53.

44. V. Ivaniv, V. Gorshkov, O. Gavlina, and E. Llyukhina. *The effect of temperature on the thermodynamics of the ion exchange separation of substances on Ionites*. Rus. J. Phy. Chem. Vol. 80, 2006, pp. 1826-1831.

45. N.M. Rice and H.M. Irving. *Nomenclature for liquid-liquid distribution (solvent extraction)*. Pure &Appl. Chem., Vol. 65, No. 11, 1993, pp. 2373-2396.

46. J. Ramkumar and T. Mukherjee. *Effect of aging on the water sorption and ion exchange studies on Nafion and Dowex resins: Transition metal ions-proton exchange systems*. Sep. and Purific. Tech., 54, 2007, 61–70.

47. P.A. Atkins and J. de Paula. *Physical Chemistry*, 7th ed. Oxford Univ. Press, 2002pp. 258.

48. J.C. Crittenden. *MWH Water Treatment: Principles and Design*, 3rd Ed, John Wiley, 2002.

49. J. W. Murray. Chapter6: Activity scales and Activity coefficients. Univ. of Washington, 2004.

50. P. Singare, R. Lokhande, and M. Dhatrak. *Study of H^+/Mg^{2+} and H^+/Ca^{2+} ion exchange reaction systems using cation exchange resin amberlite IR-120*. Oriental J. Chem., Vol. 25, No. 3, 2009, pp. 687-693.

51. J.J. Perona. *A multicomponent ion exchange equilibrium model for chabazite columns treating ORNL waste waters*. ORNL/TM-12272, 1993.

52. H. Noshin, K. Somaieh, and A. Hossei. *Equilibrium and Thermodynamic Studies of Cesium Adsorption on Natural Vermiculite and Optimization of Operation Conditions*. Iran. J. Chem. Eng. Vol. 28, No. 4, 2009, pp. 29-36.

53. J.D. Seader, and E.J. Henley. *Separation Process Principles*. Wiley, New York, 1998

54. G.M. Walker. *Industrial wastewater treatment using biological activated carbon*. PhD dissertation, *Queen's University of Belfast*, 1995.

55. S.J. Kleinubing and M.G. Silva. *Lead removal process modeling in natural Zeolita clinoptilolita through dynamic and batch systems*. Scientia Plena, Vol. 4, No. 2, 2008, pp. 024201-024209

56. D.F. Hussey. Development of a generalised multicomponent ion exchange reaction equilibrium model. MSc dissertation. Department of Chemical Engineering, Oklahoma State University, 1994.

57. C. H. Bolster and G. M. Hornberger. *On the use of linearized Langmuir equations*. SSSAJ, Vol.71, 2007, pp. 1798.

58. A.A. Zagorodni. *Ion exchange materials properties and applications*. Elsevier, Oxford, UK, 1st ed., 2006.

59. B. Subramanyam; *A. Das. Linearized and non-linearized isotherm models comparative study on adsorption of aqueous phenol solution in soil*. Int. J. Environ. Sci. Tech., Vol. 6, No. 4, 2009, pp. 633-640.

60. C.H. Bolster. *Revisiting a statistical shortcoming when fitting the Langmuir model to sorption data*. J. Environ. Qual. Vol. 37, 2008, pp. 1986-1992

61. D.A. Clifford. *Water quality and treatment: A Handbook of Community Water Supplies*. 5th ed., McGraw-Hill, NY 1999.

62. http://www.dow.com/scripts/litorder.asp?filepath=liquidseps/pdfs/noreg/177-02233.pdf. Retrieved on 2015/12/07.

63. http://www.purolite.com/default.aspx?RelID=619242:*Macroporous C150 H* strong acid cation exchange resin product data sheet. Retrieved on 2015/12/07.

64. http://www.purolite.com/relid/619235/isvars/default/strong_acid_cation_gel.htm Super gel SGC650 H strong acid cation exchange resin product data sheet. Retrieved on 2015/12/07.

65. http://www.lenntech.com/Data-sheets/Amberjet-1600-H-L.pdf. Industrial Grade High Capacity Gel Cation Exchange Resin. Product data sheet. Retrieved on 2015/12/07.

66. Dow water and Process solutions – Technical service laboratory Europe. Ion exchange analysis report no. SA10204, 2011.

67. S. Chatterjee and S. Woo. *The removal of nitrate from aqueous solutions by chitosan hydrogel beads*. J. of Hazard. Mater. Vol. 164, 2009, pp. 1012–1018.

68. A. Dabrowski. *Adsorption – from theory to practice*. Advances in Colloid and Interface Sci., Vol. 93, 2001, pp. 135-224.

69. C.A. Coles and R.N. Yong. *Use of equilibrium and initial metal concentrations in determining Freundlich isotherms for soils and sediments*. Eng. Geo., Vol. 85, 2006, pp. 19–25.

70. P.U. Singare, R.S. Lokhande, and R. D'Souza. *Selectivity behaviour of strongly acidic cation exchange resins Tulsion T-46 for univalent ions*. Ras. J. Chem., Vol.4, 2009, pp. 941.

71. http://www.chemguide.co.uk/physical/acidbaseeqia/kw.html. Retrieved on 2015/09/21.

72. T. Zuyi and W. Changshou. *Determination of ion exchange equilibrium constants for weakly dissociated ion exchange resins*. Solv. Extract. and Ion exch.,Vol.11, No. 4, 1993, pp. 1713-1728.

73. A.A. Zagorodni. *Ion exchange materials properties and applications*. Elsevier, Oxford, UK, 1st ed., 2006.

74. Rohm and Hass. Master Test Method 0265: *Cation salt splitting capacity and percent regeneration: H form resins*. Eddition 1.4, 1998.

5.4. APPENDIX

Table 7: The effect of pH on Na^+ exchange at varying reaction temperature

		Ambersep					Amberjet				
In. conc., mg/L	pH	50°C	60°C	70°C	80°C	90°C	50°C	60°C	70°C	80°C	90°C
0.0017	9.6	1.13×10^{-5}	1.13×10^{-5}	1.12×10^{-5}	1.10×10^{-5}	1.09×10^{-5}	1.13×10^{-5}	1.13×10^{-5}	1.13×10^{-5}	1.12×10^{-5}	1.10×10^{-5}
	9.8	1.12×10^{-5}	1.12×10^{-5}	1.12×10^{-5}	1.10×10^{-5}	1.09×10^{-5}	1.13×10^{-5}	1.13×10^{-5}	1.13×10^{-5}	1.12×10^{-5}	1.09×10^{-5}
	10	1.13×10^{-5}	1.12×10^{-5}	1.12×10^{-5}	1.10×10^{-5}	1.09×10^{-5}	1.13×10^{-5}	1.13×10^{-5}	1.13×10^{-5}	1.12×10^{-5}	1.09×10^{-5}
0.1033	9.6	5.74×10^{-4}	4.91×10^{-4}	3.69×10^{-4}	3.29×10^{-4}	2.59×10^{-5}	6.37×10^{-4}	6.36×10^{-4}	6.33×10^{-4}	1.17×10^{-5}	4.14×10^{-4}
	9.8	5.35×10^{-4}	4.84×10^{-4}	3.17×10^{-4}	3.05×10^{-4}	2.55×10^{-5}	5.57×10^{-4}	5.54×10^{-4}	4.59×10^{-4}	1.06×10^{-4}	9.20×10^{-5}
	10	4.96×10^{-4}	4.78×10^{-4}	3.11×10^{-4}	2.01×10^{-4}	1.96×10^{-4}	5.47×10^{-4}	5.25×10^{-4}	4.43×10^{-4}	1.03×10^{-4}	2.39×10^{-5}
0.5	9.6	3.14×10^{-3}	3.10×10^{-3}	2.95×10^{-3}	2.83×10^{-3}	2.51×10^{-3}	3.24×10^{-3}	3.19×10^{-3}	3.17×10^{-3}	3.03×10^{-3}	2.81×10^{-3}
	9.8	3.10×10^{-3}	3.05×10^{-3}	2.92×10^{-3}	2.71×10^{-3}	2.41×10^{-3}	3.20×10^{-3}	3.19×10^{-3}	2.97×10^{-3}	2.95×10^{-3}	2.76×10^{-3}
	10	2.95×10^{-3}	2.92×10^{-3}	2.89×10^{-3}	2.57×10^{-3}	2.24×10^{-3}	3.10×10^{-3}	3.10×10^{-3}	2.95×10^{-3}	2.42×10^{-3}	2.35×10^{-3}
1.257	9.6	8.07×10^{-3}	7.88×10^{-3}	7.85×10^{-3}	7.55×10^{-3}	7.07×10^{-3}	8.18×10^{-3}	8.10×10^{-3}	8.06×10^{-3}	8.03×10^{-3}	7.84×10^{-3}
	9.8	8.04×10^{-3}	7.87×10^{-3}	7.67×10^{-3}	7.48×10^{-3}	6.66×10^{-3}	8.09×10^{-3}	8.00×10^{-3}	8.06×10^{-3}	7.93×10^{-3}	7.83×10^{-3}
	10	7.98×10^{-3}	7.81×10^{-3}	7.64×10^{-3}	7.47×10^{-3}	5.85×10^{-3}	8.00×10^{-3}	7.94×10^{-3}	7.87×10^{-3}	7.80×10^{-3}	7.53×10^{-3}
		SGC					PPC				
In. conc., mg/L	pH	50°C	60°C	70°C	80°C	90°C	50°C	60°C	70°C	80°C	90°C
0.0017	9.6	1.13×10^{-5}	1.13×10^{-5}	1.13×10^{-5}	1.12×10^{-5}	1.12×10^{-5}	1.13×10^{-5}	1.13×10^{-5}	1.12×10^{-5}	1.12×10^{-5}	1.11×10^{-5}
	9.8	1.13×10^{-5}	1.13×10^{-5}	1.12×10^{-5}	1.11×10^{-5}	1.11×10^{-5}	1.13×10^{-5}	1.13×10^{-5}	1.12×10^{-5}	1.12×10^{-5}	1.11×10^{-5}
	10	1.13×10^{-5}	1.13×10^{-5}	1.12×10^{-5}	1.11×10^{-5}	1.10×10^{-5}	1.13×10^{-5}	1.12×10^{-5}	1.12×10^{-5}	1.12×10^{-5}	1.10×10^{-5}
0.1033	9.6	6.24×10^{-4}	6.03×10^{-4}	5.59×10^{-4}	3.49×10^{-4}	1.43×10^{-4}	6.53×10^{-4}	6.35×10^{-4}	6.15×10^{-4}	4.62×10^{-4}	2.53×10^{-4}
	9.8	5.73×10^{-4}	5.67×10^{-4}	4.86×10^{-4}	1.49×10^{-4}	1.43×10^{-4}	6.43×10^{-4}	5.63×10^{-4}	5.55×10^{-4}	3.77×10^{-4}	2.17×10^{-4}
	10	5.08×10^{-4}	5.31×10^{-4}	2.68×10^{-4}	1.15×10^{-4}	1.09×10^{-4}	6.21×10^{-4}	5.09×10^{-4}	4.50×10^{-4}	1.05×10^{-4}	1.89×10^{-4}
0.5	9.6	3.20×10^{-3}	3.23×10^{-3}	3.18×10^{-3}	3.11×10^{-3}	2.64×10^{-3}	3.24×10^{-3}	3.21×10^{-3}	3.15×10^{-3}	2.83×10^{-3}	2.28×10^{-3}
	9.8	3.12×10^{-3}	3.22×10^{-3}	3.18×10^{-3}	3.06×10^{-3}	2.54×10^{-3}	3.22×10^{-3}	3.13×10^{-3}	3.07×10^{-3}	2.82×10^{-3}	2.18×10^{-3}
	10	3.09×10^{-3}	3.09×10^{-3}	3.17×10^{-3}	3.01×10^{-3}	2.50×10^{-3}	3.21×10^{-3}	3.11×10^{-3}	2.88×10^{-3}	2.81×10^{-3}	2.17×10^{-3}
1.257	9.6	8.15×10^{-3}	8.05×10^{-3}	8.01×10^{-3}	7.98×10^{-3}	7.57×10^{-3}	8.15×10^{-3}	8.01×10^{-3}	8.00×10^{-3}	7.93×10^{-3}	7.45×10^{-3}
	9.8	7.91×10^{-3}	7.95×10^{-3}	7.93×10^{-3}	7.55×10^{-3}	7.36×10^{-3}	8.14×10^{-3}	7.97×10^{-3}	7.86×10^{-3}	7.56×10^{-3}	6.97×10^{-3}
	10	7.91×10^{-3}	7.77×10^{-3}	7.74×10^{-3}	7.31×10^{-3}	6.95×10^{-3}	8.04×10^{-3}	7.96×10^{-3}	7.82×10^{-3}	7.33×10^{-3}	6.94×10^{-3}

Table 8: Equilibrium quotient variation with pH at varying reaction temperature for reactions involving Ambersep 252 H

Ambersep 252 H							
Solution pH	**Initial Conc. mg/L**	**Reaction Temperature, °C**	**X_{Na^+}**	**$\Lambda_{Na^+-H^+}$**	**Solution pH**	**X_{Na^+}**	**$\Lambda_{Na^+-H^+}$**
9.8	0.0011	50	1.56E-07	5.70E-05	10	1.56E-07	5.70E-05
	0.0017		2.40E-07	1.09E-04		2.41E-07	1.10E-04
	0.1033		1.14E-05	2.95E-05		1.06E-05	2.73E-05
	0.5000		6.60E-05	5.08E-04		6.28E-05	4.83E-04
	1.2576		1.71E-04	3.40E-03		1.70E-04	3.37E-03
	0.0011	60	1.56E-07	3.88E-05		1.56E-07	3.88E-05
	0.0017		2.40E-07	3.09E-05		2.40E-07	3.09E-05
	0.1033		1.03E-05	2.35E-05		1.02E-05	2.32E-05
	0.5000		6.51E-05	4.59E-04		6.22E-05	4.39E-04
	1.2576		1.68E-04	2.29E-03		1.66E-04	2.27E-03
	0.0011	70	1.55E-07	1.20E-05		1.54E-07	1.20E-05
	0.0017		2.38E-07	1.65E-05		2.38E-07	1.65E-05
	0.1033		6.76E-06	5.58E-06		6.62E-06	5.46E-06
	0.5000		6.21E-05	4.04E-04		6.15E-05	4.00E-04
	1.2576		1.63E-04	1.69E-03		1.63E-04	1.68E-03
	0.0011	80	1.54E-07	7.91E-06		1.53E-07	7.88E-06
	0.0017		2.35E-07	7.85E-06		2.35E-07	7.85E-06
	0.1033		6.51E-06	2.70E-06		4.29E-06	1.78E-06
	0.5000		5.78E-05	1.94E-04		5.47E-05	1.84E-04
	1.2576		1.59E-04	1.31E-03		1.59E-04	1.31E-03
	0.0011	90	1.52E-07	5.12E-06		1.52E-07	5.12E-06
	0.0017		2.32E-07	5.47E-06		2.32E-07	5.46E-06
	0.1033		5.43E-06	2.17E-06		4.18E-06	1.67E-06
	0.5000		5.14E-05	1.07E-04		4.78E-05	9.93E-05
	1.2576		1.42E-04	3.32E-04		1.25E-04	2.92E-04

Table 9: Equilibrium quotient variation with pH at varying reaction temperature for reactions involving Amberjet 1600 H

Amberjet 1600 H							
Solution pH	**Initial Conc. mg/L**	**Reaction Temperature, °C**	**X_{Na^+}**	**$\Lambda_{Na^+-H^+}$**	**Solution pH**	**X_{Na^+}**	**$\Lambda_{Na^+-H^+}$**
9.8	0.0011	50	1.19E-07	4.20E-05	10	1.18E-07	2.70E-05
	0.0017		1.83E-07	5.94E-05		1.83E-07	5.80E-05
	0.1033		8.93E-06	3.58E-05		8.90E-06	3.49E-05
	0.5000		5.19E-05	1.24E-03		5.03E-05	6.71E-04
	1.2576		1.30E-04	2.83E-03		1.30E-04	2.74E-03
	0.0011	60	1.19E-07	3.17E-05		1.18E-07	1.53E-05
	0.0017		1.83E-07	7.59E-05		1.83E-07	3.68E-05
	0.1033		8.76E-06	3.19E-05		8.51E-06	2.73E-05
	0.5000		5.18E-05	1.16E-03		5.13E-05	9.50E-04
	1.2576		1.30E-04	2.73E-03		1.29E-04	2.34E-03
	0.0011	70	1.18E-07	1.17E-05		1.17E-07	8.21E-06
	0.0017		1.83E-07	3.46E-05		1.83E-07	3.31E-05
	0.1033		7.45E-06	1.50E-05		7.18E-06	1.30E-05
	0.5000		4.82E-05	3.99E-04		4.79E-05	3.71E-04
	1.2576		1.31E-04	3.31E-03		1.28E-04	1.99E-03
	0.0011	80	1.17E-07	6.65E-06		1.16E-07	5.02E-06
	0.0017		1.82E-07	1.61E-05		1.81E-07	1.22E-05
	0.1033		1.72E-06	3.13E-07		1.67E-06	2.93E-07
	0.5000		4.79E-05	3.77E-04		3.92E-05	1.04E-04
	1.2576		1.29E-04	2.30E-03		1.27E-04	1.72E-03
	0.0011	90	1.16E-07	4.44E-06		1.15E-07	3.01E-06
	0.0017		1.81E-07	1.08E-05		1.80E-07	7.39E-06
	0.1033		1.49E-06	2.31E-07		3.88E-07	1.40E-08
	0.5000		4.48E-05	2.18E-04		3.82E-05	9.24E-05
	1.2576		1.27E-04	1.82E-03		1.22E-04	1.09E-03

Table 10: Equilibrium quotient variation with pH at varying reaction temperature for reactions involving SGC 650 H

SGC 650 H							
Solution pH	**Initial Conc. mg/L**	**Reaction Temperature, °C**	**X_{Na^+}**	**$\Lambda_{Na^+-H^+}$**	**Solution pH**	**X_{Na^+}**	**$\Lambda_{Na^+-H^+}$**
9.8	0.0011	50	1.66E-07	6.06E-05	10	1.66E-07	6.06E-05
	0.0017		2.56E-07	1.61E-04		2.56E-07	1.61E-04
	0.1033		1.30E-05	3.66E-05		1.15E-05	3.25E-05
	0.5000		7.07E-05	8.97E-04		6.99E-05	8.87E-04
	1.2576		1.79E-04	3.03E-03		1.79E-04	3.02E-03
	0.0011	60	1.66E-07	5.03E-05		1.66E-07	5.03E-05
	0.0017		2.56E-07	5.82E-05		2.56E-07	5.82E-05
	0.1033		1.28E-05	4.33E-05		1.20E-05	4.05E-05
	0.5000		7.28E-05	9.29E-04		7.00E-05	8.93E-04
	1.2576		1.80E-04	2.30E-03		1.76E-04	2.25E-03
	0.0011	70	1.65E-07	1.49E-05		1.64E-07	1.49E-05
	0.0017		2.54E-07	1.79E-05		2.53E-07	1.78E-05
	0.1033		1.10E-05	7.03E-06		6.07E-06	3.88E-06
	0.5000		7.20E-05	1.45E-03		7.19E-05	1.45E-03
	1.2576		1.80E-04	2.18E-03		1.75E-04	2.13E-03
	0.0011	80	1.63E-07	7.98E-06		1.63E-07	7.98E-06
	0.0017		2.52E-07	1.23E-05		2.51E-07	1.23E-05
	0.1033		3.37E-06	6.75E-07		2.60E-06	5.20E-07
	0.5000		6.92E-05	6.47E-04		6.81E-05	6.36E-04
	1.2576		1.71E-04	1.18E-03		1.66E-04	1.15E-03
	0.0011	90	1.62E-07	5.77E-06		1.62E-07	5.76E-06
	0.0017		2.52E-07	1.23E-05		1.97E-07	9.62E-06
	0.1033		1.77E-06	3.50E-08		3.02E-07	5.98E-09
	0.5000		5.74E-05	1.74E-04		5.66E-05	1.71E-04
	1.2576		1.67E-04	8.16E-04		1.57E-04	7.71E-04

Table 11: Equilibrium quotient variation with pH at varying reaction temperature for reactions involving PPC 150 H

PPC 150 H							
Solution pH	**Initial Conc. mg/L**	**Reaction Temperature, °C**	**X_{Na^+}**	**$\Lambda_{Na^+-H^+}$**	**Solution pH**	**X_{Na^+}**	**$\Lambda_{Na^+-H^+}$**
9.8	0.0011	50	1.62E-07	3.11E-05	10	1.62E-07	3.11E-05
	0.0017		2.51E-07	5.62E-05		2.50E-07	5.61E-05
	0.1033		1.43E-05	1.31E-04		1.38E-05	1.26E-04
	0.5000		7.15E-05	1.89E-03		7.12E-05	1.88E-03
	1.2576		1.81E-04	4.25E-03		1.78E-04	4.20E-03
	0.0011	60	1.62E-07	3.17E-05		1.62E-07	3.16E-05
	0.0017		2.50E-07	3.25E-05		2.49E-07	3.24E-05
	0.1033		1.25E-05	3.56E-05		1.13E-05	3.22E-05
	0.5000		6.93E-05	9.83E-04		6.90E-05	9.78E-04
	1.2576		1.77E-04	3.33E-03		1.77E-04	3.33E-03
	0.0011	70	1.61E-07	1.19E-05		1.60E-07	1.19E-05
	0.0017		2.49E-07	2.44E-05		2.49E-07	2.44E-05
	0.1033		1.23E-05	2.33E-05		9.98E-06	1.89E-05
	0.5000		6.81E-05	4.31E-04		6.38E-05	4.04E-04
	1.2576		1.74E-04	2.46E-03		1.74E-04	2.45E-03
	0.0011	80	1.60E-07	7.09E-06		1.59E-07	7.04E-06
	0.0017		2.49E-07	1.84E-05		2.48E-07	1.83E-05
	0.1033		8.37E-06	1.52E-06		2.34E-06	4.23E-07
	0.5000		6.26E-05	3.36E-04		6.22E-05	3.34E-04
	1.2576		1.68E-04	1.18E-03		1.63E-04	1.15E-03
	0.0011	90	1.59E-07	5.01E-06		1.58E-07	4.96E-06
	0.0017		2.46E-07	7.78E-06		2.44E-07	7.72E-06
	0.1033		4.81E-06	1.82E-06		4.19E-06	1.58E-06
	0.5000		4.83E-05	9.04E-05		4.80E-05	8.99E-05
	1.2576		1.55E-04	7.51E-04		1.54E-04	7.48E-04